IDENTIFYING NOVEL UNC5B INTERACTING PARTNERS TO UNDERSTAND ITS FUNCTION IN CNS WHITE MATTER

SAMUEL CLÉMOT-DUPONT

February 2020

Integrated Program in Neuroscience

Department of Neurology and Neurosurgery

Montreal Neurological Institute

Montreal, Quebec

A Thesis submitted to McGill University in partial
fulfillment of the requirements for the degree of Master of Science

Table of Contents

ACKNOWLEDGEMENTS

I would like to start off by immensely thanking everyone mentioned in this section. Without your support, my master's degree would have been much more difficult to accomplish.

First and foremost, I would like to thank my supervisor and mentor, **Dr. Tim Kennedy** for guiding me through the hurdle that was my master's degree. Especially the times I was a lost, stressed and frustrated individual. I am very lucky to have a supervisor with so much patience and tolerance but am extremely grateful that you enabled me to explore the world of neuroscience; a field that has always fascinated me but knew very little.

I would also like to sincerely thank **Ms. Kathleen Daigneault** for basically holding my hand through essential steps needed to progress through my project. Without your help, I most likely would not have been able to reach the objectives I wanted to attain for this master's project. I would additionally like to thank **Lorne Taylor** from the proteomics platform at the RI-MUHC for his guidance and step-by-step instructions for my data analysis. I would like to thank my committee members **Dr. Jack Antel** and **Dr. Alyson Fournier**, for grounding my research project and reminding me how I should prioritize my work in order to complete my degree in a sensible amount of time.

I would also like to thank the **Multiple Sclerosis Society of Canada** for funding me and enabling me to conduct my research.

I am extremely grateful to my colleagues and friends in the Kennedy lab. **Omar** for being my first mentor (and a great one at that) when I was first a lost puppy in the lab. You really helped relieve the initial stress of joining what I found was a big lab. **Diane** for being a great and patient mentor and friend, as well as **Celina** and **Edwin** for their constant support and great friendship, most of my lab techniques were also learned from you guys. Edwin for being able to tolerate me and being a fun and great roommate! I know you'll do very well in

med-school! **Jean-David** (Jay Dee) for also being a great drinking buddy, friend and mentor. Even though we met later in my degree, we were able to form a good friendship very quickly.

A big thank you to my friends back in Ottawa! I always looked forward to catching up with you guys on the rare occasions we got to. Most importantly, I would like to endlessly thank my dearest and best friend **Fiona.** You were instrumental to my master's degree. You not only were a great roommate, but my master's would have been much more difficult if you weren't there constantly supporting me. I constantly depended on you and the memories we've formed the past years are unforgettable. I look forward to our future adventures together.

I would like to thank my **sister**; your lively and unique personality always lightened my day when I would feel particularly gloomy. Viv, never change! Finally, to **my parents**. Your guidance, life lessons and endless encouragement made me the person that I am today. I hope I made you half as proud as I admire you and am proud of having such amazing parents. This one is for you!

ABSTRACT

Netrin-1 and the netrin receptor deleted in colorectal cancer (DCC) have been demonstrated to functionally contribute to multiple stages in oligodendrocyte development and maturation in the central nervous system. Both are required for appropriate oligodendrocyte precursor cell (OPC) migration, as well as oligodendrocyte process extension, branching, and membrane elaboration. Another netrin receptor, UNC5B, is also highly expressed by OPCs and oligodendrocytes, but in contrast to netrin-1 and DCC, its functional contribution to oligodendrocyte maturation and myelination has not been studied. We have recently determined that UNC5B is enriched at the paranodal junctions that terminate the compact myelin internode. UNC5B null mice are embryonic lethal at ~E14. Thus, in order to study the contribution of UNC5B to myelination, we developed conditional knock-out (cKO) mice that selectively delete UNC5B from the oligodendrocyte lineage. Olig2 cre – UNC5Bflox/flox mice exhibit disruption of paranodal organization and an age dependent disruption of axonal subdomains. In this thesis, we further investigated the impact of UNC5B deletion on the length of myelin internodes, reporting shorter internodes in 9-month old UNC5B cKO mice compared to their wild type littermates. These findings reveal that UNC5B expression by mature myelinating oligodendrocytes is required to maintain and organize paranodal junctions. However, little is known regarding the proteins that interact with UNC5B and the signaling pathways associated with this protein. We therefore conducted a screen for UNC5B candidate interacting proteins that may function downstream of UNC5B using the biotin identification (BioID) proximity labeling assay. Our findings suggest previously unknown interaction of UNC5B with proteins associated with the cytoskeleton and with key regulators of cell polarity and vesicle trafficking.

RÉSUMÉ

La protéine nétrine-1 et son récepteur DCC (*deleted in colorectal cancer*) contribuent de façon fonctionnelle au développement et à la maturation des oligodendrocytes dans le system nerveux central. Ces deux protéines sont nécessaires à la migration des précurseurs oligodendrocytaires (OPCs), ainsi qu'à l'extension de la membrane et des ramifications des oligodendrocytes lors de la myelinisation. Un autre récepteur à la nétrine, UNC5B, est également exprimé par les OPCs et les oligodendrocytes. Cependant, sa contribution à la maturation des oligodendrocytes et à la myélinisation n'a jusqu'à présent, pas été étudiée. Nous avons récemment démontré un enrichissement de la protéine UNC5B au niveau des jonctions paranodales, qui constituent les extrémités des internoeuds de myéline compactée. La suppression totale de UNC5B provoque une léthalité embryonnaire au jour 14 (E14). Nous avons donc développé une lignée de souris où UNC5B est invalidé de façon conditionnelle dans les cellules de la lignée oligodendrocytaire afin d'étudier sa contribution à la myélinisation. Cette lignée de souris, Olig2 cre – UNC5Bflox/flox, présente une désorganisation progressive des paranoeuds, associée à une perturbation des sous-domaines axonaux à proximité des nœuds de Ranvier. Dans ce mémoire, nous étudions également l'impact de la suppression de UNC5B sur la longueur des internoeuds, révélant des intenoeuds plus courts chez les souris UNC5B cKO âgées de 9 mois que chez les souris contrôle. Ces résultats montrent que l'expression de UNC5B est nécéssaire à la préservation des jonctions paranodales. Cependant, peu d'information sont disponibles quant aux protéines interagissant avec UNC5B et aux voies de signalisation associées. Nous avons ainsi réalisé une expérience d'identification de protéine biotinylée (BioID) à proximité de UNC5B afin d'identifier des protéines candidates pouvant interagir avec UNC5B au sein des jonctions paranodales. Nos résultats suggèrent une interaction de UNC5B avec des protéines du cytosquelette, ainsi qu'avec des régulateurs clés de la polarisation cellulaire et du trafic de vésicule.

AUTHOR CONTRIBUTIONS

Samuel Clémot-Dupont: McGill University, Montreal Neurological Institute
Wrote the thesis, conducted the experiments and analyzed the data present in the thesis, apart from the work conducted by co-authors mentioned below. Provided rationale to the project.

Timothy E. Kennedy: McGill University, Montreal Neurological Institute
Edited the thesis, provided guidance and rationale to the projects and provided reagents and equipment.

Kathleen Daigneault: Shoubridge lab, McGill University, Montreal Neurological Institute
Provided guidance and rationale, generated some stable cell line colonies and provided reagents.

Hana Antonicka: Shoubridge lab, McGill University, Montreal Neurological Institute
Provided guidance and rationale for the validation of stable cell lines.

Jean-David Gothié: Kennedy lab, McGill University, Montreal Neurological Institute
Edited and translated parts of thesis.

Edwin Wong: Kennedy lab, McGill University, Montreal Neurological Institute
Edited parts of thesis.

Diane Nakamura: Kennedy lab, McGill University, Montreal Neurological Institute
Edited parts of thesis.

Omar de Faria Jr.: Káradóttir lab, University of Cambridge, MS Society Cambridge Center for Myelin Repair
Generated the UNC5B transgenic mice and sectioned mouse brain tissues on microscope slides for Immunohistochemistry.

Lorne Taylor: Proteomics Platform, RI-MUHC
Ran the Mass spectrometer, converted data into the Scaffold software and provided guidance in software usage and data analysis.

Odile Neyret and Agnes Dumont: Montreal Clinical Research Institute
Conducted DNA sequencing for generation of protein fusion constructs.

INTRODUCTION

The family of secreted netrins (comprised of netrin 1-5) are multi-functional, acting as attractant or repellent migratory cues depending on the receptors expressed by the responsive cell. Receptors for netrin-1, the most well-studied member of the family, include deleted in colorectal cancer (DCC), neogenin, and the UNC-5 homologues (UNC5A–D). Generally, DCC mediates chemoattractant responses to netrin-1 while UNC-5 homologues signal chemorepulsion (Finci et al., 2015; Hong et al., 1999; Keleman et al., 2001; Macneil et al., 2009). In studies of central nervous system (CNS) myelination, DCC was shown to have a functional role at several stages of oligodendrocyte development (Jarjour et al., 2008, 2003; Rajasekharan et al., 2009; Tsai et al., 2003). Moreover, DCC is also crucial for proper dispersal and migration of oligodendrocyte precursor cells (OPCs) emanating from the ventral ventricular zone of the developing spinal cord (Tsai et al., 2003). In contrast, a function for UNC5s in white matter remains unknown. Recently, the Kennedy lab demonstrated that UNC5B is enriched at oligodendrocyte paranodes (de Faria Jr., 2015). The paranodal regions are the anchorage sites of the myelin sheath, consolidating its interaction with the axon. It also separates the potassium channels located at the juxtaparanodes from the cluster of sodium channels found at the node of Ranvier allowing the regeneration of the axonal nerve impulse (Rios et al., 2003; Scherer, 1996; Waxman, 1980). The Kennedy lab has demonstrated that conditional deletion of UNC5B in from the oligodendrocyte lineage results in paranodal disruption in 9-month-old conditional knock out (cKO) mice, while paranodes appear relatively normal in 3-month-old cKO mice (de Faria Jr., 2015). These results revealed that UNC5B is necessary for maintaining paranodal integrity and domain organization but may be dispensable for paranode formation. However, the proteins interacting with UNC5B and the means by which they mediate its function at paranodes remain to be investigated. Paranodal disruption occurs during early stages of axonal

demyelination in periplaques of multiple sclerosis (MS), and defects in early myelination have been proposed to be a potential underlying cause of MS associated symptoms (Dziedzic et al., 2010; Kuhlmann et al., 2002). Obtaining a better understanding for UNC5 function in the oligodendrocyte lineage is thus critical to understand the mechanisms that maintain healthy myelin.

The first aim of this thesis was to compare internode lengths in 3-month old and 9-month old Olig2-Cre UNC5B transgenic mice, to better understand the implications of paranodal disruption due to functional loss of UNC5B. Additionally, to identify candidate protein interactors that may additionally function downstream of UNC5B, a protein screen was carried out using a biotin identification (BioID) assay. The assay is based on cellular over-expression of the protein of interest, which has been fused to BirA, a biotin ligase. Upon exogenous application of biotin to the overexpressing cell, BirA biotinylates proteins within a 10 nm radius of the BirA fusion protein. The BioID proximity labeling assay allows detection of potential low affinity protein-protein interaction (PPI) in a living cell (Kim et al., 2016). Overall, this work allowed us to identify many candidate proteins that may mediate UNC5B regulation of paranode maintenance.

GENERAL LITERATURE REVIEW

Post-migratory, maturing oligodendrocytes extend their processes and form elaborate lipid-rich sheets in order to wrap and insulate several different axons; forming individual myelin sheaths. This additional protective layer known as myelin, enables the acceleration and sustainability of the action potential along the axon. Furthermore, with aging, each myelin sheath remains in contact with an oligodendrocyte (Lemke, 1988). This continuous contact with the oligodendrocyte cell soma allows the transport of metabolic molecules such as lactate, to be transported to and taken up by axons, enabling oligodendrocytes to support long term axonal integrity and survival (Fünfschilling et al., 2012). A widely accepted model of myelin wrapping assumes that the leading edge of the sheet, known as the inner tongue, wraps under previously formed layers, thickening the sheath as the outermost layers extend longitudinally along the axon (Snaidero et al., 2014). This way, myelination by oligodendrocytes forms the white matter regions of the CNS (reviewed by Chang et al., 2016; Simons et al., 2016; Snaidero & Simons, 2014).

As the myelin sheath thickens, the outmost layers are the first to undergo intracellular compaction. The cytoplasm is thus squeezed to the lateral edges of the sheaths by the major myelin protein, myelin basic protein (MBP) (Ioannidou et al., 2012; Sobottka et al., 2011). In a longitudinal 2-dimensional cross-section of a myelinated axon, the coiled lateral edges of the myelin sheath can be seen as cytoplasmic filled loops (see Figure 1). This region of the myelin sheath is known as the paranode, and the compact myelin region is referred as the internode (Figure 1a). The paranodal loops are anchored to the axolemma, tethering the myelin sheath to the axon. This axo-glial interaction is enabled through the presence of an adhesive protein complex consisting of Neurofascin-155 on the glial side, and contactin with contactin associated protein (Caspr) on the axonal side (Figure 1b) (reviewed by (Rosenbluth, 2009)). Using electron microscopy (EM), axo-glial junctions can be visualized as electron

dense bands known as transverse bands, forming septate-like junctions (Tao-Cheng et al., 1983). Furthermore, axo-glial junctions were shown to be molecular barriers separating voltage gated sodium channels at the node of Ranvier from the delayed rectifying potassium channels at the juxtaparanodes; enabling the regeneration of fast action potential conduction along the axon (Figure 1a) (Rios et al., 2003; Scherer, 1996; Waxman, 1980).

Early axonal demyelination is thought to be a critical underlying cause of the debilitating symptoms associated with MS (Dziedzic et al., 2010; Kuhlmann et al., 2002). Related to this, the disruption of paranodal junctions that anchor the internode of a mature myelin sheath to an axon has been identified as an early sign of demyelination around MS lesions (Wolswijk et al., 2003). Paranodal defects typically result in disorganization of these specialized axonal domains (Wolswijk et al., 2003). At the borders of MS lesions, diffusion of both Caspr and NF-155 paranodal markers can be detected along myelinated axons, indicating a possible destabilization of bound glial loops. This observation was also seen in areas where demyelination of other axons had already occurred. Howell et al. (2006) suggested that paranodal disruption could precede other disorganization of the axo-glial apparatus (Howell et al., 2006). Comparing the distribution of NF155 and node of Ranvier (nodal) marker NF186 in areas of demyelination and normal appearing white matter, they showed that inappropriately elongated distributions of NF155 overlap with both ion channels whereas NF186 remains appropriately clustered at the node (Howell et al., 2006). Only when NF155 was absent from paranodes did potassium channels at the juxtaparanode as well as NF186 and sodium channels at the nodes become elongated and disorganized. Thus, paranodal disruption and paranodal disorganization could precede demyelination in multiple sclerosis as it was shown that paranodal markers were present in cerebrospinal fluid of children with central nervous system inflammation (Dhaunchak et al., 2012)

The UNC5 family of proteins

1.1. First Descriptions of the UNC5 family

In 1974, Brenner sought to understand how to couple the underlying genetic makeup of a species to its behavior through the intermediate organization of intricate neural connections. By screening *Caenorhabditis elegans* ethyl methanesulphonate (EMS) induced mutants, he identified the mutants displaying defective stereotypical sinusoid like movements as "uncoordinated" (unc) mutants (Brenner, 1974). In several *unc-5* mutants, the phenotype was likely due to the absence of a dorsal nerve cord (Brenner, 1974). It was later elucidated that ventral motor neurons of *unc-5* mutants had aberrant projections running longitudinally rather than orthogonally to the epidermal ridges, which is required for dorsal nerve cord formation (Hedgecock et al., 1990). Molecular cloning and sequencing experiments subsequently revealed that the *unc-5* gene encoded a single pass transmembrane protein (Leung-Hagesteijn et al., 1992). Based on the various phenotypes observed, the UNC-5 protein, expressed in ventrally derived motor neurons, was speculated to be a receptor for *C. elegans* UNC-6, a laminin related protein expressed in neuroglia at the ventral midline (Chan et al., 1996). This interaction is presently known to be essential for proper ventral to dorsal projections of the axons of the ventral motor neurons (Chan et al., 1996; Hamelin et al., 1993; Ishii et al., 1992; Su et al., 2000). It was later validated that three identified vertebrate homologues of UNC-5, UNC5H1 and UNC5H2, as well as the rostral cerebellar malformation (RCM) protein, bind the well established guidance cue netrin-1 (UNC-6 homologue in vertebrates) (Kennedy et al., 1994; Leonardo et al., 1997; Mitchell et al., 1996; Serafini et al., 1994). Thereafter the RCM protein was renamed UNCH3 (Ackerman et al., 1997; Przyborski et al., 1998).

1.2. Structure of UNC5 proteins

Mammals express four orthologues of *C. elegans* UNC-5, UNC5A-D, also known as UNC5H1-4 respectively (Hata et al., 2009; Leonardo et al., 1997; Miyamoto et al., 2010; Round et al., 2007). These transmembrane receptors are part of the immunoglobulin superfamily of proteins and have been found to regulate cell motility, survival and adhesion (Freitas et al., 2008; Huber et al., 2003; Lu et al., 2015). Their extracellular domains are composed of two immunoglobulin (Ig) repeats and two thrombospondin type I domains, with the two Ig segments demonstrated to be netrin-1 binding sites (Geisbrecht et al., 2003). The cytoplasmic tail of all UNC5s contains a ZU5 domain, also found in proteins such as ankyrinB and tight junction protein 1 (ZO-1); proteins that are important for tethering membrane bound proteins to the cytoskeleton (Yasunaga et al., 2012), and for tight and adherence junctions formation respectively (Fanning et al., 1998; Ikenouchi et al., 2007; Kausalya et al., 2004; Lockwood et al., 2009). UNC5s also contain a death domain (DD) and a DCC binding and repulsive domain, also known as the UPA domain (Hata et al., 2009; Round et al., 2007). Furthermore, a crystal structure of UNC5B's cytoplasmic domain revealed that in the absence of a ligand, the ZU5-UPA-DD supramodule adopts an L-shaped closed conformation where the ZU-5 domain interacts with both the DD and UPA domains (see Figure 2) (Wang et al., 2009). Wang et al. (2009) further predicted that the closed conformation of UNC5B's cytoplasmic tail would inhibit its angiogenic activity. They additionally showed that its apoptotic activity was inhibited when expressed at normal levels. When overexpressed, however, its apoptotic activity was enhanced. The addition of netrin-1 to cells overexpressing UNC5B was shown to decrease its apoptotic activity, presumably by stabilizing the closed conformation of UNC5B (Wang et al., 2009).

1.3. Influence of UNC5s on cerebellar development

The study of vestibular mutants in rodents led to an unexpected discovery of a new class of mutants that was previously not characterized. The mutants displayed an unbalanced forward swaying motion as homozygous mutants were initially smaller than their WT counterparts; however, they generally lived a normal life span. Histological sections of the cerebellum also showed organizational disruption of a well delineated separation between the granule cell layer from the molecular layer by Purkinje cells (Lane et al., 1992). This organizational defect was predominantly found in the rostral cerebellar region, and was therefore named the rostral cerebellar malformation (RCM) recessive mutation (Lane et al., 1992). The RCM protein, shown to play a critical role in neuronal migration and cerebellum formation, (Ackerman et al., 1997; Eisenman et al., 1998; Leonardo et al., 1997) was demonstrated to be homologous with *C. elegans* UNC-5 (approximately 30% amino acid identity) (Ackerman et al., 1997) and the mouse UNC5A and UNC5B (approximately 40% amino acid identity) proteins (Engelkamp, 2002).

The expression of the transcription factors OTX2, HOXA2 and GBX2 is critical for the spatiotemporal definition of the developing cerebellum (Joyner et al., 2000; Wingate et al., 1999). However, the morphological and volumetric appearance of the cerebellum, defined later in postnatal development, is determined by the amplification of granule precursor cells found in the external germinal layer (EGL), thus forming the surface of the cerebellum (Goldowitz et al., 1998; Wang et al., 2001). The *Unc5h3*^{rcm} mutant mouse exhibited smaller cerebella and contained fewer folia when compared to controls (Ackerman et al., 1997), showing that proper migration of both granule precursors and GABAergic Purkinje neurons required the expression of UNC5C. As their tangential migration expands rostrally in lateral regions of the developing cerebellum, mutant mice displayed the ectopic presence of both granule and Purkinje cells in the inferior colliculus of the midbrain. Netrin-

1 expressed in the floor plate at the anterior region of the cerebellum was thought to delineate the rostral boundary of the cerebellum as it would induce chemorepulsion of these migrating cells (Ackerman et al., 1997; Przyborski et al., 1998). It was later shown *in vitro* that the association of UNC5C with DSCAM in external granule layer cells, induced growth cone collapse in response to a bath application of netrin-1 through the activation of Src Family Kinases (Purohit et al., 2012). This suggested a role for UN5C/netrin-1 signaling in granule and Purkinje cell migration (Kim et al., 2011; Purohit et al., 2012). It was additionally proposed that UNC5C and other UNC5 netrin receptors could regulate the terminal position of cerebellar interneurons at the different levels of cerebellar cortex (Purohit et al., 2012).

Mouse cerebellar explants co-cultured with EBNA-293 cells overexpressing netrin-1, displayed axons extending away from the netrin-1 secreting cells, in a DCC independent manner (Guijarro et al., 2006). *In vivo,* the trajectory of migratory GABAergic interneuron was also shown to be repelled by netrin-1, which is highly expressed in the EGL of the developing cerebellum (Guijarro et al., 2006). This influence of netrin signaling was suggested to be dependent of UNC5 receptors (Guijarro et al., 2006). These findings additionally corroborated the idea that short range repulsion by netrin-1 could be DCC independent (Keleman et al., 2001; Macneil et al., 2009).

1.4. Implication of UNC5 proteins in axon guidance

UNC-5 homologues have been shown to mediate netrin-1 induced repulsion of axonal growth cones in multiple species. In *C. elegans*, UNC-5 directs motor neuron axon migration from the ventral epidermal ridge of the nerve cord to the dorsal epidermal ridge (Hedgecock et al., 1990). In worms mutant for the DCC homologue UNC-40 however, some types of motor neurons, such as ventral D (VD) motor neurons, display abnormal migratory pathways (Hedgecock et al., 1990). It was later elucidated that a balance between UNC-5 and UNC-40 expression in VD neurons is required for an asymmetrical response to UNC-6, whereby

UNC-40 would promote growth cone attraction toward the ventral midline, while heterodimeric UNC-5/UNC-40 receptor complexes repel extending axons away from it (Norris et al., 2011). Similarly in *Xenopus* and *Drosophila*, DCC and the DCC orthologue Frazzled are necessary to mediate chemorepulsion of spinal neurons and dorsal Ap neurons, respectively (Colavita et al., 1998; Hong et al., 1999; Keleman et al., 2001; Merz et al., 2001).

UNC-5 homologues can also signal chemorepellent responses independently of UNC-40 and its orthologues. In *C. elegans*, UNC-5 mutants showed misguidance of the axons of ventral DA and DB motor neurons of the nerve cord, while initial misguided defects were not observed in UNC-40 mutants (Macneil et al., 2009). UNC-40 mutants nevertheless displayed misguided axons much further dorsally in the nerve cord. In *Drosophila*, neuronal overexpression of UNC-5 inhibits midline crossing of commissural axons that in control animals are attracted by netrin expressed at the CNS ventral midline (Keleman et al., 2001). Frazzled mutants generated in *Drosophila* overexpressing UNC-5 in commissural axons also prevented midline crossing, describing a Frazzled independent repulsion at short distances from a source of netrin (Keleman et al., 2001). Nonetheless, UNC-40 and Frazzled are necessary for long-range chemorepulsion in *C. elegans* and *Drosophila* respectively, as they are needed to increase the sensitivity of the response of these axons to a progressively lower concentration of UNC6/netrin (Keleman et al., 2001; Macneil et al., 2009).

In *Xenopus*, evidence was provided that an interaction between the DCC P1 domain and UNC5B DCC binding domain (UPA) (see Figure 2.) is required to switch DCC chemoattraction to netrin-1 to chemorepulsion (Hong et al., 1999). The transmembrane and intracellular domains of UNC5B were shown to be sufficient to elicit a switch towards chemorepulsion, operating with DCC (Hong et al., 1999). Together, these findings provide evidence that UNC5 homologues have the capacity to signal chemorepellent responses to a

source of netrin-1, in some cases as a DCC/UNC5 homologue receptor complex, and in others in the absence of a DCC orthologue.

The first study that described an UNC5 axonal guidance function in vertebrates, involved the investigation of the *Unc5h3*^{rcm} mutant and its implication in aberrant axonal projections in the CNS. Layer V neuron corticospinal tracts normally decussate prior to entering the spinal cord. In *Unc5h3*^{rcm} mutant mice, anterograde tracing showed that the axon bundle splits as one half continues ipsilaterally and the other crosses the midline (Finger et al., 2002). The decussating fibers would normally turn dorsally to enter the ventral most region of the dorsal funiculus, however these fibers fail to turn in these mutants (Finger et al., 2002; Joosten, 1990). This suggests that UNC5C enables a chemorepulsive response towards the ventral midline most likely independently of both DCC and netrin-1 expressed at the ventral midline (Finger et al., 2002).

Studying the innervation defects present in *Unc5c* null mice of different genetic backgrounds elucidated additional functions for UNC5C in motor axon guidance (Ackerman et al., 1997; Burgess et al., 2006; Finger et al., 2002; Goldowitz et al., 2000). Inbred mice on a C57BL/6J (B6) background die when they are born due to breathing complications, whereas mice with a hybrid B6 and SJL background live normally (Burgess et al., 2006). It was shown that in the B6 background, there were mis-projections of the trochlear nerve as well as a severely reduced phrenic innervation to the diaphragm. Normal axonal projections in netrin-1, DCC and neogenin mutants showed that this phenotype occured independently of these proteins (Burgess et al., 2006).

Other studies however confirmed roles for netrin-1 and DCC in UNC5 homologue mediated axon guidance. During the formation of the dorsal funiculus of the spinal cord, dorsal root ganglion (DRG) cells enter the spinal cord through the dorsal root entry zone, and initially stall due to dorsal expression of netrin-1. In both netrin-1 and *unc5h3* mutant mice,

DRGs display premature and aberrant axonal projections (Watanabe et al., 2006). Similarly, the mutation of UNC5C, netrin-1 and DCC in spinal accessory motor neurons (SACMN) all impair dorsal migration of these cells away from the ventral midline expression of netrin-1 in the cervical spinal cord. Thus, instead of being adjacent to the lateral exit point allowing the formation of the spinal accessory nerve bundle, they are found at the ventrolateral region of the spinal cord (Dillon et al., 2007; Snider et al., 1990). The netrin-UNC5C/DCC signaling system also extends to the formation of the corpus callosum. More specifically, an elegant study has shown that cultured coronal brain slices from UNC5C electroporated wild type mouse embryos, positively labeled callosal that fibers mis-projected to the ipsilateral hemisphere when netrin-1 coated beads were occupying the callosal midline. More specifically, ectopic expression of UNC5C in mice lacking *Satb2*, a transcription factor that positively regulates UNC5C expression, resulted in a partial rescue of the acallosal phenotype present in these mice (Srivatsa et al., 2014). A recent study by Murcia-Belmonte et al. (2019) has also described a function for UNC5C during the development of the visual system. UNC5C is known to be expressed by a subset of retinal ganglion cells (RGC), for which the axons appear to project from one retina to the other (R-R projection). Mice knocked-out for UNC5C or expressing ectopically Zic2, a transcription factor that represses UNC5C in RGCs, fail to form the contralateral retinal connection (Murcia-Belmonte et al., 2019). These axons are thought to be repelled by netrin-1 enriched at the ventral optic chiasm (Murcia-Belmonte et al., 2019). During evolution, this transient connection is thought to be important for synchronization of both retinal waves to different areas in the brain in order to ensure proper axonal refinement that ultimately giving rise to stereoscopic vision (Godement et al., 1984; Lemke et al., 2005).

Furthermore, UNC5C not only contributes to cerebellar development but is also an axonal guidance receptor that contributes to hindbrain formation. In UNC5C null mice, cell

and axonal guidance defects were seen in the medullary precerebellar neurons as well as in hook bundles of the medial deep cerebellar nuclei, an important output innervating different parts of the brain stem (Fink et al., 2006; Kim et al., 2011). Neurons that make up precerebellar nuclei, such as the inferior olivary (IO) nucleus, migrate to the ventral medulla, where their axons cross the midline; however, in UNC5C null mice, these axons fail to project dorsally and instead turn immediately rostrally towards the cerebellum. This is also the case for the axons of pontine neurons that project laterally towards the cerebellum, however in UN5C null mice, this regular axon tract was absent. Unlike both the IO neurons and PN that eventually have their axons reach the cerebellum, albeit by an unconventional route, axons from precerebellar external cuneate nucleus degenerate and fail to innervate the cerebellum. Additionally, cerebellar commissures that normally cross dorsally at the midline of the cerebellum, instead project ipsilaterally to the mesencephalic floor plate in UNC5C null mice (Kim et al., 2011).

Neuronal migration defects have been described for paralogues of UNC5C. For instance, the ectopic expression of UNC5A in primary mouse spinal cord neurons results in axon repulsion in response to netrin-1 coated beads *in vitro*, yet only when co-expressed with DCC. That result indicates that netrin-1-induced chemorepulsion occurs through UNC5A in a DCC dependent manner in this cell type (Finci et al., 2015). Moreover, a previously unidentified RNA sequence, *svet1*, that was specifically expressed in the subventricular zone in the developing cerebral cortex, was shown to play an essential role in the tangential migration of multipolar cells that would populate the cortical plate and superficial layer. The suppression of *Svet* in mutant mice resulted in a reduced population of migrating cells in both the cortical plate and the superficial layer (Tarabykin et al., 2001). It was later shown that *svet1* corresponds to an intronic region of UNC5D, a receptor described in multipolar cells

(Sasaki et al., 2008), pointing toward a contribution of UNC5D in multipolar cell migration during cerebral cortex development.

1.5. Importance of UNC5B for vascularisation

Very much like axonal growth cones, endothelial tip cells, found at the leading edge of sprouting blood vessels, enable the process of angiogenesis by reacting to a series of environmental molecular cues through ligand/receptor binding (Gerhardt et al., 2003; Isogai et al., 2001; Shibuya, 2006). UNC5B is expressed by endothelial cells in the mouse embryo at ~E8.5 (Engelkamp, 2002; Navankasattusas et al., 2008). *In situ* hybridization for *Unc5B* revealed early expression predominant in arteries, endothelial tip cells, and capillaries surrounding the vascular plexus (Lu et al., 2004). Studies with UNC5B deficient mouse embryos showcased an increase of arterial and capillary branching. The authors speculated that this phenotype lead to increased blood flow resistance, explaining the death of these mice by heart failure at embryonic day 12.5 (Lu et al., 2004). UNC5B regulation of vascular branching was furthermore shown to be dependent on netrin-1 signaling *in vitro* and *in vivo*. For instance, exposing the human umbilical artery endothelial cell (HUAEC) line to a gradient of netrin-1 resulted in UNC5B-dependent filopodial tip retraction (Lu et al., 2004). Additionally, intra-ocular injection of recombinant netrin-1 in mice resulted in an UNC5B dependent reduction of filopodial extension of endothelial tip cells (Lu et al., 2004). This netrin/UNC5B dependent phenotype was also shown to be conserved in chick and zebrafish (Bouvrée et al., 2008; Lu et al., 2004), confirming the anti-angiogenic nature of UNC5B. Conversely, a later study displayed evidence of UNC5B being a pro-placental arteriogenic factor, as conditional deletion of UNC5B in mouse endothelial cells resulted in reduced arterioles in the placental labyrinth (Navankasattusas et al., 2008), the region of nutrient and gas exchanges between the mother and the embryo (Rossant et al., 2001). The reduction of

arterial branching led to an increase in blood flow resistance, resulting in hypoxia and ultimately embryonic lethality (Navankasattusas et al., 2008). The seemingly opposing results of these studies, attraction verses repulsion, was suggested to arise from different methods used for UNC5B deletion and from the different genetic backgrounds in which they were conducted (reviewed by Larrieu-Lahargue et al., 2012); however this discrepancy is still not fully understood. A recent publication elucidated that fibronectine leucine-rich transmembrane protein 2 (FLRT2), a known UNC5B ligand, was additionally present in the placental labyrinth endothelia (Tai-Nagara et al., 2017). The interaction of FLRT2 with UNC5B mediates endothelial cell repulsion, thus allowing proper cell alignment and enabling uteroplacental nutrient and gas exchanges (Tai-Nagara et al., 2017).

The function of UNC5B in endothelial cells is not limited to the developmental stage of an organism. In adulthood, the vasculature stabilizes and endothelial cells are in a quiescent state and express a greatly reduced amount of UNC5B protein (Larrivée et al., 2007; Lyden et al., 1999). However, in the context of pathological neo-angiogenesis such as tumorigenesis or vascular endothelial growth factor (VEGF) induced angiogenesis, an upregulation of UNC5B expression occurs in surrounding arteries and capillaries (Larrivée et al., 2007). Subcutaneous xenografts of human tumor cells overexpressing netrin-1 in nude mice exhibited delayed tumour growth. More specifically, *in situ* hybridization of the *Unc5b* expressing vasculature surrounding control or netrin-1 overexpressed transduced tumor cells were studied. In the netrin-1 overexpressing tumour cells, the vessels expressing UNC5B remained at the periphery of tumours, thus preventing nutrient delivery (Larrivée et al., 2007).

Despite netrin-1 displaying anti-angiogenic properties, the literature remains controversial over the anti- or pro-angiogenic nature of netrin-1 (Kye et al., 2004; Larrivée et al., 2007; Lu et al., 2004; Navankasattusas et al., 2008; Wilson et al., 2006). More recent

studies argue that netrin-1 is a bifunctional angiogenic cue. In attempting to settle the controversy, a study investigated the propensity of netrin-1 in influencing endothelial cell survival using the dependence receptor model. In the absence of netrin-1, UNC5B induced apoptosis of endothelial cells, supporting previous findings of increased branching vasculature in UNC5B deficient mice, and phenotypes observed in zebrafish having netrin-1a silenced (Castets et al., 2009). At low concentrations of netrin-1, a receptor named CD146 also known as melanoma cell adhesion molecule (MCAM), was discovered to bind netrin-1 with greater affinity than UNC5B, thus giving netrin-1 its pro-angiogenic role. However, higher concentrations of netrin-1 bound UNC5B and inhibited angiogenesis. It was suggested that netrin-1/UNC5B interaction may negatively regulate CD146 signaling (Tu et al., 2015). Although netrin-1's impact on vasculature remains controversial, there seems to be a general consensus that UNC5B is anti-angiogenic. Other molecular mechanisms apart from netrin-1 signaling indeed corroborated UNC5B`s role. For instance, UNC5B and UNC5C were shown to inhibit the formation of vascular-like tubules in VEGF stimulated HUAEC cells overexpressing netrin-4 and neogenin (Lejmi et al., 2008). This was dependent upon netrin-4 binding neogenin and recruiting UNC5B. Silencing netrin-4 had no effect on quiescent endothelial cells, indicating that netrin-4 and UNC5B function primarily during angiogenesis as a negative feedback response. Besides, the extracellular domain of UNC5B was shown to indirectly inhibit VEGF signaling by binding Roundabout receptor 4 (Robo4), a receptor specifically expressed in vascular endothelial cells and known to counteract VEGF induced angiogenesis (Koch et al., 2011). Further experiments confirmed a requirement for UNC5B in inhibition of Robo4 angiogenic sprouting and blood vessel integrity (Koch et al., 2011). These findings suggested that a medical treatment based on Robo4 might be a possible pathological anti-angiogenic treatment.

1.6. UNC5 expression and function in rodent CNS white matter

During brain development, glial precursor (GP) cells originating from the floor of the third ventricle migrate toward the retina along the optic nerve (Castro et al., 2013). Guidance cues, including netrin-1 and semaphorin 3A, were found to be expressed in the region of the optic chiasm. An *in vitro* study revealed that newborn rat cultured GP cells originating from the optic chiasma/nerve tract were repelled by local sources of netrin-1 (Sugimoto et al., 2001). Moreover, *in situ* hybridization revealed that NG2 positive (NG2+) GP cells express the netrin receptor UNC5A (Sugimoto et al., 2001), implicating netrin signaling in GP cells migration away from the optic chiasm. However, a different study showed in a similar *in vitro* migration assay that NG2+ and A2B5+ Oligodendrocyte Precursor Cells (OPC) from mouse embryonic day 16.5 (E16.5) were attracted to a source of netrin-1 (Spassky et al., 2002). *In situ* hybridization analysis provided evidence for an age-related shift in UNC5H1 (UNC5A) expression; only at later stages of OPC migration (postnatal day 5) in the optic nerve (ON) did the percentage of UNC5H1 expressing OPCs increase. Thus, it was hypothesized that a source of netrin-1 found at the ON/retina junction guides OPCs towards the retina at early developmental stages, whereas OPC expression of UNC5H1 at later stages would then halt their migration, preventing OPC entry into the retina.

The Kennedy lab reported that *netrin-1* is expressed in the white matter of the adult rat spinal cord using *in situ* hybridization. Through immunolabeling and *in situ* hybridization, netrin-1 protein was shown to be expressed by oligodendrocytes and enriched in periaxonal myelin, a region of non-compacted oligodendrocyte membrane (Manitt et al., 2001). A developmental shift in the relative levels of expression of netrin receptors was detected via western blotting brain and spinal cord homogenates during maturation and aging, whereas these receptors were also shown to be expressed in the white matter of the adult mammalian spinal cord using *in situ* hybridization (Manitt et al., 2004). High levels of DCC expression

were indeed detected during embryonic stages of development, while UNC5H2 expression was relatively low (Manitt et al., 2004). Inversely, UNC5H2 was upregulated in the adult CNS while DCC was downregulated. This was corroborated with *in situ* hybridization, revealing relatively faint signals for UNC5H1 (UNC5A), UNC5H3 (UNC5C) and DCC but robust signals for UNC5H2 (UNC5B) in sections of adult rat spinal cord white matter (Manitt et al., 2004).

Netrin-1 is also expressed by floor plate cells in the neural tube during developmental stages, where it acts as a repellent for OPCs migration away from the ventral ventricular zone. These OPCs expressing DCC and UNC5A migrate dorsally in the neural tube (Jarjour et al., 2003). In DCC or netrin-1 null mouse embryos, a large number of OPCs fail to migrate dorsally (Jarjour et al., 2003). Nonetheless, aberrant migration of OPCs was not investigated in UNC5A null embryos.

UNC5B is more prominent in the white matter of the adult rat spinal cord than any other UNC5 protein (Manitt et al., 2004). Investigating this, the Kennedy lab reported an enrichment of UNC5B protein at the paranodes of mature myelin sheaths (de Faria Jr., 2015). Interestingly, despite not being essential for myelin formation, UNC5B appeared critical for paranode maintenance and organization. Indeed, conditional deletion of UNC5B revealed little to no phenotypic impact on paranodes of 3 month-old mice, yet substantial paranodal disruption was visible in 9 month-old UNC5B cKO mice with detached, everted paranodal loops and reduced interloop densities (de Faria Jr., 2015). Similar, but not entirely overlapping, phenotypes were previously found *in vivo* and *in vitro* in DCC cKO mice (Bull et al., 2014; Jarjour et al., 2008). Among the distinct phenotypes detected, the apparent fragmentation of junctions made between paranodal loops was unique to UNC5B cKO but not DCC cKO mice. We speculate that this defect could be the result of tight junction radial components inappropriately invading paranodal loop-loop adhesions

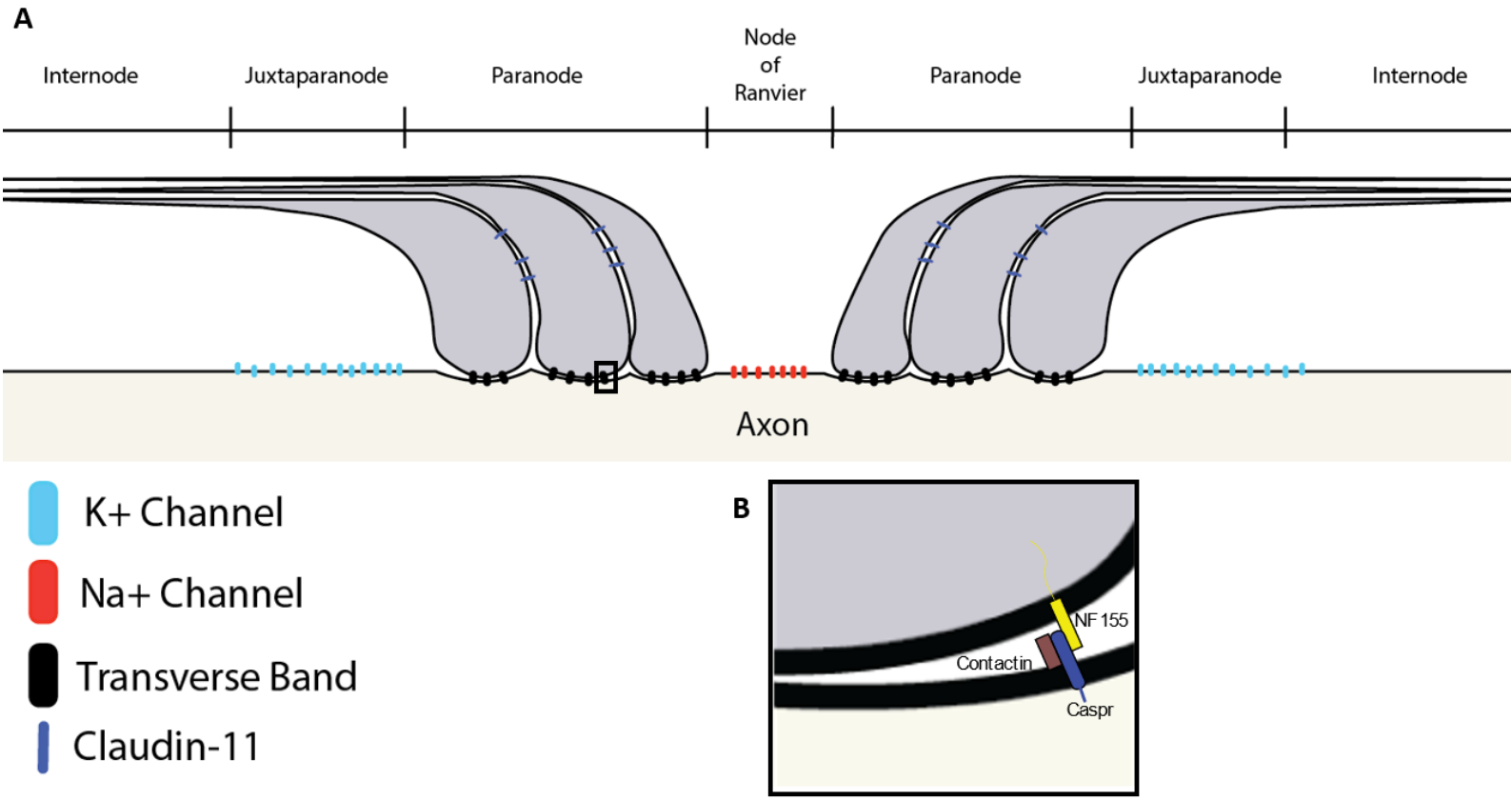

Figure 1. Paranodal domain organization.
(**A**) Depiction of a longitudinal, cross-section of a myelinated axon displaying the termination of two adjacent myelin sheaths. The cytoplasm of the multi-lamellar myelin sheath is extruded to the lateral edges of the myelin sheath upon myelin compaction. The formation of a coiled cytoplasmic channel at the edges is seen here as cytoplasmic filled loops termed paranodal loops. These loops are anchored to the axolemma through the intermediate of an adhesive protein complex consisting of oligodendroglial NF155 and axonal contactin and caspr/paranodin; all essential components required for appropriate paranode organization (**B**). This protein complex can be seen as electron dense transverse bands with EM giving the appearance of ladder-like junctions consequentially termed axo-glial septate-like junctions. Autotypic tight junctions are also found between paranodal loops consisting of claudin-11/OSP protein complexes. The paranode also acts as a molecular barrier separating potassium channels at the juxtaparanodes from the cluster of sodium channels present in the node of Ranvier, allowing the regeneration of the axonal nerve impulse.

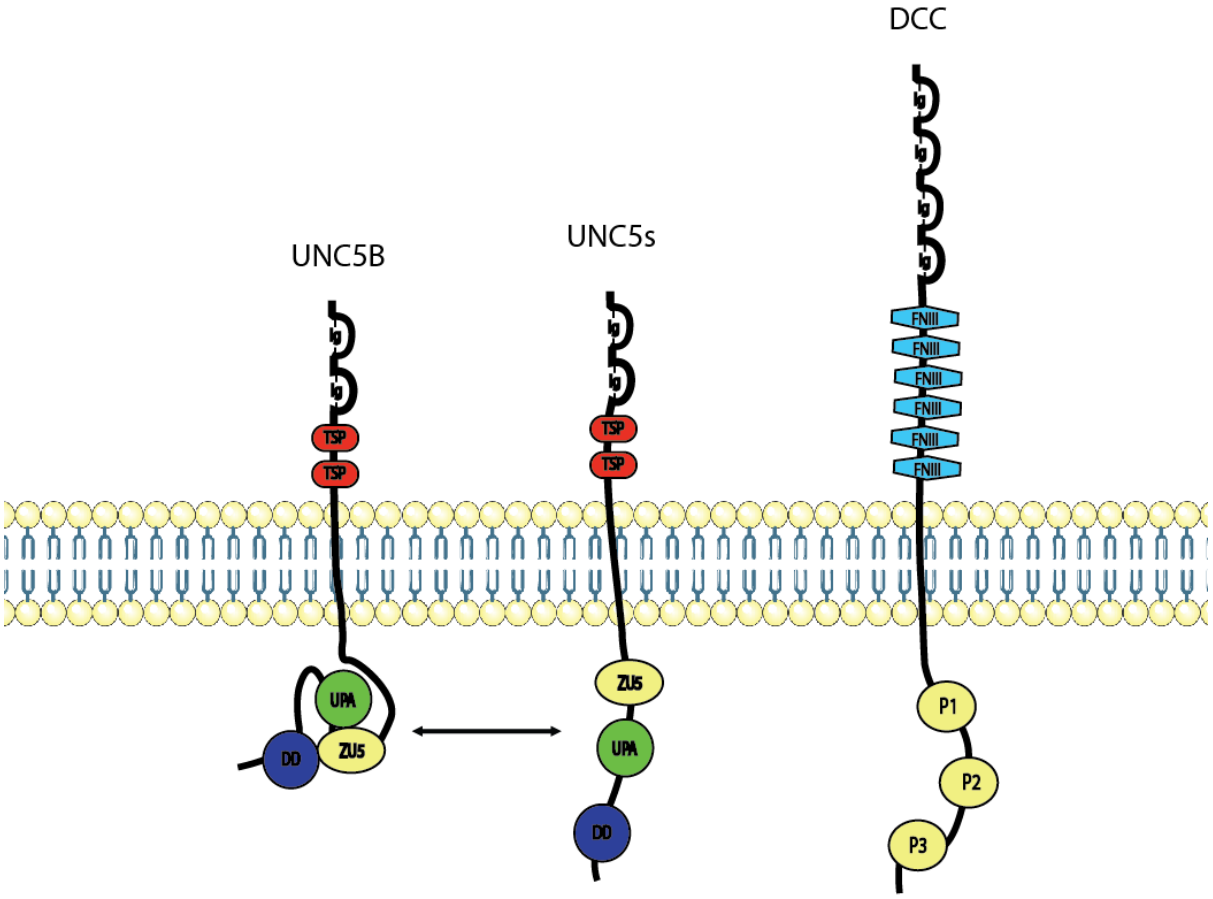

Figure 2. UNC5 homologues and DCC netrin receptors.
In vertebrates, UNC5 homologues and DCC are receptors for netrin-1, a member of the laminin superfamily, primarily known for its role as an axonal guidance cue. Both receptors are part of the immunoglobulin superfamily. Four UNC5 homologues are expressed by mammals, initially named UNC5H1-H4, but more commonly now called UNC5A-D. In the absence of netrin binding, UNC5B is thought to adopt an open conformation within its cytosolic tail allowing the recruitment of proteins enabling downstream signaling. However, netrin binding is thought to stabilize closed conformation as the UPA and DD of UNC5B both interact with the ZU5 domain, adopting an L-shaped closed conformation that prevents signaling, such as activation of apoptosis. DD: Death Domain, FNIII: Fibronectin type 3 domain, Ig: Immunoglobulin domain, P1-3, three domains that are conserved, TSP: Thrombospondin type-1 domain, UPA: conserved domain found in UNC5s, Ankyrins and p53-induced protein with a death domain (PIDD), ZU5: domain named after ZO-1 and *C. elegans* UNC-5 also present in Ankyrins.

MATERIALS AND METHODS

i) Animals

All procedures that involved the use of animals were done according to the Canadian Council on Animal Care guidelines for the use of animals in research and approved by the McGill University Animal Care Committees. Mice carrying a floxed allele of UNC5B were supplied by Dr. Susan Ackerman of the Jackson Laboratories. In this mouse line, flanking lox sites have been engineered around exon 5 of the *unc5b* gene. The Olig2-Cre mouse line (Dessaud et al., 2007) was obtained from Jackson Laboratories.

ii) Antibodies

The following primary antibodies were used: Cell Signaling Technology, rabbit anti-MBP (myelin basic protein) (D8X4Q) (1:150, #78896) and rabbit anti-UNC5B (D9M72) (1:1000 #13851); Thermo Fisher Scientific, streptavidin Alexa fluor 488 conjugate (1:1000 # S-11223) and mouse anti zo-1 (1A12) (1:1000 #339100); Neuromab, mouse anti CASPR/paranodin (1:150 # 75001); R&D Systems, mouse anti human occludin (1:1000 #690213); Sigma-Aldrich, mouse anti-Flag M2 (1:1000 and 1:500 for western blot and immunocytochemistry respectively, #F3165); Developmental Studies Hybridoma Bank, mouse anti DLG1 (1:1000 # AFFN-DLG1-4D6).

iii) Generation of the UNC5B-BirA-Flag fusion protein

To generate the UNC5B-BirA-Flag fusion protein, all subcloning techniques were carried out using Gateway® cloning technology (Invitrogen). The polymerase chain reaction (PCR) was used to amplify the coding sequence of rat *unc5b* (NCBI gene ID: 60630) and incorporate *att*B recombination sites. The following PCR primers were used.

Forward primer:

5’GGGGACAAGTTTGTACAAAAAAGCAGGCTCCACCATGGAGACAGACACA-3’

Reverse primer:

5’GGTACTGGTGACTACCGCTAACGCTGGGTCGAAAGAACATGTTTCACCAGGGG-

3’. Amplified *unc5b-attB* cDNA was purified using the Wizard® SV Gel and PCR Clean-Up System (Promega, A9281) and cloned into the pDONR221 vector using the BP clonaseII. A final recombination reaction between the *unc5b-attB* pDONR221 plasmid and the pcDNA5-pDEST-BirA-Flag-C-Terminal vector using the LR clonase generated the UNC5B-BirA-Flag fusion cDNA. Clones were validated by DNA sequencing.

iv) Generation of inducible BirA-GFP-Flag and UNC5B-BirA-Flag Flp-In T-REx HEK 293 cell lines

The Flp-In™ T-REx™ HEK 293 cell line was co-transfected in 6 well dishes with lipofectamine 2000 (Invitrogen, 11668-019) using 200 ng of the pcDNA5-UNC5B-BirA-Flag fusion plasmid and 2 µg of the pOG44 plasmid and grown overnight (ON). Cells were subsequently transferred to and expanded in 10 cm dishes, and grown in Dulbecco’s Modified Eagle Medium (DMEM) with 10% Fetal bovine Serum (FBS). On the following day, stably transfected HEK293 cells were selected in selection media, DMEM, 10% FBS and 200 µg/ml of Hygromycin B (Invitrogen, 10687-010), over the next few weeks. Monoclonal colonies present within the dish were picked, transferred and expanded in 24 well dishes. Monoclonal colonies were further expanded to 10 cm dishes and frozen for further validation.

v) Tissue collection

Generation and validation of Olig2-Cre UNC5B flox conditional knock out transgenic mice was done by Dr. Omar de Faria Jr. (de Faria Jr., 2015). Transcardiac perfusion, brain fixation and generation of coronal 20 µm thick sections was done by Dr. Omar de Faria Jr. (de Faria Jr., 2015). Slides were stored at -80º C.

vi) Immunocytochemistry

Cells cultured in DMEM with 10% FBS were fixed with 2% PFA and 10% sucrose for 10 min at 37º C. Plates were then chilled on ice for an additional 10 min. Each well was rinsed twice with 1X PBS and then stored in PBS at 4º C until use. For immunolabeling, cells were

permeabilized with 0.3% Triton X-100 in PBS for 10 min at rt. Blocking buffer (5% Bovine Serum Albumin (BSA), 0.1% triton X-100 in PBS) was then added in each well for 30 min at rt. Cells were then incubated with primary antibodies diluted in 3% BSA, 0.1% triton X-100 in PBS ON at 4º C. The next day, cells were washed three times with PBS and incubated with the appropriate Alexa 488 and 555-conjugated secondary antibodies in 3% BSA PBS for 1 hr at rt, washed three times with PBS and stained with Hoechst (1:1000 in PBS) to mark nuclei. Coverslips were quickly dipped in distilled water and mounted on glass slides using fluorogel (Electron Microscopy Sciences). For immunocytochemistry (ICC) experiments that were completed in a single day, cells were incubated with primary antibodies for 1 hr at rt.

vii) Immunohistochemistry

Slides with mounted tissue sections were thawed at rt and washed twice with PBS. Tissues were incubated in blocking buffer in a humidifying chamber for 1 hr at rt. Primary antibodies diluted in 3% BSA, 0.1% triton X-100 in PBS were added to tissue sections and incubated in a humidified chamber overnight at 4º C. Slides were then processed as described for the immunocytochemistry experiments.

viii) Western blot and immunoprecipitation

To validate the cell lines, the inducible BirA-GFP and UNC5B-BirA overexpressing cells were grown in six well dishes and lysed in RadioImmunoPrecipitation Assay (RIPA) buffer (10 mM sodium phosphate pH 7.2, 150 mM NaCl, 1% NP-40, 0.5% sodium deoxycholate and 0.1% SDS) containing a protease inhibitor cocktail tablet EDTA-free (Roche, 11873580001) with 50 mM EDTA pH 8.0, 1 mM Na_3VO_4, 1 mM PMSF and 5 mM of NaF. Cells were scraped in RIPA buffer and lysed by pulsing them up and down 50 times in a 1.5 mL Eppendorf tube before chilling on ice for 10 min. They were subsequently centrifuged at 11,000 x g for 5 min to pellet insoluble material and collect the soluble lysate. A bicinchoninic acid assay (BCA, Thermo Fisher Scientific, 23227) was performed to

determine the concentration of protein in each sample in order to load equal amounts of protein in each lane of a polyacrylamide gel. Proteins were separated using SDS-PAGE and then further transferred onto 0.45 µm pore size nitrocellulose membranes by tank (wet) electrotransfer (Bio-Rad). Blots were blocked with 3% milk in tris buffered saline tween (TBST) for 1 hr at rt and primary antibodies were applied ON at 4º C with gentle shaking. Blots were rinsed and washed 3 times in blocking buffer and secondary HRP conjugated antibodies at a 1:10,000 dilution were applied and incubated for 1 hr at rt. Blots were then washed 3 times in TBST, followed by three washes in TBS, and immunoreactivity then developed using a Chemiluminescence kit (Pierce) and X-ray films (Carestream).

For co-immunoprecipitation with the UNC5B-BirA-Flag fusion protein, cells were seeded at ~300,000 cells per well in 6 well plates. On the following day, the cultures were induced overnight with 1 µg/mL of tetracycline hydrochloride (Sigma- Aldrich T7660). Following overnight induction, the wells were washed once with PBS and lysed with 150 µl of either RIPA buffer, 1% triton buffer (1% Triton X-100, 2 mM EGTA pH 8.0, 1 mM MgCl2, 2 M Glycerol, 50 mM KCl in 10 mM HEPES pH 7.6), 1% triton and 1% NP-40 buffer or 0.1% NP-40 buffer (0.1% NP-40, 150 mM NaCl, 5 mM of EDTA pH 8.0 in 50 mM HEPES pH 7.6). Cell lysates were then precleared with 30 µl of 50% protein-G plus-agarose bead slurry (Santa Cruz Biotechnology sc-2002) for 30 min on a rotator at 4º C. Beads were pelleted by centrifugation at 250 x g for 2 min and supernatant collected. Samples were separated so that 2 µg of Flag M2 antibody was added for the IP fraction and 2 µg of mouse IgG control was added for the control fraction. Samples were incubated on a rotator for 4 hr at 4º C. A bead slurry, 30 µL of 50% dilution were added to each fraction and incubated for an additional hr at 4º C on a rotator. Beads were then pelleted at 250 x g for 2 min and cycled through a wash with lysis buffer and pelleted at 250 x g for 2 min. The pellet was then resuspended in lysis buffer and the pelleting-wash process repeated three times. Proteins were eluted from the

beads and denatured by the addition of Laemmli buffer heating to ~98º C for 5 min. Lysates were flash frozen in liquid nitrogen and stored at -80º C until processed by western blot.

ix) Streptavidin bead pull down assay

BirA-GFP and UNC5B-BirA overexpressing cells were cultured in 15 cm dishes and grown to ~95% confluency to insure cell-cell junction formation. The BioID assay was performed whereby 1 µg/ml of tetracycline and 50 µM of Biotin (Sigma-Aldrich B4639) were added to the culture. Additional conditions consisted of incubating both cell lines with 200 ng of netrin-1 ON.

Streptavidin pull-down was performed following the BioID assay in order to validate the BirA functionality. 30 µg of protein from cell lysates were incubated with 2 µL of prewashed streptavidin agarose resin (Thermo Fisher Scientific 20349) and incubated on a rotator for 2 hr at 4º C. Beads were pelleted at 1500 x g for 20 sec and washed twice with RIPA buffer. To insure that biotinylated proteins were eluted from the beads, samples were boiled and cycled through a vortex mix and centrifugation 3 times before storing samples at -80º C.

x) Silver staining prior to Mass Spectrometry

A tenth of each streptavidin bead sample was analyzed by PAGE followed by silver staining to assess the quantity and sufficiency of biotinylated proteins prior to mass spectrometry analysis. Following protein separation by SDS PAGE, gels were then fixed ON at rt in 50% methanol (MeOH). The following day, the gel was then washed twice in water followed by a 1 hr incubation on a shaker at rt in silver nitrate solution (1% AgNO3 (w/v), 60% MeOH, 1.8% Ammonium hydroxide and 0.01% NaOH). The gel was washed twice in distilled water and the silver precipitated with a quick incubation with 100 mM of NaCl at which point the gel was submerged in developing solution (0.005% citric acid (w/v) and 0.05%

formaldehyde) for 30 min. Once bands were visible on the gel, the reaction was stopped with 50% MeOH.

xi) Protein sample preparation and analysis

Following the BioID assay, cells were gently scraped in PBS, pelleted at 200 x g for 5 min, then frozen on dry ice and stored at -80º C until further use. On the day of sample preparation, pellets were thawed at 4º C on a rotator, each containing 1 mL of RIPA buffer with protease, phosphatase inhibitors and 10 µg/mL of DNAse I (Sigma-Aldrich, DN25-100mg). Cells were then sonicated on ice (three bursts of 5 seconds with 3 second rests in between at 15% amplitude) using a Bronson SFX250 Sonifier cell disruptor. Cellular debris were spun into a pellet by centrifugation at 11,000 x g for 30 min at 4º C. Cell lysates were collected and streptavidin beads added according to the volume remaining so that 50 µL of beads were added per 1 mL volume and incubated at 4º C on a rotator for 2 hr. Beads were pelleted at 1500 x g for 20 sec and washed three times with RIPA buffer. Three additional washes with ammonium bicarbonate were made before the beads were further stored in ammonium bicarbonate pH 7.8 at -20º C until shipping for mass spectrometry analysis.

Protein samples were further analyzed by the Clinical Proteomics Platform at the RI-MUHC. Briefly, each sample containing washed beads with attached proteins were loaded onto a single stacking gel band to remove lipids, detergents and salts. The single gel band containing all proteins was reduced with DTT, alkylated with iodoacetic acid and digested with trypsin. Extracted peptides were re-solubilized in 0.1% aqueous formic acid and loaded onto a Thermo Acclaim Pepmap (Thermo, 75uM ID X 2cm C18 3uM beads) precolumn and then onto an Acclaim Pepmap Easyspray (Thermo, 75uM X 15cm with 2uM C18 beads) analytical column separation using a Dionex Ultimate 3000 uHPLC at 250 nl/min with a gradient of 2-35% organic (0.1% formic acid in acetonitrile) over 3 hours . Peptides were analyzed using a Thermo Orbitrap Fusion mass spectrometer operating at 120,000 resolution

(FWHM in MS1) with HCD sequencing (15,000 resolution) at top speed for all peptides with a charge of 2+ or greater. The raw data were converted into *.mgf format (Mascot generic format) for searching using the Mascot 2.6.2 search engine (Matrix Science) against human protein sequences (Uniprot 2019). The database search results were loaded onto Scaffold Q+ Scaffold_4.9.0 (Proteome Sciences) for statistical treatment and data visualization.

xii) Imaging, quantification and statistical analysis

ICC slides were imaged using a Zeiss Axiovert S100TV and cryosections imaged using a Leica SP-8 confocal microscope. Internode length was quantified by visualizing and measuring MBP labelling that was flanked by Caspr immunofluorescence. Paranodal lengths were measured according to Caspr immunofluorescence and a presumptive node was quantified by measuring the gap between two adjacent Caspr bands. Knock outs were compared to wildtype age matched littermates. Two-tailed Mann-Whitney test; ** $p < 0.001$. A total of approximately 80 internode measures were made from 3 mice of each phenotype.

Western blots and ICC for the validation of both BirA-GFP and UNC5B-BirA overexpressing cells as well as Western blots for Un5B-BirA co-immunoprecipitation and DLG1 protein validation were assessed using Fiji (Schindelin et al., 2012). Images of western blot immunoreactivity on film were scanned and converted to 8-bit gray scale. Following mass spectrometry, identified proteins were quantified and compared between samples using spectral counts in Scaffold_4.9.0. An initial screen was performed with a one-way Analysis of Variance (ANOVA) on the normalized spectral counts between conditions, which each contained a technical replicate of 3. A refined list of proteins having an increase of spectral counts in the UNC5B-BirA conditions compared to their appropriate BirA-GFP controls, as well as other proteins of interest, were kept and further analyzed. Additionally, the identified proteins were kept only if the replicate of any condition containing the highest count had a minimum of 4 spectra. Using GraphPad Prism 6, Sidak`s multiple comparison tests were

applied to selective comparisons involving the UNC5B-BirA conditions with their appropriate control, * $p < 0.05$, ** $p < 0.01$ and *** $p < 0.001$ as well as comparisons between both UNC5B-BirA conditions and between both control conditions, # $p < 0.05$.

RESULTS

BirA-GFP-Flag and UNC5B-BirA-Flag Flp-In T-REx HEK 293 cell line validation:

The BioID proximity labeling assay screens for protein candidates that interact with a bait protein. In the version of the assay used here, UNC5B-BirA was overexpressed in an inducible stable cell line, generating a sufficient quantity of biotinylated proteins for mass spectrometry analysis. To identify candidate proteins that may specifically interact with UNC5B, a control cell line (BirA-GFP) expressing BirA linked to GFP was also made.

Prior to performing the BioID assay, it was critical to validate the cell lines. Cells were seeded on glass coverslips for ICC or in 6-well plates for Western blot analysis and expression of the transgene induced ON with 1 µg/ul of tetracycline hydrochloride. Following fixation, cells were immunocytochemically labeled with a mouse anti-flag M2 antibody to visualize the induced protein. In both the BirA-GFP and the UNC5B-BirA cell lines, fluorescence in non-induced conditions was undetectable compared to the induced conditions (Figure 3). This was further confirmed using the mouse flag M2 antibody for Western blot analysis of the UNC5B-BirA cell line. It was also important to confirm that BirA did not impede proper trafficking of UNC5B-BirA to expected regions of the cell, such as the plasma membrane. UNC5B is a transmembrane protein and using ICC, we detected UNC5B at intercellular junctions, delineated by apposed cell membranes (Figure 3). We conclude that transgene expression is successfully induced in the cell line, and that the ectopic UNC5B protein is detected at expected locations within the cell.

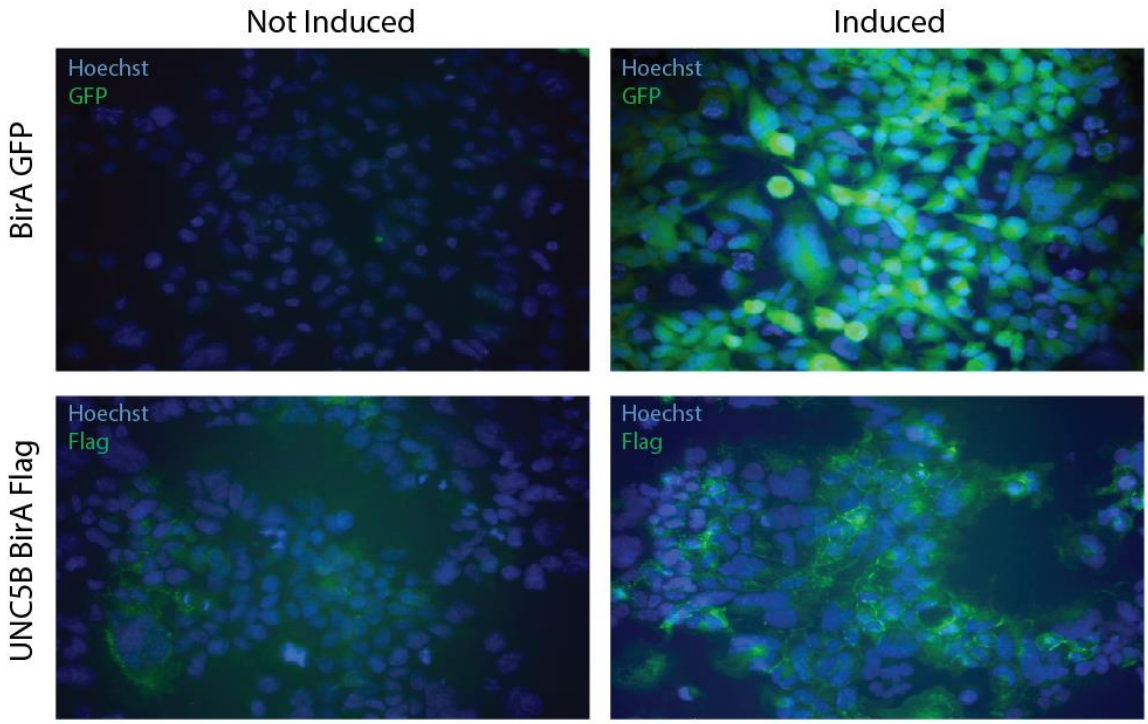

Figure 3. Induction of BirA GFP and UNC5B-BirA Flag expression with expected subcellular localization in HEK293 cells. Stably transfected HEK 293 Flp-In™ T-REx™ cell line with either BirA- GFP or UNC5B-BirA flag cDNA cultured and treated over-night with 1 µg/mL tetracycline hydrochloride to induce transgene expression. Representative images were taken for each condition and fluorescence of GFP or Flag antibodies were qualitatively compared between induced and non-induced conditions.

The BirA biotin ligase is an essential component of the BioID assay; thus, it is important to validate BirA functionality in the expressed chimeric protein. In this case, the induced cell lines were exposed to 50 µM of biotin overnight. Subsequent ICC revealed an overlap between biotin and flag immunofluorescence, albeit with the biotin fluorescence being more diffuse and not as concentrated at cell junctions (Figure 4A). BirA functionality was also demonstrated through streptavidin pull-down assays. Biotinylated proteins have an extremely strong affinity for streptavidin, which can be linked to beads. Biotinylated proteins were isolated using streptavidin bead pull-down assays, then separated by PAGE and electroblotted for western blot analysis using streptavidin-HRP detection. A substantially larger quantity of biotinylated proteins was detected in pull-downs from control BirA-GFP

cells, in terms of band intensity and the sheer number of bands present, compared to UNC5B-BirA expressing cells (Figure 4C). This was expected since the UNC5B-BirA fusion protein primarily biotinylates proteins at the cell membrane whereas cytoplasmic BirA-GFP may biotinylate neighboring proteins throughout much of the cell. Importantly, we detected bands that are clearly differentially and uniquely biotinylated in the UNC5B-BirA condition. We concluded that the BirA biotin ligase is functional in both cell lines. To assess whether a sufficient amount of protein is being isolated by the streptavidin beads, we analyzed a fraction of the pull-down assay by PAGE and then silver stained the polyacrylamide gel (Figure 4B). Bands were readily detected in every condition indicating the presence of sufficient amounts of biotinylated protein for mass spectrometry analysis (Finehout et al., 2004; Kang et al., 2002).

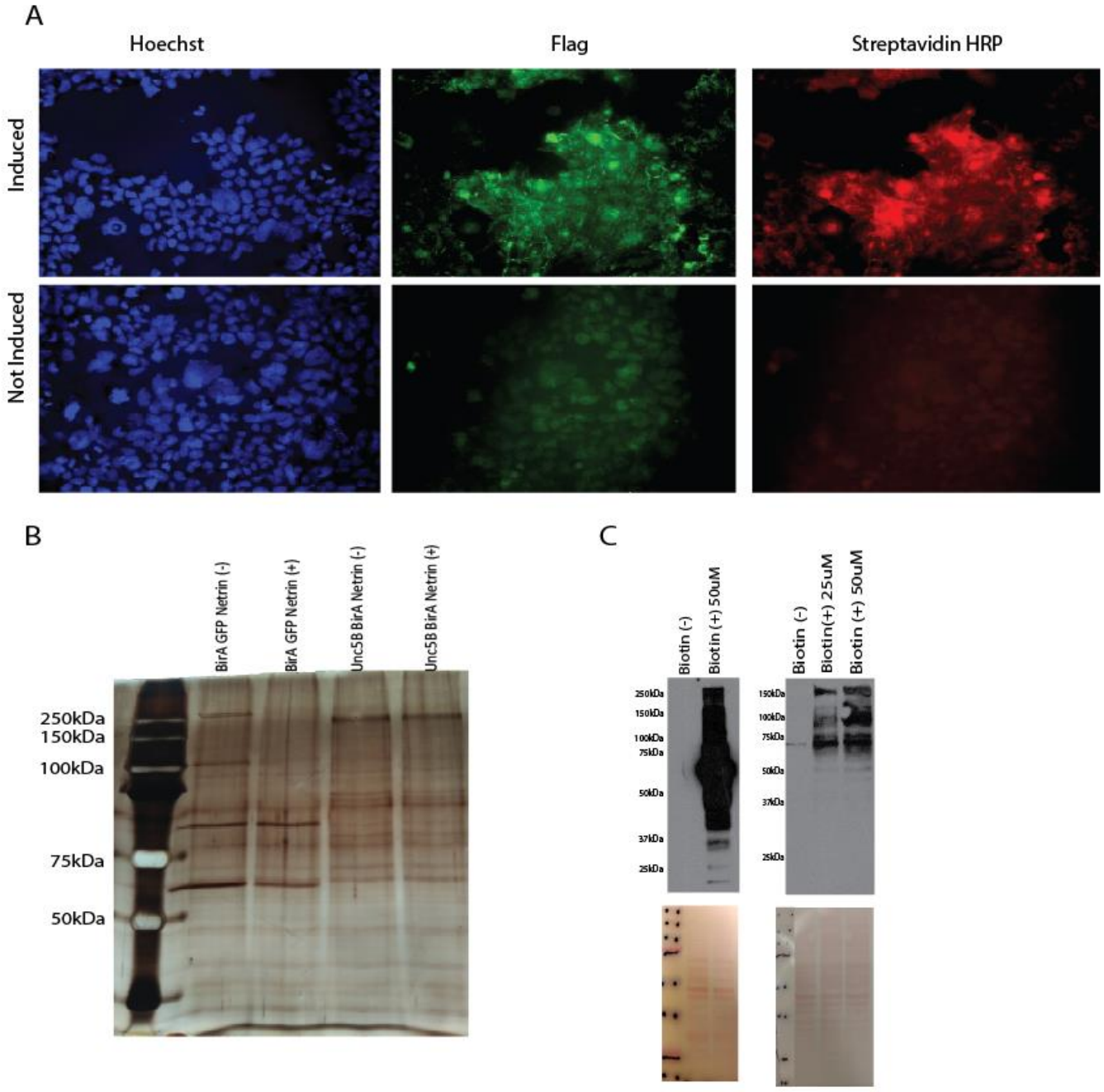

Figure 4. BirA-GFP and UNC5B-BirA Flag cell lines display functional BirA biotinylation. Stably transfected cells were cultured and incubated with 1µg/mL of tetracycline hydrochloride and 50 µM of biotin overnight. (**A**) Representative images comparing immunofluorescence of UNC5B and biotinylated proteins in UNC5B-BirA-Flag HEK 293 cell lines. (**B**) Image of the silver stained gel containing each sample that was sent for mass spectrometry. Approximately one tenth of each sample was run to assess whether each sample contained sufficient protein for mass spectrometry analysis. (**C**) Western blot analysis of the streptavidin bead pull-down assay peformed on the HEK 293 cell lines overexpressing either BirA or UNC5B when subjected to different concentrations of biotin. The ponceau stain for each blot is shown underneath the corresponding blot. For comparison, each blot was exposed for 2 min.

Mass spectrometry screen reveals subsets of proteins as UNC5B interacting candidates

The molecular mechanism underlying the contribution of UNC5B to the maintenance of CNS paranodes and preservation of the molecular integrity of different axonal-myelin domains remains unknown. It is thus paramount to identify the subset of proteins that interact with this transmembrane protein; however, protein insolubility and the study of protein interaction in reproducible physiological conditions remain challenging obstacles to overcome. Protein identification by biotinylation allows the BioID assay to address protein interaction within physiological conditions regardless of protein solubility, with less concern for detrimental protein modification due to extraneous factors (Kim et al., 2016). By overexpressing a bioengineered fusion protein consisting of a BirA biotin ligase fused at the C-terminal end of UNC5B, neighbouring proteins are subsequently biotinylated and identified through mass spectrometry. Netrin-1 is a ligand for the UNC5 family of proteins. We therefore included an additional condition in which cells overexpressing either fusion protein were exposed to exogenous netrin-1 overnight. Technical triplicates were each run on separate occasions and identified proteins were visualized using the proteomics software Scaffold.

Analysis of the control BirA-GFP condition identified over 1000 biotinylated proteins and the UNC5B-BirA condition identified over 800 biotinylated proteins for a total of approximately 2000 proteins detected. In comparison, the transcriptome of the HEK293 cell line contains over 11,000 detectable gene products indicating that BirA and UNC5B each interacted with a select network of proteins within the cell line (http://www.proteinatlas.org, Uhlén et al., 2015).

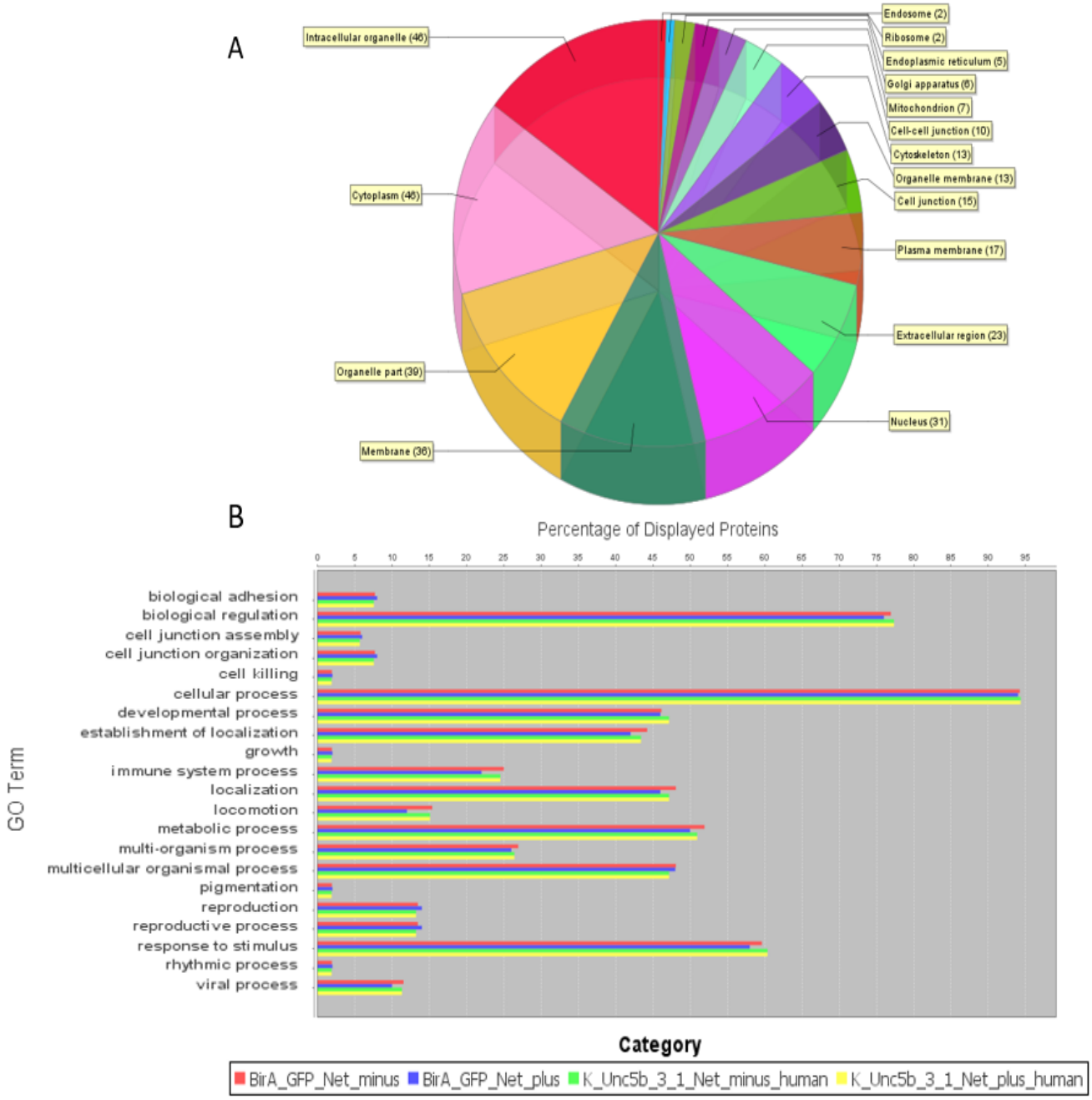

Figure 5. Gene Ontology terms associated with the UNC5B BioID assay. Using a Thermo Orbitrap Fusion mass spectrometer, proteins bound to streptavidin coated beads following the UNC5B-BirA BioID assay were identified and assessed using Scaffold_4.9.0. Approximately 300 proteins were identified following an initial screen using a one-way ANOVA on the normalized spectral counts of each protein between conditions. (**A** and **B**) are depictions of a refined list of proteins for which only proteins with higher spectral counts in the UNC5B conditions compared to their appropriate controls were kept. (**A**) Pie chart displaying the cellular locations for a refined list of proteins, encapsulating only significant protein hits that scored above a threshold with an increase of spectral counts in the UNC5B-BirA condition. (**B**) A bar graph was generated using Scaffold, illustrating the proteins present in each condition organized by Gene Ontology (GO) terms for biological processes.

To identify and filter out background proteins, a one-way ANOVA using Scaffold was conducted on the spectral counts for each protein across the four conditions. The filtered list contained over 300 proteins that were significantly different between conditions. To better focus on the subset of proteins that were specifically associated with UNC5B, only the proteins for which the spectral counts were higher in the UNC5B conditions were kept. This reduced the list to 52 proteins (including UNC5B) (Table1), henceforth referred as the refined list of proteins. Using the gene ontology terms, the refined list of proteins was organized using the NCBI database for cellular components and biological processes (Figure 5A and B respectively). Briefly, approximately 7% of these proteins were associated with biological adhesion, 8% and 6% were associated with cell junction organization and assembly, respectively. Additionally, 36 of the 52 proteins were associated with the cell membrane, 17 with the plasma membrane, 13 and 10 proteins in the list were associated with the cytoskeleton and cell-cell junctions, respectively.

To more stringently distinguish which of these proteins were enriched in the UNC5B conditions compared to the BirA-GFP control, the Sidak's multiple comparison test on the spectral counts was applied for selective comparisons between conditions. Approximately half of the proteins remained significant at least across one of the selected comparisons (Figure 6A-K). An important indication of the validity of this assay is the presence of UNC5B solely in the UNC5B overexpressing conditions with no significant difference resulting from the addition of exogenous netrin-1 (Figure 6B).

An interesting family of proteins detected in this screen are the septins (Figure 6A). These GTP binding proteins are a component of the cytoskeleton that have only been studied relatively recently and found to be involved in vesicle trafficking, and cell compartmentalization (Spiliotis et al., 2008). Spectral counts associated with Septins 2, 7, 8 and 11 were significantly higher in the UNC5B condition lacking netrin-1 compared to its

control, however there seems to be a general decrease of septin spectra when netrin-1 is present with UNC5B. Many tubulin isoforms (TBA1A, TBA1B, TBB2B, TBB3, TBB5 and TBB4B) were present in the screen. The mean value for tubulin spectra were increased in the UNC5B condition compared to BirA control albeit the differences between conditions were non-significant, likely due to the variation between each replicate (Figure 6E). Many polarity, cytoskeletal or junctional proteins were present in the list including: Disks large homologue1 (DLG1) (Figure 6B), Desmoglein-2 (DSG2), alpha and gamma adducin (ADDA and ADDG respectively) (Figure 6D), Lethal(2) giant larvae protein homolog 1 (L2GL1) and Vang-like protein 1 (VANG1) (Figure 6J). All had spectral counts significantly higher in the UNC5B conditions compared to their respective control except for DSG2 and ADDA as the netrin (+) condition was not significant compared to BirA netrin(+) control. However, none of these proteins had any significant spectral changes between their netrin-1/UNC5B conditions.

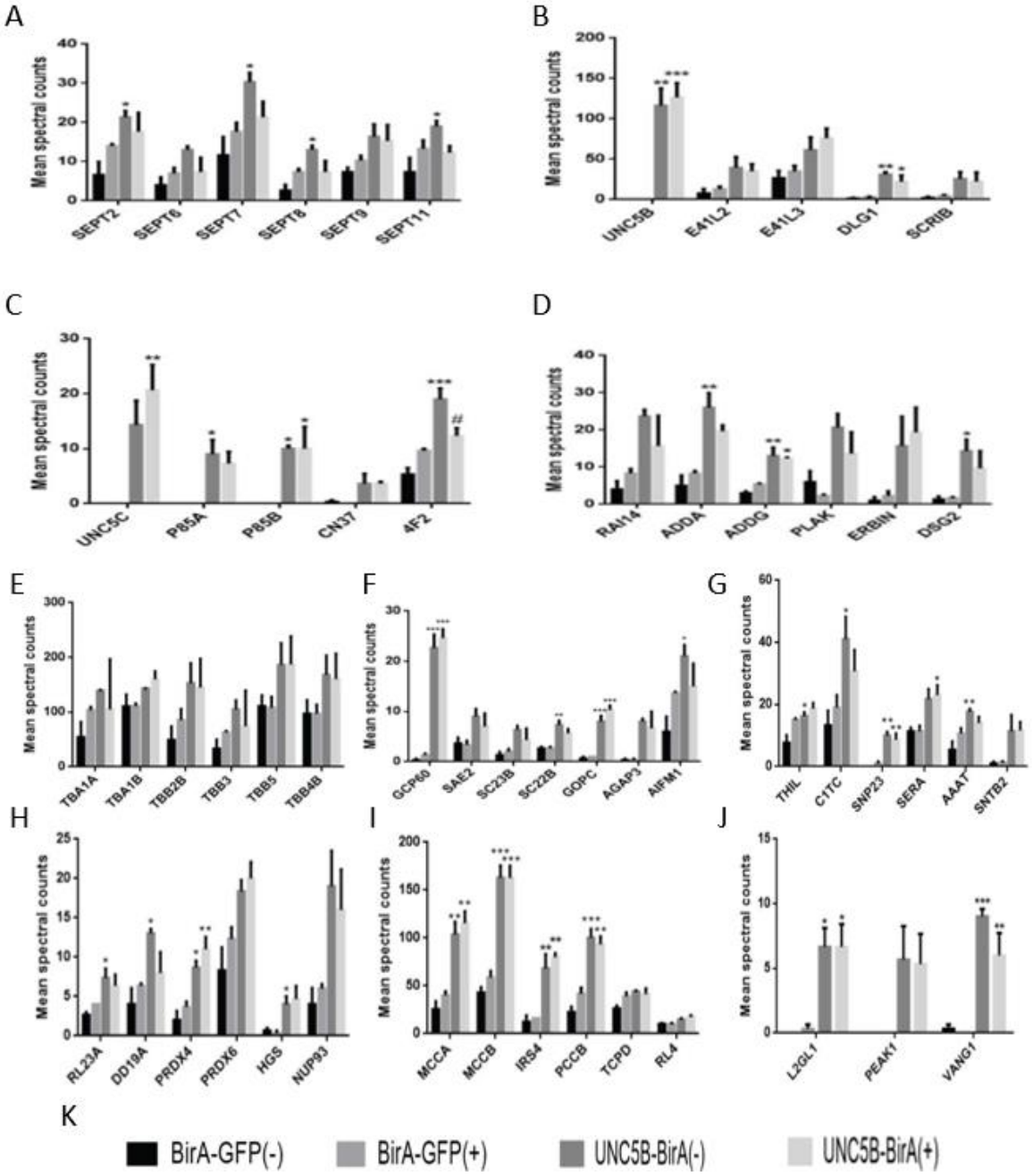

Figure 6. Proteomic analysis of the UNC5B BioID assay. The refined list contains 52 proteins. Proteins are written as their UniProt accession number (**A-J**). The normalized spectral counts of the significant differences and/or proteins of interest are shown and organized through bar graphs for each condition (**K**) where + and – indicate conditions with and without netrin-1 respectively. Using GraphPad Prism 6, Sidak`s multiple comparison tests were applied to selective comparisons involving the UNC5B-BirA conditions with their appropriate GFP control, ***** $p < 0.05$, ****** $p < 0.01$ and ******* $p < 0.001$ as well as comparisons between both UNC5B-BirA conditions and between both control conditions, # $p < 0.05$. Error bars are displayed as standard error means and spectral counts were normalized through the Scaffold software.

Many polarity and junctional proteins were detected. In addition, there was a similar abundance of proteins associated with maintenance of the golgi apparatus, vesicle formation and trafficking. These proteins incuded Golgi resident protein (GCP60), Golgi-associated PDZ and coiled-coiled motif-containing protein (GOPC), Vesicle-trafficking protein (SEC22B) (Figure 6F), Synaptosomal-associated protein 23 (SNP23) as well as proteins involved in the transport of large amino acids such as Neutral amino acid transporter B(0) (AAAT) (Figure 6G) and 4F2 cell-surface antigen heavy chain (4F2) (Figure 6C) which all had significantly higher spectral counts in the UNC5B conditions. Metabolic proteins such as Acetyl-CoA acetyltransferase, mitochondrial (THIL), C-1-tetrahydrofolate synthase, cytoplasmic (C1TC) and D-3-phosphoglycerate dehydrogenase (SERA) were also found to be significantly increased in the UNC5B conditions, with (SERA) or without netrin-1 (THIL and C1TC) in this list (Figure 6G).

To investigate if candidate interacting proteins obtained through the BioID screen might be parts of the same functional pathways, the refined list of protein was input to the web-based tool Database for Annotation, Visualisation and Integrated Discovery (DAVID) (https://david.ncifcrf.gov/, Huang et al., 2009a, 2009b). Since the input constitutes a relatively short list of proteins, only a few proteins were detected to be involved in functional pathways such as SNP23, SEC22B and C, which are both part of vesicular transport involving SNAREs (Figure 7A). Apoptosis-Inducing Factor 1 (AIFM1) is involved in caspase independent apoptosis (Figure 7B) and Insulin receptor substrate 4 (IRS4) with P85A and B, regulatory subunits of Phosphatidylinositol 3-kinase, are involved in insulin/Akt signaling pathway (Figure 6C) (Kanehisa, 2019; Kanehisa et al., 2000, 2019). Additionally, to examine whether the larger list could complement the pathways described above, the larger list of protein was also input in DAVID. None of the proteins complemented the previous pathways further validating that BirA and UNC5B interact with distinct networks of protein.

A

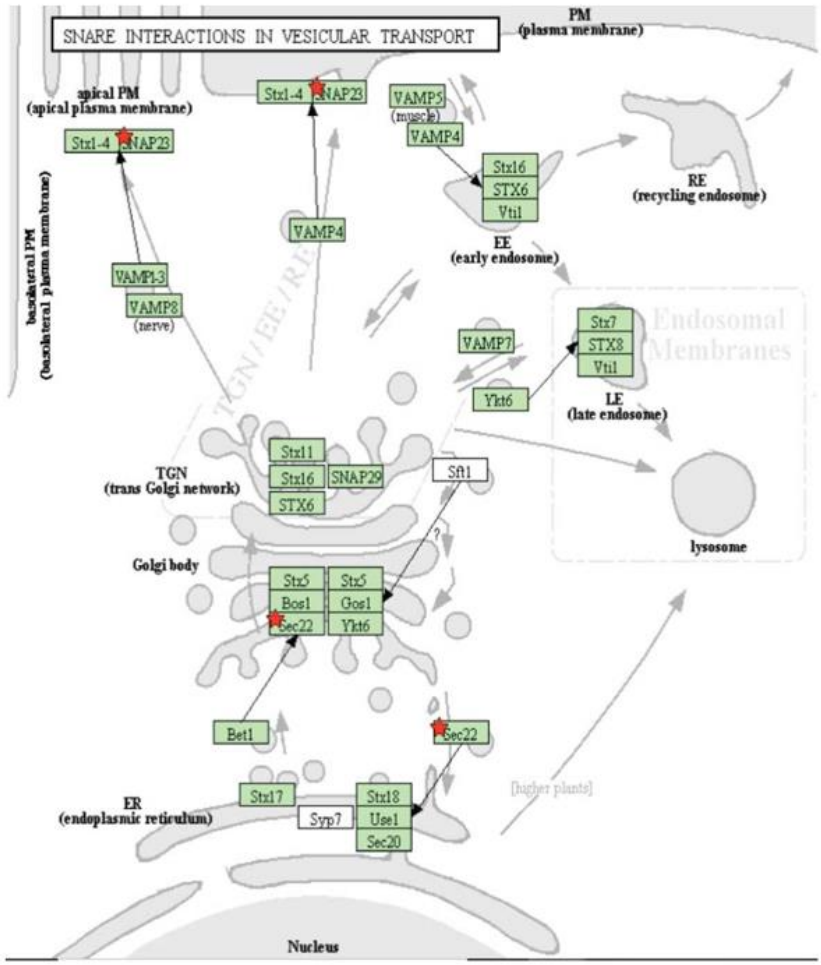
SNARE INTERACTIONS IN VESICULAR TRANSPORT
PM
(plasma membrane)
apical PM
(apical plasma membrane)
basolateral PM
(basolateral plasma membrane)
Stx1-4
SNAP23
VAMP5
(muscle)
VAMP4
Stx16
STX6
Vti1
RE
(recycling endosome)
EE
(early endosome)
VAMP3
VAMP8
(nerve)
Endosomal Membranes
VAMP7
Stx7
STX8
Vti1
Ykt6
LE
(late endosome)
Stx11
Stx16
STX6
SNAP29
Sft1
TGN
(trans Golgi network)
Golgi body
lysosome
Stx5
Bos1
Sec22
Gos1
Ykt6
Bet1
Sec22
Stx17
Stx18
Use1
Sec20
Syp7
ER
(endoplasmic reticulum)
[higher plants]
Nucleus

B

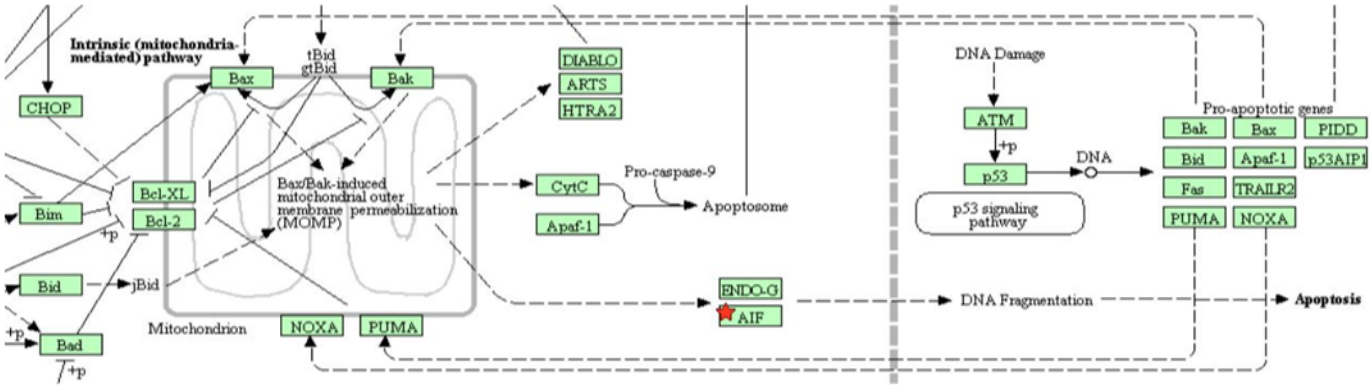
Intrinsic (mitochondria-mediated) pathway
CHOP
Bax
tBid
gtBid
Bak
DIABLO
ARTS
HTRA2
Bcl-XL
Bcl-2
Bim
Bid
jBid
Bad
+p
Bax/Bak-induced mitochondrial outer membrane permeabilization (MOMP)
Mitochondrion
NOXA
PUMA
CytC
Apaf-1
Pro-caspase-9
Apoptosome
ENDO-G
AIF
DNA Damage
ATM
p53
p53 signaling pathway
DNA
Pro-apoptotic genes
Bak
Bax
PIDD
Bid
Apaf-1
p53AIP1
Fas
TRAILR2
PUMA
NOXA
DNA Fragmentation
Apoptosis

C

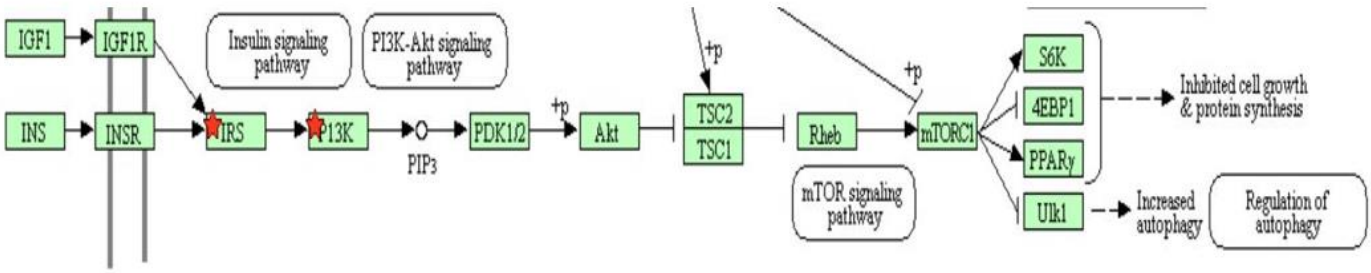
IGF1
IGF1R
INS
INSR
Insulin signaling pathway
PI3K-Akt signaling pathway
IRS
PI3K
PIP3
PDK1/2
+p
Akt
TSC2
TSC1
Rheb
mTOR signaling pathway
mTORC1
S6K
4EBP1
PPARγ
Ulk1
Inhibited cell growth & protein synthesis
Increased autophagy
Regulation of autophagy

Figure 7. Candidates involved in molecular pathways generated by KEGG through the web-based tool DAVID. The refined list encapsulating 52 proteins was input in the Database for Annotation, Visualisation and Integrated Discovery (DAVID) against the UniProt ID database. Using the functional annotation tool, pathways in which certain candidates were involed could be visualised using the Kyoto Encyclopedia of Genes and Genomes (KEGG) bioinformatics database. (**A**) Vesicular transport parthway involving SNAREs, candidates include SNP23 and Sec22B. (**B**) A caspase independent apoptotic pathway includes candidate AIFM1. (**C**) The insulin signaling pathway comprising candidates IRS4 and PI3 Kinase subunits P85A and P85B. The red stars indicate the proteins that are present in the mass spectrometry screen.

Thus far, the analysis was restricted to differences in spectral counts between the UNC5B conditions and the corresponding GFP-BirA controls. To better illustrate the spectral differences that result from netrin-1 addition in UNC5B expressing conditions, scatterplots were generated to depict spectral counts between two conditions. Comparing the netrin (+) conditions, the spectra of significant proteins were either skewed towards the UNC5B or BirA-GFP conditions (Figure 8). Netrin (-) conditions were similarly skewed (Figure 9). Notably, the addition of netrin-1 did not have a dramatic effect on many proteins detected to interact with UNC5B as spectral counts between both conditions remained relatively similar (Figure 10). However one protein had spectral counts that were significantly decreased in the UNC5B condition with netrin-1 added: 4F2, also called CD98, (Figure 6C), is an integrin associated protein that is the high molecular weight subunit of the large neutral amino acid transporter (LAT1) (Kanai et al., 1998).

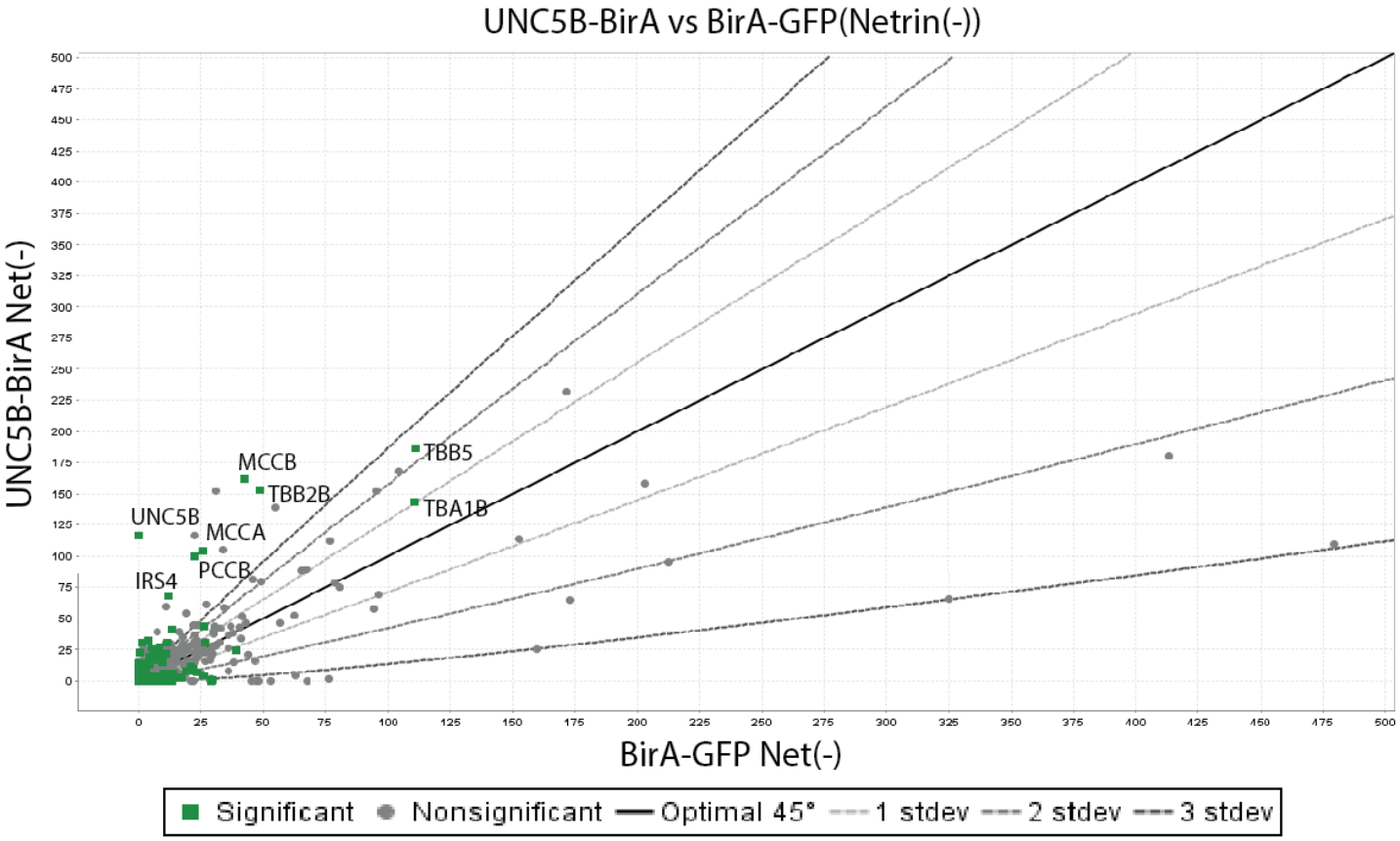

Figure 8. UNC5B-BirA compared to BirA-GFP netrin (-) conditions. Scatterplot of the spectral count fold change between UNC5B-BirA and BirA-GFP without netrin-1 conditions. Each individual dot represents the spectral count mean from triplicates of both conditions. Proteins represented in green are significant hits, products from the one way ANOVA analysis conducted by Scaffold. The optimal line indicates the line at which spectral counts in both conditions are equivalent.

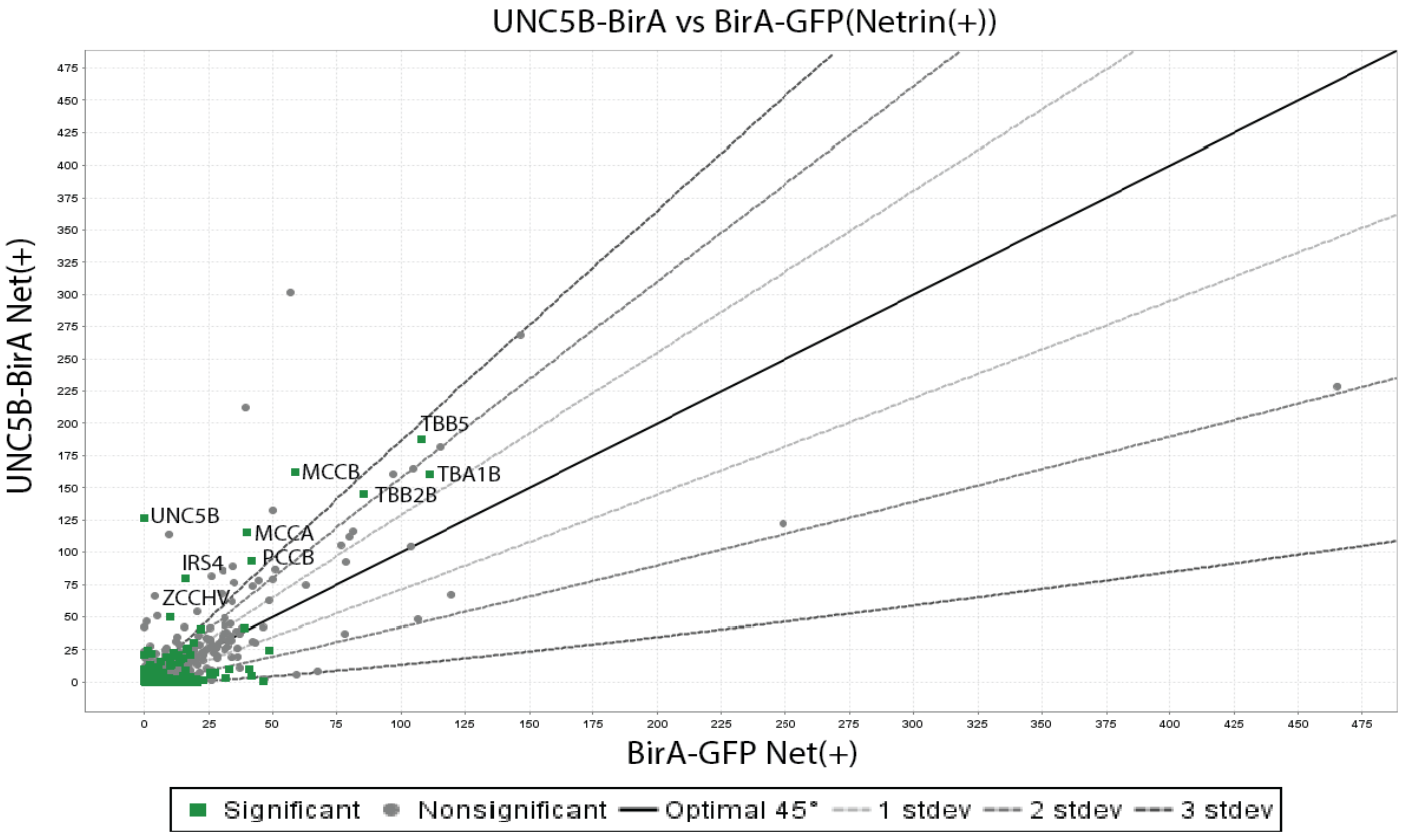

Figure 9. UNC5B-BirA compared to BirA-GFP netrin (+) conditions. Scatterplot of the spectral count fold change between UNC5B-BirA and BirA-GFP with netrin-1 conditions. Each individual dot represents the spectral count mean from triplicates of both conditions. Proteins represented in green are significant hits, products from the one way ANOVA analysis conducted by Scaffold. The optimal line indicates the line at which spectral counts in both conditions are equivalent.

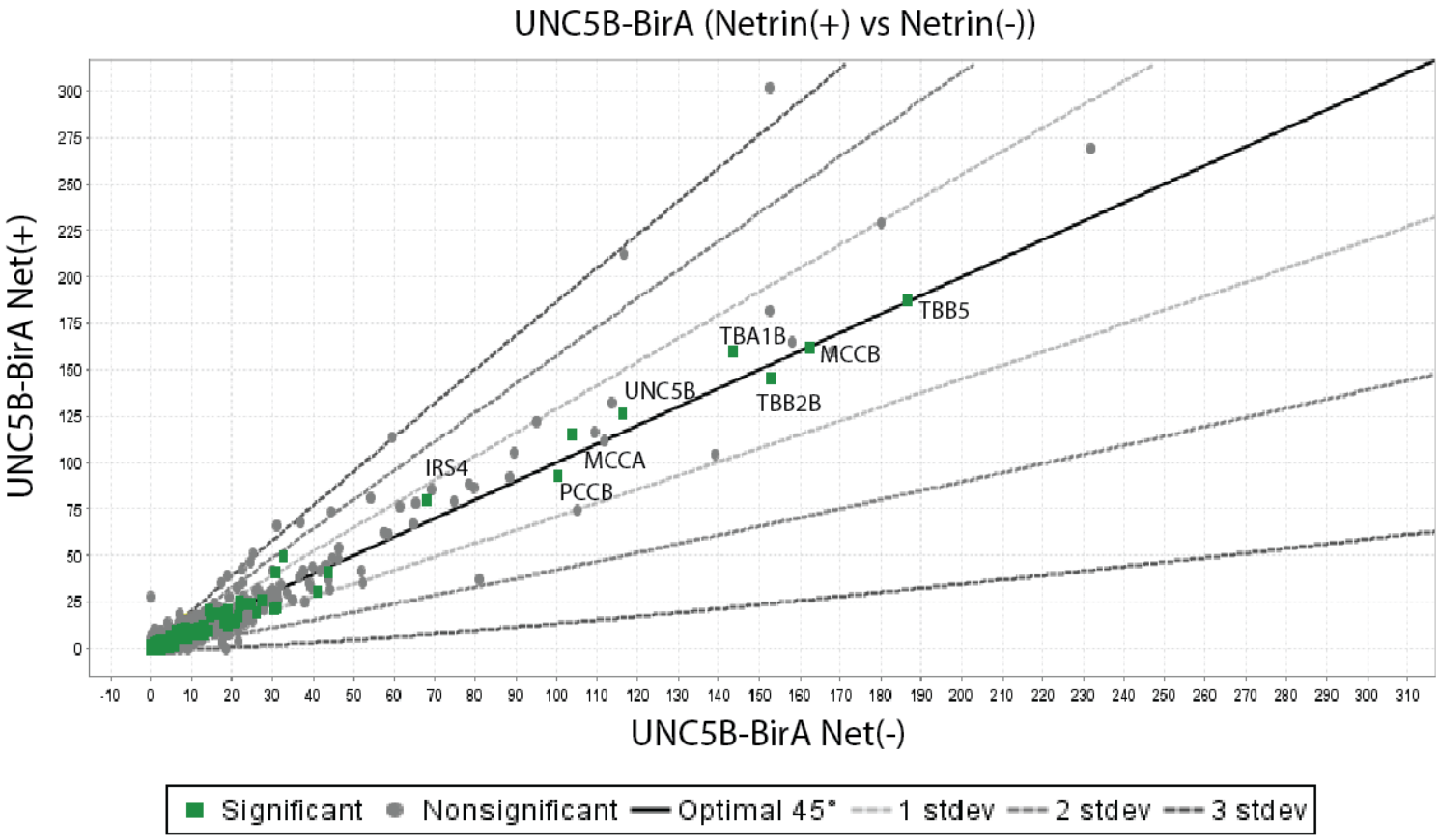

Figure 10. UNC5B-BirA netrin conditions comparison. Scatterplot of the spectral count fold change between UNC5B-BirA with and without netrin-1 conditions. Each individual dot represents the spectral count mean from triplicates of both conditions. Proteins represented in green are significant hits, products from the one way ANOVA analysis conducted by Scaffold. The optimal line indicates the line at which spectral counts in both conditions are equivalent.

Polarity protein DLG1 but not tight junction proteins ZO-1 and occludin co-immunoprecipitate with UNC5B-BirA fusion protein in HEK 293 cells

UNC5B contains a ZU-5 domain within its cytoplasmic domain that is homologous to the ZU-5 domain in the tight junction protein ZO-1. The ZU-5 domain in ZO-1 is responsible for tethering the cytoplasmic domains of transmembrane proteins to the cytoskeleton (Yasunaga et al., 2012). Hence, we investigated whether UNC5B might interact with tight junction proteins such as ZO-1 and occludin. UNC5B-BirA fusion protein was immunoprecipitated

from induced UNC5B-BirA over expressing cells using an anti-Flag antibody and blotted with an antibody directed against UNC5B. The UNC5B-BirA fusion protein was successfully pulled down. However, no co-immunoprecipitation of ZO-1 or occludin with UNC5B was detected (Figure 11). This suggests UNC5B may not interact directly with ZO-1 or occludin in HEK293 cells. The scarcity of spectral counts for both these tight junction proteins in the three UNC5B-BirA replicate conditions also supports the conclusion that UNC5B in HEK 293 cells do not interact with these subsets of tight junction proteins. It also raises the possibility that the ZU5 domain in the UNC5B intracellular domain does not function as part of a tight junction complex, but rather may mediate an UNC5B-cytoskeletal interaction similar to that made by ZO-1. It also remains possible that the addition of BirA to the carboxyl terminus may disrupt certain protein-protein interactions (Kim et al., 2016), and that tight junction proteins may be sensitive to this.

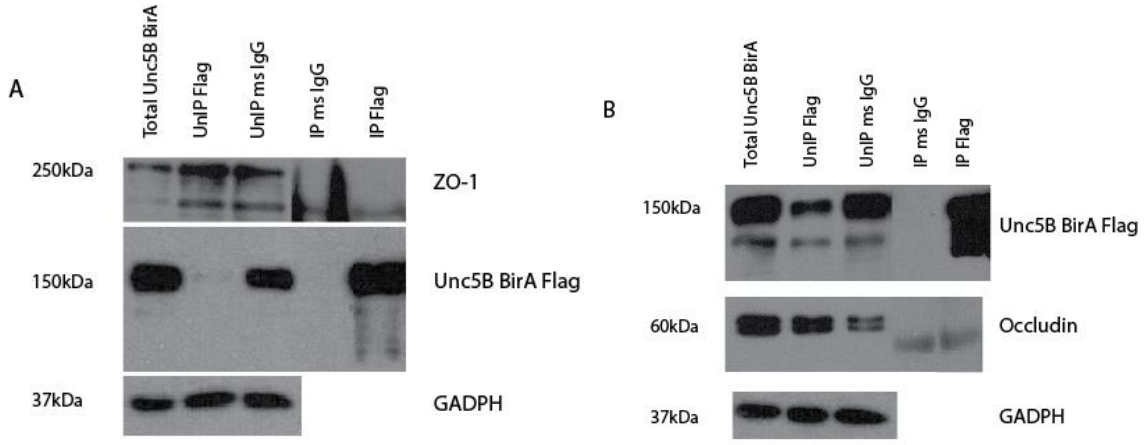

Figure 11. Tight junction proteins ZO-1 and occludin fail to immunoprecipitate with UNC5B-BirA Flag. Pull down was performed using cell lysates and a flag antibody. Blots were immunolabeled with a primary antibody directed against UNC5B. (**A**) Western blot of UNC5B co-immunoprecipitation from UNC5B-BirA HEK cells also labeled for tight junction protein ZO-1. (**B**) Co-immunoprecipitation with UNC5B also labeled for tight junction protein occludin. Total = total cell lysate after cell lysis, UnIP = remaining cell lysis after immunoprecipitation, IP = proteins bound to the beads after immunoprecipitation.

To further validate candidate UNC5B interacting proteins identified via the BioID screen mass spectrometry analysis, streptavidin bead pull-down assays were conducted and

assessed using Western blot analysis to independently determine if these biotinylated proteins were present. An interesting candidate interacting protein that we confirmed is present using this method is the polarity and scaffold protein DLG1 (Figure 12B). To further investigate this interaction, UNC5B-BirA was immunoprecipitated with the anti-flag antibody, and the immunoprecipitated western blot probed using a DLG1 antibody (Figure 12A). A faint band was detected, providing evidence that DLG1 can be coimmunoprecipitated with UNC5B, suggesting that the two proteins may interact directly, or indirectly as part of a protein complex.

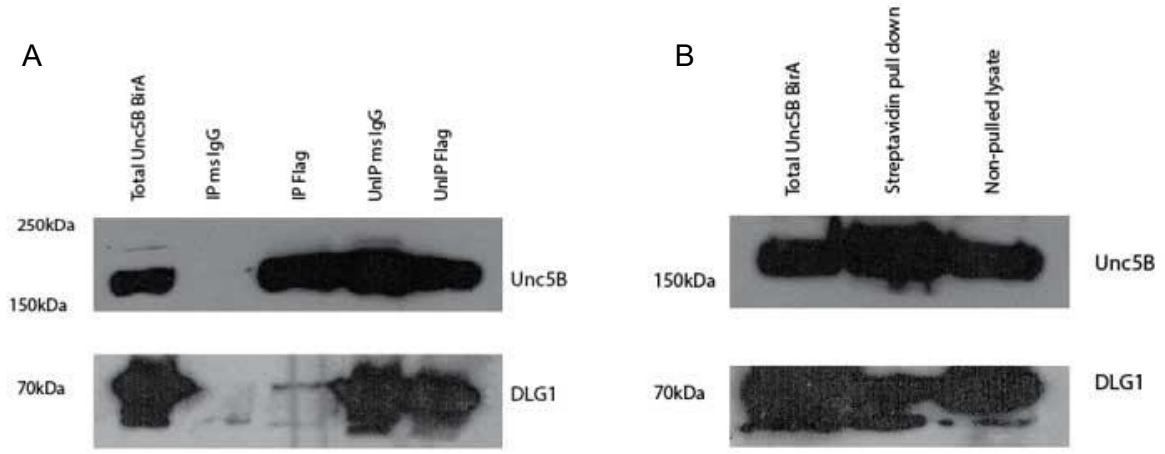

Figure 12. Validation and co-immunoprecipitation of Disks large homologue 1. Cell lysates were pulled down with an antibody against the flag epitope tag (**A)** or streptavidin coated beads (**B**) and blots were immunolabeled with a primary antibody directed against UNC5B or DLG1. (**A**) Western blot of UNC5B co-immunoprecipitation from UNC5B-BirA HEK cells also labeled for DGL1. (**B**) Western blot of a streptavidin coated bead pull-down assay from UNC5B-BirA HEK cells labeled for UNC5B and DLG1. Total = total cell lysate after cell lysis, UnIP = remaining cell lysis after immunoprecipitation, IP = proteins bound to the beads after immunoprecipitation.

Internodes are shorter in UNC5B cKO mice at 6 to 9 months of age but not at 3 months

The Kennedy lab has previously provided evidence supporting a requirement for UNC5B function at paranodes (de Faria Jr., 2015). In Olig2-Cre UNC5B conditional knock out mice

(Olig2-Cre UNC5B cKO), these studies reveal the progressive disorganization of myelin domains and severe disruption of paranode organization in 9-month-old mice compared to 3-month-old mice. By characterizing paranodes in 3 month old mice, an age at which myelination is almost complete (Snaidero & Simons, 2014) and 9-month-old mice, the relative importance of UNC5B in paranode formation verses maintenance was addressed. Previous studies indicated that disorganization of nodal and paranodal markers could precede or be an early sign of demyelination in the brain of MS patients (Howell et al., 2006; Wolswijk et al., 2003). We therefore investigated the possibility that UNC5B might influence internode length. Shorter internodes could result in reduced conduction velocity of signal propagation which is thought to be a contributing factor to early symptoms of MS (Wolswijk et al., 2003; Wu et al., 2012).

Coronal sections of 3-month and 9-month-old Olig2-Cre UNC5B cKO and WT mouse neocortex were immunolabeled for Caspr and MBP, markers of paranode and compact myelin internode, respectively (Figure 13A). In 3-month-old mice, no differences in internode length were detected between UNC5B cKO and WT mice (22.8 ± 0.751 μm and 21.97 ± 0.554 μm respectively) (Figure 13B). In contrast, 9-month-old UNC5B cKO mice have significantly shorter internodes than WT age-matched littermates (22.03 ± 0.946 μm and 28.1 ± 1.29 μm respectively) (Figure 13C). These results further support the conclusion that conditional loss of UNC5B expression by oligodendrocytes results in a phenotype that progressively worsens; in agreement with previous findings (de Faria Jr., 2015).

A

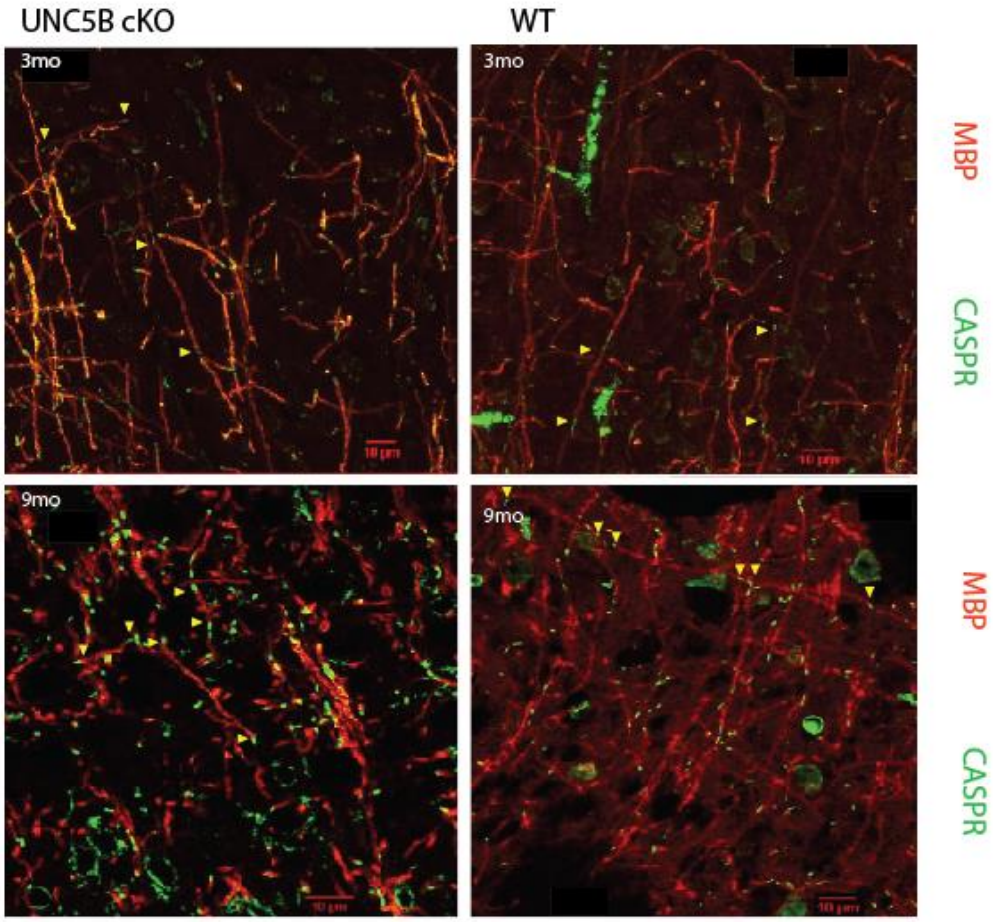
UNC5B cKO
WT
3mo
3mo
9mo
9mo
MBP
CASPR
MBP
CASPR

B

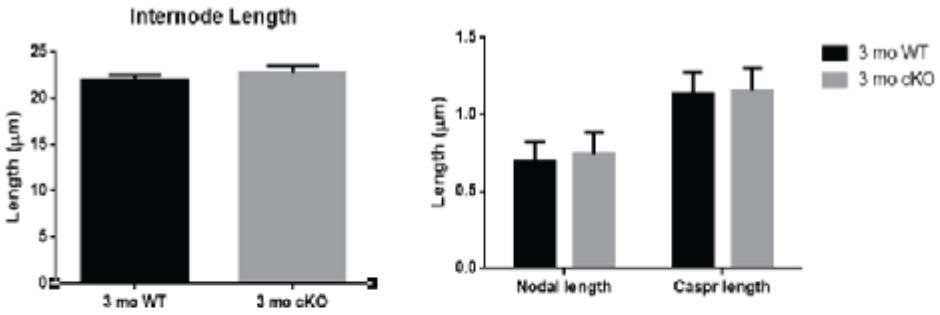
Internode Length
Length (µm)
25
20
15
10
5
0
3 mo WT
3 mo cKO
Length (µm)
1.5
1.0
0.5
0.0
Nodal length
Caspr length
3 mo WT
3 mo cKO

C

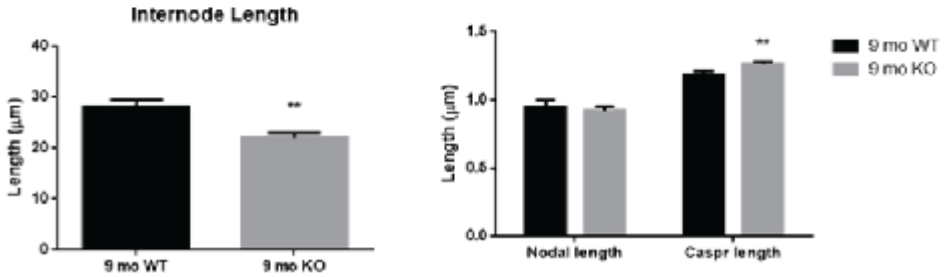
Internode Length
Length (µm)
40
30
20
10
0
**
9 mo WT
9 mo KO
Length (µm)
1.5
1.0
0.5
0.0
**
Nodal length
Caspr length
9 mo WT
9 mo KO

Figure 13. 9-month-old UNC5B cKO mice present shorter internodes.
(**A**) Representative images of sections of neocortex from wild type and UNC5B cKO mice immunolabeled for MBP and Caspr (coronal sections). Yellow arrowheads indicate the borders of internodes measured, flanked by Caspr + signal marking the paranode. Internode length, Caspr domain length and presumptive node lengths were measured in neocortical gray matter just dorsal to the corpus callosum. Internode lengths were measured when an MBP+ fiber was flanked by Caspr + paranodal junctions. Lengths were measured with Fiji using the straight-line tool. (**B** and **C**) Average internode length, paranodal (Caspr) and presumptive node (gaps between two Caspr devoid of fluorescence) lengths were determined in 3-month and 9-month old mice respectively. Knockouts were compared to their wild type littermates. Two-tailed Mann-Whitney test; ** $p < 0.001$. A total of approximately 80 internode measures were made from 3 mice for each phenotype.

The length of caspr-positive paranodes and the presumptive length of nodes of Ranvier (gap between Caspr labeling) were measured in the deep layers of the neocortex, just dorsal to the corpus callosum. Neither Caspr nor node lengths were altered in 3-month-old UNC5B cKO mice compared to WT (1.16 ± 0.015 µm and 1.14 ± 0.014 µm, 0.744 ± 0.014 µm and 0.721 ± 0.016 µm respectively) (Figure 13B). In contrast, Caspr-positive paranode lengths significantly increase in 9-month-old cKO mice compared to WT counterparts (1.27 ± 0.019 µm and 1.18 ± 0.026 µm) but no change in the gap length between Caspr positive domains were detected between the two genotypes (0.925 ± 0.031 µm and 0.952 ± 0.048 µm) (Figure 13C). These findings support the conclusion that the organization of paranodes degrades during aging in UNC5B cKO mice.

TABLE 1

Refined list of protein biotinylated by the UNC5B-BirA biotin ligase

*** INF: infinite, no spectra were found in the BirA-GFP control**

UniProt ID	Name	Description/function (UniProt)	Cellular localization (UniProt)	Fold change (Unc5B/BirA) netrin(-)	Fold change (Unc5B/BirA) netrin(+)	Reference(s)
4F2	4F2 cell-surface antigen heavy chain	Part of many heterodimeric complexes involved in the uptake of large neutral amino acids	Lysosome/ Cell membrane	3.4	1.3	(Milkereit et al., 2015; Torrents et al., 1998)
AAAT	Neutral amino acid transporter B(0)	Sodium dependent transporter of neutral amino acids	Cell membrane	3.3	1.3	(Garaeva et al., 2018)
ADDA	Alpha-adducin	Component of the membrane-cytoskeleton, binds to spectrin and actin meshwork	Cell membrane/ Cytoskeleton	5.2	2.3	(Hughes et al., 1995)
ADDG	Gamma-adducin	Component of the membrane-cytoskeleton, capping of actin filament	Cell membrane/ Cytoskeleton	4.5	2.3	(Gaudet et al., 2011; Katagiri et al., 1996)
AGAP3	Arf-GAP with GTPase, ANK repeat and PH domain-containing protein 3	GTPase involved in polyglutamine protein degradation	Cytoplasm	43	27	(Qin et al., 2006)
AIFM1	Apoptosis-inducing factor 1	Proapoptotic factor utilizing a caspase independent pathway	Cytoplasm/ Mitochondria	3.6	1.1	(Delettre et al., 2006; Hangen et al., 2010; Son et al., 2009)
C1TC	C-1-tetrahydrofolate synthase, cytoplasmic	Tetrahydrofolate conversion and One-carbon metabolism	Cytoplasm	3.0	1.6	(Burda et al., 2015; Hum et al., 1991)
CDK4	Cyclin-dependent kinase 4	Cell cycle regulator of G1/S phase	Nucleus/ Cytoplasm	20	INF*	(Medema et al., 1995)
CDN2A	Cyclin-dependent kinase inhibitor 2A	Interacts with CDK4 as a negative regulator of cell proliferation	Nucleus/ Cytoplasm	INF*	INF*	(Bockstaele et al., 2006; Huang et al., 2007)
CTND1	Catenin delta-1	Binds cadherins	Cytoplasm/ cell membrane	9.5	22	(Katafiasz et al., 2003)
DD19A	ATP-dependent RNA helicase DDX19A	Transportation of mRNA out of the nucleus	Nuclear pore complex	3.1	1.2	(Gaudet et al., 2011)
DLG1	Disks large homolog 1	Scaffold protein that compartmentalize proteins to specific domains of the plasma membrane also involved in adherens junction assembly	Cell junction/ Apical cell membrane	20	7.8	(Godreau et al., 2002; Laprise et al., 2004; Lue et al., 1994)
DSG2	Desmoglein-2	Cell-cell adhesion involving intermediate filaments and desmosome junctions	Cell membrane	12	6.1	(Cirillo et al., 2008; Pilichou et al., 2006)
GAB1	GRB2-associated-binding protein 1	Adapter protein involved in actin cytoskeleton reorganization	Cell-cell junction/ cytosol	INF*	4.0	(Laramé et al., 2007; Xu et al., 2016)
GCP60	Golgi resident protein GCP60	Maintenance of Golgi structure and regulation of protein transportation between ER and Golgi	Cytoplasmic membrane of Golgi apparatus	70	23	(Klima et al., 2016; Sohda et al., 2001)
GLYR1	Putative oxidoreductase GLYR1	Chromatin binding	Nucleus	17	5.7	(Fei et al., 2018)
GOPC	Golgi-associated PDZ and coiled-coil motif-containing protein	Protein trafficking from Golgi to plasma membrane and apical protein localization	Plasma membrane/ Golgi apparatus	18	12	(Cheng et al., 2002)
HGS	Hepatocyte growth factor-regulated tyrosine kinase substrate	Possible effector for PI3-kinase in vesicle trafficking. Signal transduction from cytokines and growth factors	Endosome/ Cytoplasm	8.4	9.3	(Holleman et al., 2014; Lee et al., 2012; Pons et al., 2008)
HNRH1	Heterogeneous nuclear ribnucleoprotein H	RNA binding	nucleoplasm	2.8	1.5	(Bateman, 2019; Paul et al., 2006)

HNRPM	Heterogeneous nuclear ribnucleoprotein M	RNA binding	nucleolus	3.2	1.6	(Bateman, 2019; Castello et al., 2012)
IRS4	Insulin receptor substrate 4	Promotes the AKT1 and insulin receptor 55ignalling pathway	Cell membrane	5.5	5.0	(Fantin et al., 1998; Uchida et al., 2000)
L2GL1	Lethal(2) giant larvae protein homolog 1	Maintenance of cell polarity and tissue organization of neuroepithelial cells and cortical actin cytoskeleton	Cytoskeleton	INF*	20	(Strand et al., 1995; Yamanaka et al., 2003)
MCCA	Methylcrotonoyl-CoA carboxylase subunit alpha	Subunit of the 3-methylcrotonyl-CoA carboxylase important for leucine catabolism	Mitochondrial matrix	4.0	2.9	(Chu et al., 2007; Stadler et al., 2005)
MCCB	Methylcrotonoyl-CoA carboxylase beta chain, mitochondrial	Subunit of the 3-methylcrotonyl-CoA carboxylase important for leucine catabolism	Mitochondrial matrix	3.8	2.8	(Chu et al., 2007; Stadler et al., 2005)
NUCL	Nucleolin	Induction of chromatin decondensation and ribosomal assembly	Nucleus/ cell cortex	1.2	1.9	(Huang et al., 2006; Parada et al., 1999)
NUP93	Nuclear pore complex protein	Assembly and maintenance of the nuclear pore complex	Nuclear membrane	4.7	2.5	(Krull et al., 2004)
P85A	Phosphatidylinositol 3-kinase regulatory subunit alpha	PIK3 binding and regulator activity involved in Akt pathway and plays an important response to FGFR signaling	Cell membrane/ Cytoplasm	62	INF*	(Argetsinger et al., 1995; Winnay et al., 2010)
P85B	Phosphatidylinositol 3-kinase regulatory subunit beta	PIK3 binding and regulator activity generating PIP3 and involved in Akt pathway	Cytoplasm	INF*	INF*	(Krull et al., 2004)
PCCB	Propionyl-CoA carboxylase beta chain, mitochondrial	Bio-synthesis of succinyl-CoA through degradation of propanoyl-CoA	Mitochondrion	4.4	2.2	(Lamhonwah et al., 1994; Stadler et al., 2005)
PCH2	Pachytene checkpoint protein 2	ATP binding	Nucleus	2.7	3.5	(Bateman, 2019; Yasugi et al., 1997)
PLAK	Junction plakoglobin	Junctional plaque protein binding to cadherin and anchors cytoskeleton to plasma membrane	Cytoskeleton/ Adherens junction	3.3	6.7	(Kirchner et al., 2012; Knudsen et al., 1992; Roberts et al., 2013)
PRDX4	Peroxiredoxin-4	Cell protection against oxidative stress, regulates NF-kappa-B activation	Endoplasmic Reticulum/ Cytoplasm	4.3	2.9	(Jin et al., 1997; Tavender et al., 2008)
PRDX6	Peroxiredoxin-6	Cell protection against oxidative stress and has phospholipase activity	Cytoplasm	2.2	1.6	(Chen et al., 2000; Kang et al., 1998)
RALY	RNA-binding protein Raly	RNA binding	Nucleus	5.7	0.8	(Bateman, 2019; Castello et al., 2012)
RL23A	60S ribosomal protein L23a	Ribosomal component binds 26S rRNA	Cytosol	2.5	1.7	(Datta et al., 2015; Odintsova et al., 2003)
RL4	60S ribosomal protein L4	Ribosomal component	Cytosol	1.5	1.8	(Odintsova et al., 2003)
SC22B	Vesicle-trafficking protein SEC22b	Transport vesicle fusion and targeting between the Golgi and ER	Golgi apparatus/ Endoplasmic reticulum	2.9	1.9	(Nakajima et al., 2004)
SEPT2	Septin-2	Cytoskeletal GTPase stabilizes microtubules for vesicle transport in polarized columnar epithelium	Cytoskeleton/ Cytoplasm	3.3	1.3	(Spiliotis et al., 2008, 2005)
SEPT7	Septin-7	Cytoskeletal GTPase involved in actin cytoskeleton organization and cytokinesis	Cytoskeleton/ Cytoplasm	2.6	1.2	(Kremer et al., 2007; M. Zhu et al., 2008)
SEPT8	Septin-8	Cytoskeletal GTPase involved in synaptic vesicle SNARE formation	Cytoskeleton/ Cytoplasm	4.3	1.0	(Bläser et al., 2004)
SERA	D-3-phosphoglycerate dehydrogenase	Biosynthesis of L-serine	cytosol	1.9	2.0	(Pind et al., 2002)
SNP23	Synaptosomal-associated protein 23	Constituent of the membrane fusion machinery and important in docking	Cytoplasm	68	12	(Gaudet et al., 2011; Lu et al., 2008)

		and fusion of transport vesicles				
SYDC	Aspartate—tRNA ligase, cytoplasmic	Attachment of an amino acid with its appropriate tRNA	Cytoplasm	3.3	1.6	(Escalante et al., 1993)
TBA1B	Tubulin alpha-1B chain	Component of microtubules and of the cytoskeleton	Cytoskeleton/ Cytoplasm	1.3	1.4	(Bharti et al., 2011; Gaudet et al., 2011)
TBB2B	Tubulin beta-2B chain	Component of microtubules and of the cytoskeleton and involved in neuronal migration	Cytoskeleton/ Cytoplasm	3.1	1.7	(Bharti et al., 2011; Gaudet et al., 2011; Jaglin et al., 2009)
TBB5	Tubulin beta chain	Component of microtubules and of the cytoskeleton	Cytoskeleton/ Cytoplasm	1.7	1.7	(Bharti et al., 2011; Gaudet et al., 2011)
TCPD	T-complex protein 1 subunit delta	Molecular chaperone involved in protein folding during ATP hydrolysis	Cytoskeleton/ Cytoplasm	1.7	1.1	(Seo et al., 2010)
THIL	Acetyl-CoA acetyltransferase, mitochondrial	Beta-oxidation and ketone body metabolism	mitochondrion	2.1	1.2	(Fukao et al., 1990; Haapalainen et al., 2007)
UNC5C	Netrin receptor UNC5C	Axon guidance, microtubule interaction	Cell membrane	INF*	INF*	(Shao et al., 2017; Wetzel-Smith et al., 2014)
VANG1	Vang-like protein 1	Planar cell polarity	Cell membrane	50	INF*	(Arenas, 2014)
ZCCHV	Zinc finger CCCH-type antiviral protein 1	Inhibitor of viral replication	Cytoplasm/Nucleus	8.6	5.1	(Hayakawa et al., 2011; Zhu et al., 2011)

DISCUSSION

UNC5B has been demonstrated to be essential for proper development in mice. Existing literature documents roles for UNC5B regulating cell-cell interaction to promote cell-cell alignment, dispersal and movement during development in endothelial cells, in addition to being a receptor for repellent axonal and neuronal guidance cues (Larrivée et al., 2007; Lu et al., 2004; Navankasattusas et al., 2008; Tai-Nagara et al., 2017). A recent finding in the Kennedy lab provides an interesting parallel. Conditional knock-out mice that selectively delete UNC5B from the oligodendrocyte lineage, exhibit gradual axonal-myelin domain disorganization and paranodal disruption in the CNS during aging, with the lack of UNC5B resulting in the destabilization and disorganization of autotypic paranodal loop-loop interactions (de Faria Jr., 2015). The underlying molecular mechanism employed by UNC5B to maintain paranodal junctions remains unknown. The primary aim of this thesis was to investigate UNC5B function to better understand its role in CNS white matter stabilizing paranodal junctions.

Shorter internodes in 9-month-old UNC5B conditional knock out mice.

Previous studies from the Kennedy laboratory revealed severe disruption of paranode ultrastructure in 9-month-old UNC5B cKO mice, while paranodal integrity was unchanged in 3-month-old UNC5B cKO mice. To determine whether these paranodal disruptions might influence the structure of the internode, we measured internode lengths immediately dorsal to the corpus callosum in coronal sections of neocortex. We detected a significant decrease in internode length in 9-month-old cKO mice compared to their wild type littermates, with no significant difference detected in 3-month old mice. This finding complements previous findings from the Kennedy lab supporting the conclusion that the loss of UNC5B expression by oligodendrocytes results in a progressive, rather than an acute phenotype (de Faria Jr., 2015).

The observations made here, and in a manuscript in preparation that describes the resulting phenotypes, provide evidence that loss of UNC5B from OLs leads to destabilization of the myelin sheath. Our finding supports the conclusion that this results from disrupting the organization of paranodal junctions, and that this ultimately leads to shorter myelin internodes. The underlying molecular mechanism responsible for these changes remains unknown. Interestingly, the concept of active myelin remodeling may provide some insight into the phenotype of these mice. In the CNS of aging mice, there is a general increase of oligodendrogenesis and studies have shown that the myelin sheath shortens as the quantity of paranodes increase (Hamilton et al., 2017; Lasiene et al., 2009). Immunofluorescence studies of mouse optic nerve sections showed that adult-born OLs generated greater numbers of myelin sheaths, albeit shorter, whereas early-born OLs made fewer but longer internodes. Young et al. (2013) provided further evidence of myelin remodeling, reporting that adult-born OLs replace early-born or dying OLs as a possible means to adapt to non cell

autonomous factors such as neuronal activity due to experience as the mice age (Etxeberria et al., 2016; Young et al., 2013). Evidence for d*e novo* myelination by adult-born OLs of partially myelinated or unmyelinated axons is also of relevance, another study disclosed that more than half of the OLs were produced in the mouse cerebral cortex after four months of age (Hughes et al., 2018). Therefore, *de novo* myelination of partially myelinated axons may require dynamic structural adjustments to be made by pre-existing internodes. Although this concept has been addressed by several studies, an undeniable demonstration has remained elusive due a lack of physical evidence (Lasiene et al., 2009; Young et al., 2013). Recent studies in zebrafish have provided better insight as internodes were seen to expand and retract using time-lapse imaging and internode displacement following OL ablation (Auer et al., 2018; Baraban et al., 2018; Krasnow et al., 2018). However, a study of the developing mouse somatosensory cortex reported that over 80% of internodes visualized were stable and only a subset of internodes showed further extension or retraction (Hill et al., 2018).

Paranodal disruption and disorganization occur with aging and a lack of UNC5B could expedite myelin sheath destabilization by increasing internode dynamics during *de novo* myelination. In addition, however, the Kennedy lab previously reported the lengthening of K+ channels at juxtaparanodes in mice that lack DCC or UNC5B expression by oligodendrocytes (Bull et al., 2014; de Faria Jr., 2015), which has not been reported to occur in aging mice (Shepherd et al., 2012). This indicates that the loss of these netrin receptors results in aspects of myelin segment destabilization that is not seen in aging mice. The Kennedy lab has previously reported that paranodal length was significantly shorter in 3 month old UNC5B conditional knockout mice that selectively lack expression by oligodendrocytes (de Faria Jr., 2015). Here, we demonstrate that internode lengths of older UNC5B cKO mice were similar to those of 3-month-old mice, as the 9-month-old wild type mice had significantly longer internodes. The approximate age at which internode elongation

peaks, before the average internode length either stops elongating or begins to shorten, and the time course of these changes in specific CNS subregions, has not been determined. Importantly, we do not rule out a possible role for UNC5B promoting internode extension (de Faria Jr., 2015).

Shorter internodes are normally accompanied by reduced conduction velocity resulting in possible deficits in motor behavior (reviewed by (Peters, 2002)). The Kennedy lab previously described a lack of behavioral deficits in the UNC5B cKO animals at both 3 and 9-months of age, in spite of the paranodal disruption and disorganization of axonal-myelin subdomain disorganization in 9-month-old mice (de Faria Jr., 2015). Similarly, mouse knockouts for another late myelin protein, Myelin and Lymphocyte (MAL), also lack detectable motor impairments, in spite of progressive paranodal disorganization in the PNS of older mice (Schaeren-Wiemers et al., 2004). The possible relationship between shorter neocortical internodes and a possible reduction in axon conduction velocity in older UNC5B cKO mice remains to be determined.

Several studies have examined the relationship between nodal distance (i.e. internode length) and conduction velocity. As what is speculated to be a protective measure, these distances were found to commonly surpass a length at which the conduction velocity would reach a "flat maximum" (Brill et al., 1977; Waxman, 1980). Notably, there are other dimensional and structural elements that influence signal propagation. Factors such as myelin thickness, axonal caliber, periaxonal space, nodal length and ion channel density at the node of Ranvier may all affect the velocity of an action potential along an axon (Arancibia-Cárcamo et al., 2017; Friede et al., 1984; Gillespie et al., 1983; Young et al., 2013). Interestingly, the Kennedy lab has also shown that cKO mice that selectively delete DCC from oligodendrocytes display motor impairment and also delayed conduction velocity (Bull et al., 2014). DCC, which is also found at paranodes, was found to be required for paranodal

maintenance and organization. However, a lack of transverse bands (TB) detected in DCC cKO mice was a distinct phenotype that was not found in mice lacking UNC5B. These electron dense bands visualized by electron microscopy, are thought to stabilize the linkage of the myelin loops to the axolemma as they are removed during myelin reorganization. They are also thought to provide a molecular barrier that contributes to segregate the sodium channels from the potassium channels. This is thought to contribute to preservation of the conduction velocity, as certain mice lacking TBs had more severe motor deficits and shorter lifespans than those who had TBs (Mierzwa et al., 2010; Shepherd et al., 2012). It has also been suggested that the continued presence of DCC and netrin-1 may partially mitigate and delay the severity of the UNC5B cKO phenotype, perhaps due to some functional redundancy in netrin receptor function (de Faria Jr., 2015).

To elucidate the relationship between UNC5B, internode length, and impairment of motor/cognitive behavior, measuring internode lengths in different areas of the UNC5B cKO CNS and in the DCC cKOs could be beneficial and would be of relevance. Additionally, the literature has repeatedly report myelin destabilization as a consequence of aging. In mice, cortical myelin debris and single internode loss was only present past 2 years of age (Hill et al., 2018). Thus, it would also be of relevance to further study the effects of UNC5B in mice older than 9 months of age, more specifically at 2 years should the UNC5B cKO mice live that long.

UNC5B-BirA-Flag Flp-In T-REx HEK 293 cell line validation

The mechanism by which UNC5B maintains paranodal stability and the integrity of axonal-myelin subdomains is not known, however several pieces of evidence obtained by the Kennedy lab suggest that UNC5B acts at the autotypic paranodal junctions. Additionally, components of the cytoskeleton such as tight junction proteins and gap junction proteins are

present between paranodal loops(Gow et al., 1999; Kamasawa et al., 2005). This suggests that these adhesions between loops contribute to maintaining loop stability.

HEK293 cells are not oligodendrocytes, but they do express many proteins characteristic of neural and epithelial cell lineages (Shaw et al., 2002). Taking advantage of the utility of this cell line, we screened for candidate UNC5B interacting proteins using the BioID assay in a genetically modified HEK293 cell line (Schultz et al., 1998; Shaw et al., 2002). The proximity labeling BioID assay allowed us to identify protein candidates in physiological conditions, as opposed to previous methods to screen for interacting proteins, such as affinity complex purification or the yeast-2-hybrid assay (Kim et al., 2016). Using Gateway® cloning technology, we generated a cell line in which induced overexpression of the protein of interest is regulated by the Tet operon. In both the UNC5B-BirA and BirA-GFP cell lines, we confirmed that the gene of interest was properly induced (Figure 3). Immunocytochemically, we detected UNC5B associated with cell-cell junctions, whereas the BirA GFP signal was diffuse throughout the cytoplasm, showing selective spatial localization of the overexpressed UNC5B. Additionally, using a streptavidin bead pull-down assay, fewer, and condition specific, bands were detected in the UNC5B overexpressing condition compared to BirA-GFP, consistent with biotinylation labeling subsets of proteins specific to the localization and function of these proteins. Silver staining the polyacrylamide gel further supported these conclusions and revealed the presence of sufficient amounts of biotinylated proteins for identification by mass spectrometry analysis. The presence of unique bands, comparing the UNC5B and control BirA lanes, is an indication of differential protein biotinylation between the two conditions.

Candidate UNC5B interacting proteins identified using the BioID assay

DLG-1 and Scribble:

The mass spectrometry output of the BioID assay resulted in over 2000 protein hits. Strikingly, one of the strongest signals and most significantly different hits between the UNC5B conditions and the BirA-GFP control was Disks Large homologue 1 (DLG1). The *dlg1* gene was first identified in *Drosophila*, coding for DLGA, a membrane-associated guanylate kinase (MAGUK) protein localized at septate junctions; arguably equivalent to paranodal septate-like junctions in vertebrates (Hortsch et al., 2003; Woods et al., 1991). This scaffolding protein has been shown to contribute to the formation of both adherens and tight junctions and the maintenance of the apical-basal polarity of septate junctions (Firestein et al., 2001; Stucke et al., 2007; Woods et al., 1991, 1996). DLG1 is also part of the Scribble polarity complex which consists or three tumour suppressor proteins, DLG1, Scribble and Lethal giant Larvae (reviewed by (Su et al., 2012)) . Interestingly, Scribble was also detected in the BioID screen, albeit below the level of an individual significant hit. There was however an increasing trend in the amount of Scribble present in the UNC5B condition compared to control. Scribble is a Leucine-Rich-Repeat(LRR) And PDZ (PSD 95, Discs-large and ZO-1) (LAP) protein which regulates protein-protein interactions and protein distribution. In particular, PDZ domains were shown to enhance the capacity of LRR domains to localize proteins at septate junctions (Bilder et al., 2000; Zeitler et al., 2004).

Interestingly, both DLG1 and Scribble are present in white matter. DLG1 has contrasting functions in the PNS and CNS. In Schwann cells, DLG1 interacts with PTEN to inhibit the PI3K-Akt-mTOR pathway, which consequentially reduces myelin thickness. In contrast, DLG1 in oligodendrocytes interact directly with the p85 regulatory subunit of PI3K to promote myelination (Noseda et al., 2016). Notably, two p85 isoforms, p85α and p85β, had significantly higher spectra in UNC5B expressing conditions compared to control. DLG1

has been localized to Schwann cell paranodes and the lack of DLG1in these cells leads to hypermyelination and ultimately demyelination due to destabilization of the myelin sheath (Cotter et al., 2010). In oligodendrocytes, conditional knock out of Scribble results in paranodal disruption that is similar to that seen in UNC5B cKO mice. Additional functions for Scribble are argued to be to negatively regulate myelination, regulate myelin initiation and sheath extension (Jarjour et al., 2015).

Band 4.1-like proteins:

DLG1 also interacts with other components of the cytosleleton and adhesion proteins. The band 4.1 family of proteins interact with DLG1. Notably, band 4.1 like protein B and G (E41L3 and E41L2 respectively) were both increased in the UNC5B expression condition, albeit without reaching the level of individual significance (Lue et al., 1996, 1994). 4.1B co-immunoprecipitates with paranodal marker Caspr and juxtaparanodal marker Caspr2 in both CNS and PNS, and 4.1B has been shown to promote the maintenance of paranodal junctions, likely by stabilizing an interaction between transmembrane Caspr and intracellular F-actin (Buttermore et al., 2011; Denisenko-Nehrbass et al., 2003). Although 4.1B is found on the axonal side of the junctional connection, 4.1G is expressed by myelinating Schwann cells at paranodes. 4.1G null mice exhibit progressive disorganization of the PNS axo-myelin subdomains and although 4.1G has not been found in oligodendrocytes, 4.1G has a role in formation of tight junctions by the OLN-93 oligodendrocyte cell line (Ivanovic et al., 2012; Ohno et al., 2006; Xia et al., 2011), and has been extensively reviewed (Susuki et al., 2016).

Tubulins and CNP:

A number of other cytoskeletal constituents, including isoforms of tubulins and septins all had increased spectra in the UNC5B condition with some significantly increased compared to control. Microtubule dynamics and organization in oligodendrocytes are influenced by CNP

(shown as CN37 in Figure 3), a major myelin protein that enables OL process arborisation. In CNP null mice, myelination occurs normally, however paranodal disruption becomes progressively worse with age due to a putative loss of structural stability provided by microtubules. Both CNP and microtubules are present in paranodal loops (Lee et al., 2005; Li et al., 2005; Rasband et al., 2005).

Septins:

In contrast, a role for septins at PNS and CNS paranodes has not been described (Buser et al., 2009). Septins are GTP binding proteins that were first identified in yeast due to their importance in cytokinesis (Hartwell, 1971). Generally, septins were thought to be high order scaffolding proteins for cell cycle regulators, however, more recent publications demonstrate that septins are involved in cell compartmentalization, vesicle transport, as well as regulators of actin and microtubule organization (Kinoshita, 2006; Kremer et al., 2007; Mostowy et al., 2012; Spiliotis, 2010; Spiliotis et al., 2008). Epithelial cell polarity is regulated by the association of septin 2 to polyglutamated tubulin tracks which facilitates the transportation of vesicles containing membrane proteins that define apical and basolateral cell polarity (Spiliotis et al., 2008). In oligodendrocytes, septin 2, 4, 7 and 8 form longitudinal filaments on the adaxonal side of the internodal myelin sheath at a late stage of myelination. This promotes the stability of the myelin sheath and prevents myelin outfolding (Erwig et al., 2019; Patzig et al., 2016). The affinity of septins for each other could determine the filamentous structure particular septins adopt, as their affinity is dependent on the curvature of the membrane with which they are associated (Cannon et al., 2019).

Adducins:

Actin isoforms present in the BioID screen exhibited no clear trends between conditions. Nevertheless, spectra of actin binding proteins and proteins associated with adherens junctions were increased in the UNC5B expressing conditions. α and γ-adducin were both

significantly increased in the UNC5B conditions compared to control. Adducins cap F-actin filaments and function as an integral link between the cortical actin cytoskeleton and the epithelial plasma membrane via the adducin-spectrin skeleton. This meshwork of proteins is essential to maintain epithelial apical junctions such as adherens and tight junctions as both α and γ-adducin colocalize at adherens junctions (Abdi et al., 2008; Hughes et al., 1995; Kuhlman et al., 1996; Mische et al., 1987). Furthermore, the inactivation of adducins was suggested as the initial step in apical junction disassembly induced by phorbol ester (Naydenov et al., 2010). On the other hand, adducins were also shown to promote apical junction remodeling by enabling disassembly of these junctions as adducins and spectrins were shown to colocalize with the actomyosin contractile rings of calcium depleted epithelial cells (reviewed by (Naydenov et al., 2010)).

In CACO-2 cells, the synapse associated protein 97 (SAP97), a homologue of DLG-1, was found to colocalize with α-adducin and E-cadherin at cell junctions. This identified SAP97 as a part of the cortical actin cytoskeleton (Reuver et al., 1998). DLG-1 was also shown to be critical for adherens junction formation in *C. elegans* (Firestein et al., 2001).

Adducins are also present in other cell types such as endothelial cells, neurons and neuronal stem cell (NSC) derived oligodendrocytes (Hauser et al., 2018; Kugelmann et al., 2015; Xu et al., 2013). In endothelial cells, α-adducin co-localizes with VE-cadherins at adherens junctions in human dermal microvascular endothelial cells (HDMEC). Subsequent downregulation of α-adducin using siRNA revealed conspicuous VE-cadherin mislocalization and fragmentation. Additional experiments revealed that adducin at the cell membrane, is important in adherens junction remodeling as well as enabling barrier function integrity (Kugelmann et al., 2015). Furthermore, VE-cadherin is known to regulate vessel permeability and intercellular adhesion by stabilizing endothelial adherens junctions. Inhibition of VE-cadherins and ultimately adherens junctions disassembly, is a mechanism by

which VEGF induces angiogenesis (reviewed by(Radeva et al., 2018)). Interestingly, UNC5B is thought to negatively regulate VEGF signaling and function as an anti-angiogenic molecule (Koch et al., 2011).

In neurons, adducins are a component of the membrane-associated periodic skeleton (MPS) first reported using stochastic optical reconstruction super resolution microscopy (STORM) (Xu et al., 2013). The MPS is defined by the actin-spectrin skeleton visualised as periodic actin rings orthogonal to the longitudinal plane of the axon. These rings are separated by spectrin filaments. The MPS is present in mature axons including the axon initial segment (AIS) and the immature axon as its function is not fully understood (Leterrier et al., 2015). In basal conditions, the MPS is not essential to sustain axonal integrity. However, axons undergoing physical stress lacking an MPS are more easily damaged (Hammarlund et al., 2007). Consequentially, the stabilization of the actin filament in an axon-pruning assay protected against axon fragmentation and the MPS was not lost (Unsain et al., 2018). Although adducins were shown to be dispensable for MPS formation, they are thought to regulate actin filament length by strengthening the actin-spectrin interaction (reviewed by (Unsain et al., 2018)). Adducins were also shown in NSC derived oligodendrocyte processes as a one-dimensional periodic cytoskeleton using 3D STORM microscopy, however if adducins are present at paranodes is not known (Hauser et al., 2018).

Junction plakoglobin:

Other proteins involved with the association of actin filaments or adherens junctions include proteins such as junction plakoglobin and retinoic acid-induced protein 14 (RAI14). Although plakoglobin, also known as γ-catenin, is best known in association with desmosomes, its presence has also been characterized in AJs (Korman et al., 1989; Lewis et al., 1997). Plakoglobin is closely related to β-catenin with approximately 80% sequence similarity and similarly interacts with E-cadherin, however, plakoglobin has greater affinity for desmosomal

cadherins such as desmoglein-2 (Ozawa et al., 1995); a protein that also exhibits increased spectral counts in the UNC5B condition compared to control, albeit not to a level beyond significance. Its intercellular adhesive function is not well understood, however, similar to β-catenin, it promotes the linkage of membrane associated proteins via cadherins to actin filaments (Lewis et al., 1997). A study using a squamous epithelial cell line indicated that although plakoglobin is not essential for AJs formation, it serves as an intermediate and signaling molecule for downstream formation of desmosomes (Lewis et al., 1997). Additionally, in human umbilical vein endothelial cells (HUVEC), plakoglobin in basal conditions promoted cell-cell adhesion with VE-cadherin, however plakoglobin is also essential for vascular permeabilization upon VEGF stimulation (Muramatsu et al., 2017). Junction plakoglobin was also present in rat whole brain myelin fractions, however its function in oligodendrocytes is not well understood (Baer et al., 2009).

RAI14:

RAI14 was characterized as an F-actin protein regulator (reviewed by (Qian et al., 2013)). Its gene product was coincidentally discovered both in rat liver and in human retinal pigment epithelium, and named ankycorbin and NORPEG respectively. Being characterized as a component of the cortical actin skeleton, RAI14 was shown to be present at adherens junctions in rat liver and at cell-cell junctions in rat epithelia (Kutty et al., 2001; Peng et al., 2000). RAI14 has also been shown to regulate actin in Sertoli cells. In this context, roles were described promoting of blood testis barrier (BTB) integrity and the process of spermatogenesis (Qian et al., 2013). More specifically, RAI14 was shown to maintain actin bundles for proper BTB function and to enable the bundling/de-bundling (actin branching) process of actin filaments needed for spermatogenesis (for more information see review by (Qian et al., 2013)). Very recently, RAI14 was classified as an N-Ank protein which are ankyrin repeat containing proteins that shape and sense membrane curvature (Wolf et al.,

2019). RAI14 contains an N-terminal amphipathic helix that allows its association with the plasma membrane. This along with its ankyrin repeats facilitates dendritic formation and branching during neural development (Wolf et al., 2019).

Effect of netrin-1 in the UNC5B Bio ID assay

Surprisingly, no dramatic effect was seen upon addition of netrin-1 to HEK 293 cells over expressing UNC5B-BirA. The level of protein spectra remained relatively similar in both conditions. Therefore, differences seen between UNC5B and BirA expressing cells appear to be independent of netrin-1. Although netrin-1 is a major ligand for Unc-5 homologues in development, there are instances where UNC5 exerts its function on migrating cells and axons independently of netrin-1. This was initially suggested when cerebellar abnormalities normally seen in *Unc5h3* (*Unc5hc*) deficient mice were not seen in *netrin-1* deficient mice (Przyborski et al., 1998). Similar issues were seen in *Unc5c*$^{-/-}$ null mice pertaining to the projections of corticospinal tract axons during pyramidal decussation and phrenic axon projection, that were not seen in netrin-1 deficient mice (Burgess et al., 2006). UNC5B interacts with proteins, independent of netrin-1 as a ligand as well. The G protein, $G_{i\alpha 2}$, was shown to interact with the cytosolic tail of UNC5B without ligand binding and could additionally associate with neogenin as a co-receptor for repulsive guidance molecule A (RGMa) signaling; a molecule involved in the collapse of cerebellar granule neuron growth cones (Komatsuzaki et al., 2002). The FLRT family of proteins are chemorepellent cues that associates with the UNC5 family (Karaulanov et al., 2009; Visser et al., 2015; Yamagishi et al., 2011). More specifically, FLRT2 acts as a ligand for UNC5B, mediating inter-endothelial repulsion in the developing placental labyrinth. This repulsion was shown to organize and control the layering of these endothelial cells as endothelial cells lacking FLRT2 resulted in mice dying mid-gestation due to hypoxia (Tai-Nagara et al., 2017).

Although the literature reveals numerous cases of UNC5B function without netrin-1 (reviewed by (Larrieu-Lahargue et al., 2012)), it remains surprising that no effect of netrin-1 was seen. The ZU5-UPA-DD supramodule of UNC5B adopts an L-shaped closed conformation, with apoptosis signaling occurring upon opening. Addition of netrin-1 is argued to stabilize the closed conformation, thereby preventing the initiation of apoptosis (Wang et al., 2009). The addition of a 35kDa biotin ligase to the C-terminal end of UNC5B could forcibly open the conformation of the UNC5B intracellular domain, which is predicted to nullify netrin-1 signaling (Kim et al., 2016); however we did not detect an increase in cell death due to UNC5B-BirA expression. Alternatively, the over-expression of UNC5B in HEK293 cells could result in some level of constitutive activation, similar to netrin-1 binding, and thereby independently recruit signaling proteins that normally require netrin-1.

UNC5B co-immunoprecipitations with tight junction proteins and DLG1

Older UNC5B cKO mice exhibit detached paranodal loops that may be everted from the axolemma, along with reduced interloop densities. Claudin-11, a tight junction protein that is uniquely expressed by oligodendrocytes, is found within tight junctions between paranodal loops (Gow et al., 1999). We speculated that UNC5B could be interacting with components of tight junctions as interloop densities are lost in the UNC5B conditional knockouts mice. We investigated whether UNC5B would co-immunoprecipitate with tight junction proteins such as ZO-1 and occludin; however, overexpressing UNC5B in the UNC5B-BirA-Flag 293 cell line, we were unable to co-immunoprecipitate these tight junction proteins with UNC5B. We were similarly unsuccessful using more gentle lysis buffers, in case RIPA buffer was too stringent and disrupted protein-protein interactions. These findings suggest that UNC5B may not interact with tight junction proteins, and if it does interact with tight junction proteins, the putative interaction is not sufficiently robust to survive co-immunoprecipitation.

Since DLG1 was a strong hit in the BioID screen, we then tried to validate this hit by performing a streptavidin-biotinylation pull down assay from UNC5B-BirA overexpressing cells. The presence of DLG1 on the beads provides validation of the identification of DLG1 in the screen and encouraged us to further investigate whether DLG1 might co-immunoprecipitate with UNC5B-BirA. The presence of a faint band in Figure 6a suggests sufficient interaction between the two proteins for co-immunoprecipitation. The molecular mechanism mediating an interaction between UNC5B and DLG1 has not been investigated, however it has previously been shown that the DD of UNC5B can interact with PDZ domains, and DLG1 contains three (González-Mariscal et al., 2000; Hata et al., 2009). UNC5A also contains a PDZ binding domain within its DD. This PDZ binding domain along with the last three amino acids of UNC5A interacted with the PDZ domain of protein interacting with C-kinase 1 (PICK1). UNC5B was also shown to co-immunoprecipitate with PICK1 and the last three amino acids of UNC5B are similar to UNC5A, which are GDC versus AEC respectively (Williams et al., 2003). The notion that the last three amino acids of UNC5B interact with DLG1 might clarify the relatively weak co-IP band detected for DLG1 and possibly the lack of tight junction protein interaction. Specifically, the addition of the biotin ligase to the C-terminus of UNC5B could impede these interactions by hindering the binding availability of the last three amino acids (Kim et al., 2016). Therefore, if a successful co-immunoprecipitation occurred with a full length UNC5B expressed in HEK 293 cells, viral infections with different UNC5B cDNA constructs could elucidate which UNC5B domain interacts with DLG1. Such a system could then be used to further investigate whether netrin-1 may stabilize this interaction. Ongoing studies in the Kennedy lab aim to visualize the subcellular localizations of tight junction proteins with UNC5B in the UNC5B HEK 293 expressing cell line, as well as in the human colorectal adenocarcinoma CACO-2 epithelial cell line.

GENERAL DISCUSSION

Performing a BioID screen on HEK 293 cells over expressing UNC5B has provided insight into the subset of proteins UNC5B may interact with, informing our understanding of its function at paranodes. Notably, the major constituents of the cytoskeleton were not detected as significant hits in the screen. A trend toward an increased presence of tubulin was detected when UNC5B was overexpressed and UNC5C has been previously shown to immunoprecipitate with the tubulin subunit TUBB3 (Shao et al., 2017). While these findings suggest that UNC5B may not directly interact with tubulins, molecules such as septins have been shown to remodel the microtubule cytoskeleton and multiple septins were detected in the current screen (Spiliotis, 2010). Actin isoforms were also present in the screen, but the quantitative spectra were so variable across replicates and conditions that they were excluded from the list of significant hits. In contrast, several actin binding proteins, proteins associated and known to promote adherens junction integrity were significantly enriched in the UNC5B conditions; most notably the adducin subunits. Other proteins such as RAI14 and plakoglobin/γ-catenin were also increased in the UNC5B conditions.

Based solely on this protein screen, we can only speculate on what are the myriad of possible molecular mechanisms by which UNC5B enables the maintenance and integrity of paranodal loops in oligodendrocytes. Figure 14 depicts a model in which putative UNC5B molecular interactions would facilitate its function at the paranodes. More precisely, the model proposes UNC5B could promote the structural stability of mature paranodes, necessary for the maintenance of a dynamic structure, by binding to the adducin-actin-spectrin skeleton. Spectrin localized to the glial side of the paranode were shown to be vital for paranode formation and maintenance in both the CNS and PNS in mice (Susuki et al., 2018). Additionally, DLG1 and scribble have been characterized in oligodendrocytes and

roles identified in the development and organization of paranodal loops (Jarjour et al., 2015). Thus, these cytoskeleton binding proteins could potentially interact with UNC5B and F-actin to further stabilize the contacts between paranodal loops.

Several proteins involved in vesicle trafficking were also detected in the screen, specifically SNP23, Septin2, SC22B, GOPC, GCP60 (see table1). These findings suggest that UNC5B over expression could modulate vesicle trafficking and protein recruitment. The idea that UNC5B could impact local protein or vesicle recruitment to maintain the loop-loop junctional integrity would be a novel role for UNC5B. This could be a means by which polarity and scaffold proteins necessary for stabilization or proper alignment of the cytoplasmic filled wraps that define paranodal loops are recruited to these autotypic junctions. In addition to the earlier discussion concerning DLG1, it has also been shown to regulate Sec8, a member of the exocyst complex of proteins that regulate local polarity and membrane addition including in oligodendrocytes and Schwann cells (Anitei et al., 2006; Bolis et al., 2009).

These findings support the speculation that DLG1, or a related member of the MAGUK family, could direct the local recruitment of polarity and other signaling proteins to the paranode plasma membrane via UNC5B, thereby contributing to stabilizing and maintaining paranode integrity. Further, a putative interaction of UNC5B with DLG1 and microtubules, which are the tracks for cargo vesicle transport, could also stabilize the paranodal loops by locally recruiting proteins necessary for the maintenance of these autotypic junctions. Finally, the repellent function of UNC5B for motile cells, could perhaps translate at paranode autotypic junctions to mediate mechanisms that regulate loop spacing and appropriate glial loop layering.

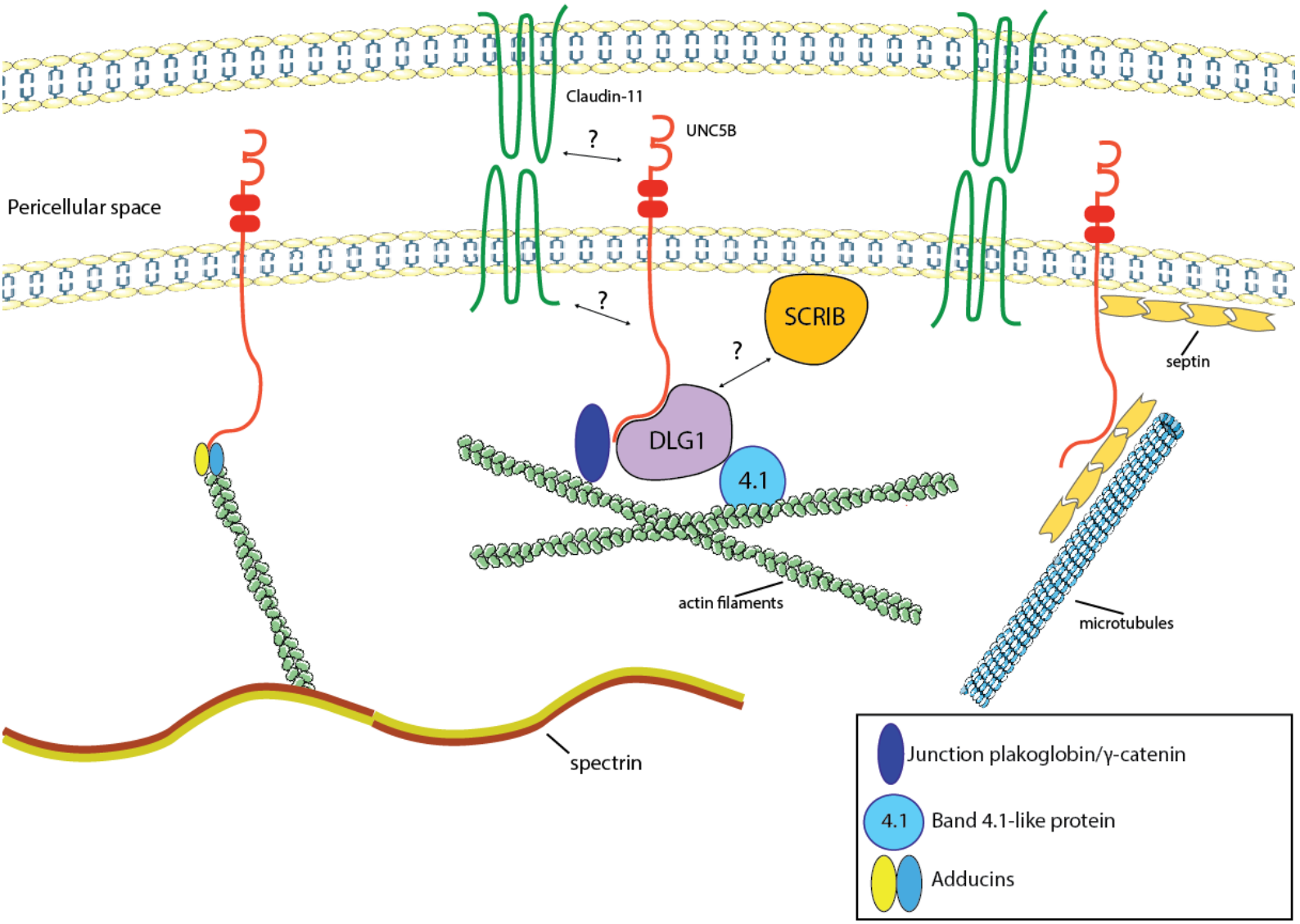

Figure 14. Model of putative UNC5B molecular interactions at oligodendrocyte paranodal junctions. UNC5B localized to autotypic junctions between oligodendrocyte paranodal loops maintains paranodes with aging. Candidate UNC5B interacting proteins identified in the BioID protein screen provide insight into molecular interactions that support UNC5B paranode maintenance. The actin-spectrin cytoskeleton, which is known to maintain cell-cell junctions, could, acting through the F-actin capping proteins adducins, bind UNC5B to enable loop-loop junction integrity. Polarity protein Scribble and scaffold protein DLG1 could also provide junction stability by linking UNC5B to F-actin. Tubulin isoforms, the detection of vesicle regulating proteins and microtubule regulating proteins such as septins, suggest roles regulating microtubule and in vesicle recruitment. UNC5B binding septins regulating microtubules could recruit proteins to junctions to promote paranodal maintenance.

SUMMARY AND CONCLUSION

Maintaining healthy paranodes is likely to be key to preventing the onset of demyelination and be a potential therapeutic target in demyelinating diseases such as MS. The Kennedy lab has previously provided evidence that the netrin receptor UNC5B is essential for paranode maintenance. The aim of this thesis was to identify and recognize some key molecules that could clarify the way UNC5B functions to regulate paranodal maintenance. Using the BioID proximity labeling assay, we observed that many polarity and scaffold proteins, such as DLG1, as well as components of the cytoskeleton and components of vesicle trafficking mechanisms, are enriched in the UNC5B-BirA screen. This suggests that UNC5B is part of a structural complex that is necessary to maintain paranodal autotypic junctions as well as possibly recruiting other proteins necessary for paranode maintenance.

Further, we measured internode length in 3 and 9 month-old mice in order to understand the implications of conditionally knocking down UNC5B from oligodendrocytes. We report that 9 month-old UNC5B cKO mice have significantly smaller internodes than their wildtype counter parts. This strongly suggests that with time, the lack of UNC5B will have adverse effects on myelin sheath stability.

Further studies in both projects described in this thesis are required to better understand the network of UNC5B interacting proteins and their full functional significance at paranodes. Identifying UNC5B candidate interactors paves the way for a plethora of experiments to ultimately elucidate the role of UNC5B in myelin formation, maintenance, demyelination, and remyelination.

REFERENCES

Abdi, K. M., & Bennett, V. (2008). Adducin Promotes Micrometer-Scale Organization of B2-Spectrin in Lateral Membranes of Bronchial Epithelial Cells. *Molecular Biology of the Cell*, *19*(February), 536–545. doi:10.1091/mbc.E07

Ackerman, S. L., Kozak, L. P., Przyborski, S. A., Rund, L. A., Boyer, B. B., & Knowles, B. B. (1997). The mouse rostral cerebellar malformation gene encodes an UNC-5-like protein. *Nature*, *386*(6627), 838–842. doi:10.1038/386838a0

Anitei, M., Ifrim, M., Ewart, M., Cowan, A. E., Carson, J. H., Bansal, R., & Pfeiffer, S. E. (2006). A role for Sec8 in oligodendrocyte morphological differentiation. *Journal of Cell Science*, *119*, 807–818. doi:10.1242/jcs.02785

Arancibia-Cárcamo, I. L., Ford, M. C., Cossell, L., Ishida, K., Tohyama, K., & Attwell, D. (2017). Node of ranvier length as a potential regulator of myelinated axon conduction speed. *ELife*, *6*, 1–15. doi:10.7554/eLife.23329

Arenas, E. (2014). WNT signaling in midbrain dopaminergic neuron development and regenerative medicine for Parkinson's disease. *Journal of Molecular Cell Biology*, *6*, 42–53. doi:10.1186/2193-1801-4-S1-L49

Argetsinger, L. S., Hsu, G. W., Myers, J. M. G., Billestrup, N., White, M. F., & Carter-Su, C. (1995). Growth Hormone, Interferon-gamma, and Leukemia Inhibitory Factor Promoted Tyrosyl Phosphorylation of Insulin Receptor Substrate-1. *The Journal of Biological Chemistry*, *270*(24), 14685–14692.

Auer, F., Vagionitis, S., & Czopka, T. (2018). Evidence for Myelin Sheath Remodeling in the CNS Revealed by In Vivo Imaging. *Current Biology*, *28*(4), 549–559. doi:10.1016/j.cub.2018.01.017

Baer, A. S., Syed, Y. A., Kang, S. U., Mitteregger, D., Vig, R., Ffrench-Constant, C., Franklin, R. J. M., Altmann, F., Lubec, G., & Kotter, M. R. (2009). Myelin-mediated inhibition of oligodendrocyte precursor differentiation can be overcome by pharmacological modulation of Fyn-RhoA and protein kinase C signalling. *Brain*, *132*(2), 465–481. doi:10.1093/brain/awn334

Baraban, M., Koudelka, S., & Lyons, D. A. (2018). Ca 2+ activity signatures of myelin sheath formation and growth in vivo. *Nature Neuroscience*, *21*(1), 19–25. doi:10.1038/s41593-017-0040-x

Bateman, A. (2019). UniProt: A worldwide hub of protein knowledge. *Nucleic Acids Research*, *47*(D1), D506–D515. doi:10.1093/nar/gky1049

Bharti, P., Schliebs, W., Schievelbusch, T., Neuhaus, A., David, C., Kock, K., Herrmann, C., Meyer, H. E., Wiese, S., Warscheid, B., Theiss, C., & Erdmann, R. (2011). PEX14 is required for microtubule-based peroxisome motility in human cells. *Journal of Cell Science*, *124*(10), 1759–1768. doi:10.1242/jcs.079368

Bilder, D., & Perrimon, N. (2000). Localization of apical epithelial determinants by the basolateral PDZ protein Scribble. *Nature*, *403*(6770), 676–680. doi:10.1038/35001108

Bläser, S., Horn, J., Würmell, P., Bauer, H., Strümpell, S., Nurden, P., Pagenstecher, A., Busse, A., Wunderle, D., Hainmann, I., & Zieger, B. (2004). The novel human platelet septin SEPT8 is an interaction partner of SEPT4. *Thrombosis and Haemostasis*, *91*(5), 959–966. doi:10.1160/TH03-09-0578

Bockstaele, L., Kooken, H., Libert, F., Paternot, S., Dumont, J. E., de Launoit, Y., Roger, P. P., & Coulonval, K. (2006). Regulated Activating Thr172 Phosphorylation of Cyclin-Dependent Kinase 4(CDK4): Its Relationship with Cyclins and CDK "Inhibitors." *Molecular and Cellular Biology*, *26*(13), 5070–5085. doi:10.1128/mcb.02006-05

Bolis, A., Coviello, S., Visigalli, I., Taveggia, C., Bachi, A., Chishti, A. H., Hanada, T., Quattrini, A., Previtali, S. C., Biffi, A., & Bolino, A. (2009). Dlg1, Sec8, and Mtmr2 regulate membrane homeostasis in Schwann cell myelination. *Journal of Neuroscience*, *29*(27), 8858–8870. doi:10.1523/JNEUROSCI.1423-09.2009

Bouvrée, K., Larrivée, B., Lv, X., Yuan, L., DeLafarge, B., Freitas, C., Mathivet, T., Bréant, C., Tessier-Lavigne, M., Bikfalvi, A., Eichmann, A., & Pardanaud, L. (2008). Netrin-1 inhibits sprouting angiogenesis in developing avian embryos. *Developmental Biology*, *318*(1), 172–183. doi:10.1016/j.ydbio.2008.03.023

Brenner, S. (1974). The genetics of *Caenorabditis elegans*. *Genetics*, *77*(May), 71–94. doi:10.1016/S0047-2484(78)80101-8

Brill, M. H., Waxman, S. G., Moore, J. W., & Joyner, R. W. (1977). Conduction velocity and spike configuration in myelinated fibres: Computed dependence on internode distance. *Journal of Neurology, Neurosurgery and Psychiatry*, *40*(8), 769–774. doi:10.1136/jnnp.40.8.769

Bull, S.-J., Bin, J. M., Beaumont, E., Boutet, A., Krimpenfort, P., Sadikot, A. F., & Kennedy, T. E. (2014). Progressive Disorganization of Paranodal Junctions and Compact Myelin Due to Loss of DCC Expression by Oligodendrocytes. *Journal of Neuroscience*, *34*(29), 9768–9778. doi:10.1523/JNEUROSCI.0448-14.2014

Burda, P., Kuster, A., Hjalmarson, O., Suormala, T., Bürer, C., Lutz, S., Roussey, G., Christa, L., Asin-Cayuela, J., Kollberg, G., Andersson, B. A., Watkins, D., Rosenblatt, D. S., Fowler, B., Holme, E., Froese, D. S., & Baumgartner, M. R. (2015). Characterization and review of MTHFD1 deficiency: four new patients, cellular delineation and response to folic and folinic acid treatment. *Journal of Inherited Metabolic*

Disease, *38*(5), 863–872. doi:10.1007/s10545-015-9810-3

Burgess, R. W., Jucius, T. J., & Ackerman, S. L. (2006). Motor Axon Guidance of the Mammalian Trochlear and Phrenic Nerves : Dependence on the Netrin Receptor Unc5c and Modifier Loci. *Journal of Neuroscience*, *26*(21), 5756–5766. doi:10.1523/JNEUROSCI.0736-06.2006

Buser, A. M., Erne, B., Werner, H. B., Nave, K. A., & Schaeren-Wiemers, N. (2009). The septin cytoskeleton in myelinating glia. *Molecular and Cellular Neuroscience*, *40*(2), 156–166. doi:10.1016/j.mcn.2008.10.002

Buttermore, E. D., Dupree, J. L., Cheng, G., An, X., Tessarollo, L., & Bhat, M. A. (2011). The cytoskeletal adaptor protein band 4.1B is required for the maintenance of paranodal axoglial septate junctions in myelinated axons. *Journal of Neuroscience*, *31*(22), 8013–8024. doi:10.1523/JNEUROSCI.1015-11.2011

Cannon, K. S., Woods, B. L., Crutchley, J. M., & Gladfelter, A. S. (2019). An amphipathic helix enables septins to sense micrometer-scale membrane curvature. *Journal of Cell Biology*, *218*(4), 1128–1137. doi:10.1083/jcb.201807211

Castello, A., Fischer, B., Eichelbaum, K., Horos, R., Beckmann, B. M., Strein, C., Davey, N. E., Humphreys, D. T., Preiss, T., Steinmetz, L. M., Krijgsveld, J., & Hentze, M. W. (2012). Insights into RNA Biology from an Atlas of Mammalian mRNA-Binding Proteins. *Cell*, *149*(6), 1393–1406. doi:10.1016/j.cell.2012.04.031

Castets, M., Coissieux, M. M., Delloye-Bourgeois, C., Bernard, L., Delcros, J. G., Bernet, A., Laudet, V., & Mehlen, P. (2009). Inhibition of Endothelial Cell Apoptosis by Netrin-1 during Angiogenesis. *Developmental Cell*, *16*(4), 614–620. doi:10.1016/j.devcel.2009.02.006

Castro, F. De, Bribián, A., & Ortega, C. (2013). Regulation of oligodendrocyte precursor migration during development , in adulthood and in pathology. *Cellular and Molecular Life Sciences*, *70*, 4355–4368. doi:10.1007/s00018-013-1365-6

Chan, S. S. Y., Zheng, H., Su, M. W., Wilk, R., Killeen, M. T., Hedgecock, E. M., & Culotti, J. G. (1996). UNC-40, a C. elegans homolog of DCC (Deleted in Colorectal Cancer), is required in motile cells responding to UNC-6 netrin cues. *Cell*, *87*(2), 187–195. doi:10.1016/S0092-8674(00)81337-9

Chang, K. J., Redmond, S. A., & Chan, J. R. (2016). Remodeling myelination: Implications for mechanisms of neural plasticity. *Nature Neuroscience*, *19*(2), 190–197. doi:10.1038/nn.4200

Chen, J.-W., Dodia, C., Feinstein, S. I., Jain, M. K., & Fisher, A. B. (2000). 1-Cys Peroxiredoxin, a Bifunctional Enzyme with Glutathione Peroxidase and Phospholipase A $_2$ Activities. *Journal of Biological Chemistry*, *275*(37), 28421–28427. doi:10.1074/jbc.M005073200

Cheng, J., Moyer, B. D., Milewski, M., Loffing, J., Ikeda, M., Mickle, J. E., Cutting, G. R., Li, M., Stanton, B. A., & Guggino, W. B. (2002). A golgi-associated PDZ domain protein modulates cystic fibrosis transmembrane regulator plasma membrane expression. *Journal of Biological Chemistry*, *277*(5), 3520–3529. doi:10.1074/jbc.M110177200

Chu, C. H., & Cheng, D. (2007). Expression, purification, characterization of human 3-methylcrotonyl-CoA carboxylase (MCCC). *Protein Expression and Purification*, *53*(2), 421–427. doi:10.1016/j.pep.2007.01.012

Cirillo, N., Lanza, M., De Rosa, A., Cammarota, M., La Gatta, A., Gombos, F., & Lanza, A. (2008). The most widespread desmosomal cadherin, desmoglein 2, is a novel target of caspase 3-mediated apoptotic machinery. *Journal of Cellular Biochemistry*, *103*(2), 598–606. doi:10.1002/jcb.21431

Colavita, A., & Culotti, J. G. (1998). Suppressors of ectopic UNC-5 growth cone steering identify eight genes involved in axon guidance in Caenorhabditis elegans. *Developmental Biology*, *194*, 72–85. Retrieved from http://www.wormbase.org/db/misc/paper?name=WBPaper00003014

Cotter, L., Özçelik, M., Jacob, C., Pereira, J. A., Locher, V., Baumann, R., Relvas, J. B., Suter, U., & Tricaud, N. (2010). Dlg1-PTEN Interaction Regulates Myelin Thickness to Prevent Damaging Peripheral Nerve Overmyelination. *Science*, *328*(June), 1415–1419.

Datta, D., Anbarasu, K., Rajabather, S., Priya, R. S., Desai, P., & Mahalingam, S. (2015). Nucleolar GTP-binding protein-1 (NGP-1) promotes G<inf>1</inf>to S phase transition by activating cyclin-dependent kinase inhibitor p21$^{Cip1/Waf1}$. *Journal of Biological Chemistry*, *290*(35), 21536–21552. doi:10.1074/jbc.M115.637280

de Faria Jr., O. (2015). *New regulators of oligodendrocyte development and CNS myelin organization*. McGill University.

Delettre, C., Yuste, V. J., Moubarak, R. S., Bras, M., Lesbordes-Brion, J. C., Petres, S., Bellalou, J., & Susin, S. A. (2006). AIFsh, a novel apoptosis-inducing factor (AIF) pro-apoptotic isoform with potential pathological relevance in human cancer. *Journal of Biological Chemistry*, *281*(10), 6413–6427. doi:10.1074/jbc.M509884200

Denisenko-Nehrbass, N., Oguievetskaia, K., Goutebroze, L., Galvez, T., Yamakawa, H., Ohara, O., Carnaud, M., & Girault, J. A. (2003). Protein 4.1B associates with both Caspr/paranodin and Caspr2 at paranodes and juxtaparanodes of myelinated fibres. *European Journal of Neuroscience*, *17*, 411–416. doi:10.1046/j.1460-9568.2003.02441.x

Dessaud, E., Yang, L. L., Hill, K., Cox, B., Ulloa, F., Ribeiro, A., Mynett, A., Novitch, B. G., & Briscoe, J. (2007). Interpretation of the sonic hedgehog morphogen gradient by a temporal adaptation mechanism. *Nature*, *450*(7170), 717–720. doi:10.1038/nature06347

Dhaunchak, A. S., Becker, C., Schulman, H., De Faria, O., Rajasekharan, S., Banwell, B., Colman, D. R., & Bar-Or, A. (2012). Implication of perturbed axoglial apparatus in early pediatric multiple sclerosis. *Annals of Neurology*, *71*(5), 601–613. doi:10.1002/ana.22693

Dillon, A. K., Jevince, A. R., Hinck, L., Ackerman, S. L., Lu, X., Tessier-Lavigne, M., & Kaprielian, Z. (2007). UNC5C is required for spinal accessory motor neuron development. *Molecular and Cellular Neuroscience*, *35*(3), 482–489. doi:10.1016/j.mcn.2007.04.011

Dziedzic, T., Metz, I., Dallenga, T., König, F. B., Müller, S., Stadelmann, C., & Brück, W. (2010). Wallerian Degeneration : A Major Component of Early Axonal Pathology in Multiple Sclerosis. *Brain Pathology*, *20*, 976–985. doi:10.1111/j.1750-3639.2010.00401.x

Eisenman, L. M., & Brothers, R. (1998). Rostral Cerebellar Malformation (rcm/rcm): A Murine Mutant to Study Regionalization of the Cerebellum. *Journal of Comparative Neurology*, *394*, 106–117.

Engelkamp, D. (2002). Cloning of three mouse Unc5 genes and their expression patterns at mid-gestation. *Mechanisms of Development*, *118*, 191–197. doi:10.1016/S0925-4773(02)00248-4

Erwig, M. S., Patzig, J., Steyer, A. M., Dibaj, P., Heilmann, M., Heilmann, I., Jung, R. B., Kusch, K., Möbius, W., Jahn, O., Nave, K. A., & Werner, H. B. (2019). Anillin facilitates septin assembly to prevent pathological outfoldings of central nervous system myelin. *ELife*, *8*, 1–18. doi:10.7554/eLife.43888

Escalante, C., & Yang, D. C. H. (1993). Expression of human Aspartyl-tRNA synthetase in Escherichia coli. *Journal of Biological Chemistry*, *268*(8), 6014–6023.

Etxeberria, A., Hokanson, K. C., Dao, D. Q., Mayoral, S. R., Mei, F., Redmond, S. A., Ullian, E. M., & Chan, J. R. (2016). Dynamic modulation of myelination in response to visual stimuli alters optic nerve conduction velocity. *Journal of Neuroscience*, *36*(26), 6937–6948. doi:10.1523/JNEUROSCI.0908-16.2016

Fanning, A. S., Jameson, B. J., Jesaitis, L. A., & Anderson, J. M. (1998). The tight junction protein ZO-1 establishes a link between the transmembrane protein occludin and the actin cytoskeleton. *Journal of Biological Chemistry*, *273*(45), 29745–29753. doi:10.1074/jbc.273.45.29745

Fantin, V. R., Sparling, J. D., Slot, J. W., Keller, S. R., Lienhard, G. E., & Lavan, B. E. (1998). Characterization of insulin receptor substrate 4 in human embryonic kidney 293 cells. *Journal of Biological Chemistry*, *273*(17), 10726–10732. doi:10.1074/jbc.273.17.10726

Fei, J., Ishii, H., Hoeksema, M. A., Meitinger, F., Kassavetis, G. A., Glass, C. K., Ren, B., & Kadonaga, J. T. (2018). NDF, a nucleosome-destabilizing factor that facilitates transcription through nucleosomes. *Genes and Development*, *32*(9–10), 682–694. doi:10.1101/gad.313973.118

Finci, L., Zhang, Y., Meijers, R., & Wang, J. H. (2015). Signaling mechanism of the netrin-1 receptor DCC in axon guidance. *Progress in Biophysics and Molecular Biology*, *118*(3), 153–160. doi:10.1016/j.pbiomolbio.2015.04.001

Finehout, E. J., & Lee, K. H. (2004). An Introduction to Mass Spectrometry Applications in Biological Research *, 93–100.

Finger, J. H., Bronson, R. T., Harris, B., Johnson, K., Przyborski, S. A., & Ackerman, S. L. (2002). The netrin 1 receptors Unc5h3 and Dcc are necessary at multiple choice points for the guidance of corticospinal tract axons. *Journal of Neuroscience*, *22*(23), 10346–10356. doi:10.1523/jneurosci.22-23-10346.2002

Fink, A. J., Englund, C., Daza, R. A. M., Pham, D., Lau, C., Nivison, M., Kowalczyk, T., & Hevner, R. F. (2006). Development of the deep cerebellar nuclei: Transcription factors and cell migration from the rhombic lip. *Journal of Neuroscience*, *26*(11), 3066–3076. doi:10.1523/JNEUROSCI.5203-05.2006

Firestein, B. L., & Rongo, C. (2001). DLG-1 is a MAGUK similar to SAP97 and is required for adherens junction formation. *Molecular Biology of the Cell*, *12*(11), 3465–3475. doi:10.1091/mbc.12.11.3465

Freitas, C., Larrivée, B., & Eichmann, A. (2008). Netrins and UNC5 receptors in angiogenesis. *Angiogenesis*, *11*(1), 23–29. doi:10.1007/s10456-008-9096-2

Friede, R. L., Benda, M., Dewitz, A., & Stoll, P. (1984). Relations between axon length and axon caliber. Is maximum conduction velocity the factor controlling the evolution of nerve structure? *Journal of the Neurological Sciences*, *63*(3), 369–380. doi:10.1016/0022-510X(84)90160-6

Fukao, T., Yamaguchi, S., Kano, M., Orii, T., Fujiki, Y., Osumi, T., & Hashimoto, T. (1990). Molecular cloning and sequence of the complementary DNA encoding human mitochondrial acetoacetyl-coenzyme a thiolase and study of the variant enzymes in cultured fibroblasts from patients with 3-ketothiolase deficiency. *Journal of Clinical Investigation*, *86*(6), 2086–2092. doi:10.1172/JCI114946

Fünfschilling, U., Supplie, L. M., Mahad, D., Boretius, S., Saab, A. S., Edgar, J., … Nave, K. A. (2012). Glycolytic oligodendrocytes maintain myelin and long-term axonal integrity. *Nature*, *485*(7399), 517–521. doi:10.1038/nature11007

Garaeva, A. A., Oostergetel, G. T., Gati, C., Guskov, A., Paulino, C., & Slotboom, D. J. (2018). Cryo-EM structure of the human neutral amino acid transporter ASCT2. *Nature Structural and Molecular Biology*,

25(6), 515–521. doi:10.1038/s41594-018-0076-y
Gaudet, P., Livstone, M. S., Lewis, S. E., & Thomas, P. D. (2011). Phylogenetic-based propagation of functional annotations within the Gene Ontology consortium. *Briefings in Bioinformatics*, *12*(5), 449–462. doi:10.1093/bib/bbr042
Geisbrecht, B. V., Dowd, K. A., Barfield, R. W., Longo, P. A., & Leahy, D. J. (2003). Netrin binds discrete subdomains of DCC and UNC5 and mediates interactions between DCC and heparin. *Journal of Biological Chemistry*, *278*(35), 32561–32568. doi:10.1074/jbc.M302943200
Gerhardt, H., Golding, M., Fruttiger, M., Ruhrberg, C., Lundkvist, A., Abramsson, A., Jeltsch, M., Mitchell, C., Alitalo, K., Shima, D., & Betsholtz, C. (2003). VEGF guides angiogenic sprouting utilizing endothelial tip cell filopodia. *Journal of Cell Biology*, *161*(6), 1163–1177. doi:10.1083/jcb.200302047
Gillespie, M. J., & Stein, R. B. (1983). The relationship between axon diameter, myelin thickness and conduction velocity during atrophy of mammalian peripheral nerves. *Brain Research*, *259*(1), 41–56. doi:10.1016/0006-8993(83)91065-X
Godement, P., Salaün, J., & Imbert, M. (1984). Prenatal and postnatal development of retinogeniculate and retinocollicular projections in the mouse. *Journal of Comparative Neurology*, *230*(4), 552–575. doi:10.1002/cne.902300406
Godreau, D., Vranckx, R., Maguy, A., Rücker-Martin, C., Goyenvalle, C., Abdelshafy, S., Tessier, S., Couétil, J. P., & Hatem, S. N. (2002). Expression, regulation and role of the MAGUK protein SAP-97 in human atrial myocardium. *Cardiovascular Research*, *56*(3), 433–442. doi:10.1016/S0008-6363(02)00602-8
Goldowitz, D., & Hamre, K. (1998). The cells and molecules that make a cerebellum. *Trends in Neuroscience*, *21*(9), 375–382.
Goldowitz, D., Hamre, K. M., Przyborski, S. A., & Ackerman, S. L. (2000). Granule cells and cerebellar boundaries: Analysis of Unc5h3 mutant chimeras. *Journal of Neuroscience*, *20*(11), 4129–4137. doi:10.1523/jneurosci.20-11-04129.2000
González-Mariscal, L., Betanzos, A., & Ávila-Flores, A. (2000). MAGUK proteins: Structure and role in the tight junction. *Seminars in Cell and Developmental Biology*, *11*(4), 315–324. doi:10.1006/scdb.2000.0178
Gow, A., Southwood, C. M., Li, J. S., Pariali, M., Riordan, G. P., Brodie, S. E., Danias, J., Bronstein, J. M., Kachar, B., & Lazzarini, R. A. (1999). CNS Myelin and Sertoli Cell Tight Junction Strands Are Absent in Osp / Claudin-11 Null Mice. *Cell*, *99*, 649–659.
Guijarro, P., Simó, S., Pascual, M., Abasolo, I., Del Río, J. A., & Soriano, E. (2006). Netrin1 exerts a chemorepulsive effect on migrating cerebellar interneurons in a Dcc-independent way. *Molecular and Cellular Neuroscience*, *33*(4), 389–400. doi:10.1016/j.mcn.2006.08.010
Haapalainen, A. M., Meriläinen, G., Pirilä, P. L., Kondo, N., Fukao, T., & Wierenga, R. K. (2007). Crystallographic and kinetic studies of human mitochondrial acetoacetyl-CoA thiolase: The importance of potassium and chloride ions for its structure and function. *Biochemistry*, *46*(14), 4305–4321. doi:10.1021/bi6026192
Hamelin, M., Zhou, Y., Su, M.-W., Scott, I. M., & Culotti, J. G. (1993). Expression of the UNC-5 guidance receptor in the touch neurons of C. elegans steers their axons dorsally. *Nature*, *364*, 327–330. Retrieved from http://www.wormbase.org/db/misc/paper?name=WBPaper00021198
Hamilton, N. B., Clarke, L. E., Arancibia-Carcamo, I. L., Kougioumtzidou, E., Matthey, M., Káradóttir, R., Whiteley, L., Bergersen, L. H., Richardson, W. D., & Attwell, D. (2017). Endogenous GABA controls oligodendrocyte lineage cell number, myelination, and CNS internode length. *Glia*, *65*(2), 309–321. doi:10.1002/glia.23093
Hammarlund, M., Jorgensen, E. M., & Bastiani, M. J. (2007). Axons break in animals lacking β-spectrin. *Journal of Cell Biology*, *176*(3), 269–275. doi:10.1083/jcb.200611117
Hangen, E., De Zio, D., Bordi, M., Zhu, C., Dessen, P., Caffin, F., … Modjtahedi, N. (2010). A brain-specific isoform of mitochondrial apoptosis-inducing factor: AIF2. *Cell Death and Differentiation*, *17*(7), 1155–1166. doi:10.1038/cdd.2009.211
Hartwell, L. H. (1971). Genetic Control of the Cell Division Cycle in Yeast. *Experimental Cell Research*, *69*(2), 265–276.
Hata, K., Kaibuchi, K., Inagaki, S., & Yamashita, T. (2009). Unc5B associates with LARG to mediate the action of repulsive guidance molecule. *Journal of Cell Biology*, *184*(5), 737–750. doi:10.1083/jcb.200807029
Hauser, M., Yan, R., Li, W., Repina, N. A., Schaffer, D. V, & Xu, K. (2018). The Spectrin-Actin-Based Periodic Cytoskeleton as a Conserved Nanoscale Scaffold and Ruler of the Neural Stem Cell Lineage. *Cell Reports*, *24*, 1512–1522. doi:10.1016/j.celrep.2018.07.005
Hayakawa, S., Shiratori, S., Yamato, H., Kameyama, T., Kitatsuji, C., Kashigi, F., … Takaoka, A. (2011). ZAPS is a potent stimulator of signaling mediated by the RNA helicase RIG-I during antiviral responses. *Nature Immunology*, *12*(1), 37–44. doi:10.1038/ni.1963
Hedgecock, E. M., Culotti, J. G., & Hall, D. H. (1990). The unc-5, unc-6, and unc-40 genes guide circumferential migrations of pioneer axons and mesodermal cells on the epidermis in C. elegans. *Neuron*,

4, 61–85.
Hill, R. A., Li, A. M., & Grutzendler, J. (2018). Lifelong cortical myelin plasticity and age-related degeneration in the live mammalian brain. *Nature Neuroscience*, *21*(5), 683–695. doi:10.1038/s41593-018-0120-6
Holleman, J., & Marchese, A. (2014). The ubiquitin ligase deltex-3l regulates endosomal sorting of the G protein-coupled receptor CXCR4. *Molecular Biology of the Cell*, *25*(12), 1892–1904. doi:10.1091/mbc.E13-10-0612
Hong, K., Hinck, L., Poo, M., Nishiyama, M., Stein, E., & Tessier-Lavigne, M. (1999). A Ligand-Gated Association between Cytoplasmic Domains of UNC5 and DCC Family Receptors Converts Netrin-Induced Growth Cone Attraction to Repulsion. *Cell*, *97*(7), 927–941. doi:10.1016/s0092-8674(00)80804-1
Hortsch, M., & Margolis, B. (2003). Septate and paranodal junctions: kissing cousins. *Trends in Cell Biology*, *13*(11), 557–561. doi:10.1016/j.tcb.2003.09.003
Howell, O. W., Palser, A., Polito, A., Melrose, S., Zonta, B., Scheiermann, C., Vora, A. J., Brophy, P. J., & Reynolds, R. (2006). Disruption of neurofascin localization reveals early changes preceding demyelination and remyelination in multiple sclerosis. *Brain*, *129*(12), 3173–3185. doi:10.1093/brain/awl290
Huang, D. W., Sherman, B. T., & Lempicki, R. A. (2009a). Bioinformatics enrichment tools: Paths toward the comprehensive functional analysis of large gene lists. *Nucleic Acids Research*, *37*(1), 1–13. doi:10.1093/nar/gkn923
Huang, D. W., Sherman, B. T., & Lempicki, R. A. (2009b). Systematic and integrative analysis of large gene lists using DAVID bioinformatics resources. *Nature Protocols*, *4*(1), 44–57. doi:10.1038/nprot.2008.211
Huang, X., Shi, Z., Wang, W., Bai, J., Chen, Z., Xu, J., Zhang, D., & Fu, S. (2007). Identification and characterization of a novel protein ISOC2 that interacts with p16INK4a. *Biochemical and Biophysical Research Communications*, *361*(2), 287–293. doi:10.1016/j.bbrc.2007.06.181
Huang, Y., Shi, H., Zhou, H., Song, X., Yuan, S., & Luo, Y. (2006). The angiogenic function of nucleolin is mediated by vascular endothelial growth factor and nonmuscle myosin. *Blood*, *107*(9), 3564–3571. doi:10.1182/blood-2005-07-2961
Huber, A. B., Kolodkin, A. L., Ginty, D. D., & Cloutier, J.-F. (2003). SIGNALING AT THE GROWTH CONE : Ligand-Receptor Complexes and the Control of Axon Growth and Guidance. *Annual Review of Neuroscience*, *26*(1), 509–563. doi:10.1146/annurev.neuro.26.010302.081139
Hughes, C. A., & Bennett, V. (1995). Adducin: a Physical Model with Implications for Function in Assembly of Spectrin-Actin Complexes. *The Journal of Biological Chemistry*, *270*(32), 18990–18996.
Hughes, E. G., Orthmann-murphy, J. L., Langseth, A. J., & Bergles, D. E. (2018). Myelin remodeling through experience-dependent oligodendrogenesis in the adult somatosensory cortex. *Nature Neuroscience*, *21*, 696–706. doi:10.1038/s41593-018-0121-5
Hum, W., & Mackenzie, R. E. (1991). Expression of active domains of a human folate-dependent trifunctional enzyme in escherichia coli. *Protein Engineering, Design and Selection*, *4*(4), 493–500. doi:10.1093/protein/4.4.493
Ikenouchi, J., Umeda, K., Tsukita, S., Furuse, M., & Tsukita, S. (2007). Requirement of ZO-1 for the formation of belt-like adherens junctions during epithelial cell polarization. *Journal of Cell Biology*, *176*(6), 779–786. doi:10.1083/jcb.200612080
Ioannidou, K., Anderson, K. I., Strachan, D., Edgar, J. M., & Barnett, S. C. (2012). Time-lapse imaging of the dynamics of CNS glial-axonal interactions in vitro and ex vivo. *PLoS ONE*, *7*(1). doi:10.1371/journal.pone.0030775
Ishii, N., Wadsworth, W. G., Stern, B. D., Culotti, J. G., & Hedgecock, E. M. (1992). UNC-6, a laminin-related protein, guides cell and pioneer axon migrations in C. elegans. *Neuron*, *9*(5), 873–881. doi:10.1016/0896-6273(92)90240-E
Isogai, S., Horiguchi, M., & Weinstein, B. M. (2001). The vascular anatomy of the developing zebrafish: An atlas of embryonic and early larval development. *Developmental Biology*, *230*(2), 278–301. doi:10.1006/dbio.2000.9995
Ivanovic, A., Horresh, I., Golan, N., Spiege, I., Sabanay, H., Frechter, S., Ohno, S., Terada, N., Möbius, W., Rosenbluth, J., Brose, N., & Peles, E. (2012). The cytoskeletal adapter protein 4.1G organizes the internodes in peripheral myelinated nerves. *Journal of Cell Biology*, *196*(3), 337–344. doi:10.1083/jcb.201111127
Jaglin, X. H., Poirier, K., Saillour, Y., Buhler, E., Tian, G., Bahi-Buisson, N., … Chelly, J. (2009). Mutations in the B-tubulin gene TUBB2B result in asymmetrical polymicrogyria. *Nature Genetics*, *41*(6), 746–752. doi:10.1038/ng.380
Jarjour, A. A., Boyd, A., Dow, L. E., Holloway, R. K., Goebbels, S., Humbert, P. O., Williams, A., & Ffrench-Constant, C. (2015). The Polarity Protein Scribble Regulates Myelination and Remyelination in the Central Nervous System. *PLoS Biology*, 1–23. doi:10.1371/journal.pbio.1002107
Jarjour, A. A., Bull, S.-J., Almasieh, M., Rajasekharan, S., Baker, K. A., Mui, J., Antel, J. P., Di Polo, A., &

Kennedy, T. E. (2008). Maintenance of Axo-Oligodendroglial Paranodal Junctions Requires DCC and Netrin-1. *Journal of Neuroscience*, *28*(43), 11003–11014. doi:10.1523/JNEUROSCI.3285-08.2008
Jarjour, A. A., Manitt, C., Moore, S. W., Thompson, K. M., Yuh, S., & Kennedy, T. E. (2003). Netrin-1 Is a Chemorepellent for Oligodendrocyte Precursor Cells in the Embryonic Spinal Cord. *Journal of Neuroscience*, *23*(9), 3735–3744.
Jin, D. Y., Chae, H. Z., Rhee, S. G., & Jeang, K. T. (1997). Regulatory role for a novel human thioredoxin peroxidase in NF-κB activation. *Journal of Biological Chemistry*, *272*(49), 30952–30961. doi:10.1074/jbc.272.49.30952
Joosten, E. A. J. (1990). An ultrastructural double-labelling method: immunohistochemical localization of cell adhesion molecule L1 on HRP-labelled developing corticospinal tract axons in the rat. *Histochemistry*, *94*(6), 645–651. doi:10.1007/BF00271992
Joyner, A. L., Liu, A., & Millet, S. (2000). Otx2, Gbx2 and Fgf8 interact to position and maintain a mid-hindbrain organizer. *Current Opinion in Cell Biology*, *12*(6), 736–741. doi:10.1016/S0955-0674(00)00161-7
Kamasawa, N., Sik, A., Morita, M., Yasumura, T., Davidson, K. G. V., Nagy, J. I., & Rash, J. E. (2005). Connexin-47 and connexin-32 in gap junctions of oligodendrocyte somata, myelin sheaths, paranodal loops and Schmidt-Lanterman incisures: Implications for ionic homeostasis and potassium siphoning. *Neuroscience*, *136*(1), 65–86. doi:10.1016/j.neuroscience.2005.08.027
Kanai, Y., Segawa, H., Miyamoto, K. I., Uchino, H., Takeda, E., & Endou, H. (1998). Expression cloning and characterization of a transporter for large neutral amino acids activated by the heavy chain of 4F2 antigen (CD98). *Journal of Biological Chemistry*, *273*(37), 23629–23632. doi:10.1074/jbc.273.37.23629
Kanehisa, M. (2019). Toward understanding the origin and evolution of cellular organisms. *Protein Science*, (August), 1947–1951. doi:10.1002/pro.3715
Kanehisa, M., & Goto, S. (2000). KEGG: Kyoto Encyclopedia of Genes and Genomes. *Nucleic Acids Research*, *28*(1), 27–30.
Kanehisa, M., Sato, Y., Furumichi, M., Morishima, K., & Tanabe, M. (2019). New approach for understanding genome variations in KEGG. *Nucleic Acids Research*, *47*(D1), D590–D595. doi:10.1093/nar/gky962
Kang, D., Gho, Y. S., Suh, M., & Kang, C. (2002). Highly Sensitive and Fast Protein Detection with Coomassie Brilliant Blue in Sodium Dodecyl Sulfate-Polyacrylamide Gel Electrophoresis, *23*(11), 1511–1512.
Kang, S. W., Baines, I. C., & Rhee, S. G. (1998). Characterization of a mammalian peroxiredoxin that contains one conserved cysteine. *Journal of Biological Chemistry*, *273*(11), 6303–6311. doi:10.1074/jbc.273.11.6303
Karaulanov, E., Böttcher, R. T., Stannek, P., Wei, W., Rau, M., Ogata, S., Cho, K. W. Y., & Niehrs, C. (2009). Unc5B interacts with FLRT3 and Rnd1 to modulate cell adhesion in Xenopus embryos. *PLoS ONE*, *4*(5), 2–9. doi:10.1371/journal.pone.0005742
Katafiasz, B. J., Nieman, M. T., Wheelock, M. J., & Johnson, K. R. (2003). Characterization of cadherin-24, a novel alternatively spliced type II cadherin. *Journal of Biological Chemistry*, *278*(30), 27513–27519. doi:10.1074/jbc.M304119200
Katagiri, T., Ozaki, K., Fujiwara, T., Shimizu, F., Kawai, A., Okuno, S., Suzuki, M., Nakamura, Y., Takahashi, E., & Hirai, Y. (1996). Cloning, expression and chromosome mapping of adducin-like 70 (ADDL), a human cDNA highly homologous to human erythrocyte adducin. *Cytogenetic and Genome Research*, *74*, 90–95.
Kausalya, J. P., Phua, D. C. Y., & Hunziker, W. (2004). Association of ARVCF with Zonula Occludens (ZO)-1 and ZO-2: Binding to PDZ-Domain Proteins and Cell-Cell Adhesion Regulate Plasma Membrane and Nuclear Localization of ARVCF. *Molecular Biology of the Cell*, *15*(December), 5503–5515. doi:10.1091/mbc.E04
Keleman, K., & Dickson, B. J. (2001). Short- and long-range repulsion by the Drosophila Unc5 Netrin receptor. *Neuron*, *32*(4), 605–617. doi:10.1016/S0896-6273(01)00505-0
Kennedy, T. E., Serafini, T., de la Torre, J. R., & Tessier-Lavigne, M. (1994). Netrins are diffusible chemotropic factors for commissural axons in the embryonic spinal cord. *Cell*, *78*(3), 425–435. doi:10.1016/0092-8674(94)90421-9
Kim, D., & Ackerman, S. L. (2011). The UNC5C netrin receptor regulates dorsal guidance of mouse hindbrain axons. *Journal of Neuroscience*, *31*(6), 2167–2179. doi:10.1523/JNEUROSCI.5254-10.2011
Kim, D. I., & Roux, K. J. (2016). Filling the Void : Proximity- Based Labeling of Proteins in Living Cells. *Trends in Cell Biology*, *26*(11), 804–817. doi:10.1016/j.tcb.2016.09.004
Kinoshita, M. (2006). Diversity of septin scaffolds. *Current Opinion in Cell Biology*, *18*(1), 54–60. doi:10.1016/j.ceb.2005.12.005
Kirchner, F., Schuetz, A., Boldt, L. H., Martens, K., Dittmar, G., Haverkamp, W., Thierfibroer, L., Heinemann, U., & Gerull, B. (2012). Molecular insights into arrhythmogenic right ventricular cardiomyopathy caused by plakophilin-2 missense mutations. *Circulation: Cardiovascular Genetics*, *5*(4), 400–411.

doi:10.1161/CIRCGENETICS.111.961854
Klima, M., Tóth, D. J., Hexnerova, R., Baumlova, A., Chalupska, D., Tykvart, J., Rezabkova, L., Sengupta, N., Man, P., Dubankova, A., Humpolickova, J., Nencka, R., Veverka, V., Balla, T., & Boura, E. (2016). Structural insights and in vitro reconstitution of membrane targeting and activation of human PI4KB by the ACBD3 protein. *Scientific Reports*, *6*(December 2015), 1–11. doi:10.1038/srep23641
Knudsen, K. A., & Wheelock, M. J. (1992). Plakoglobin, or an 83-kD homologue distinct from β-catenin, interacts with E-cadherin and N-cadherin. *Journal of Cell Biology*, *118*(3), 671–679. doi:10.1083/jcb.118.3.671
Koch, A. W., Mathivet, T., Larrivée, B., Tong, R. K., Kowalski, J., Pibouin-Fragner, L., … Eichmann, A. (2011). Robo4 Maintains Vessel Integrity and Inhibits Angiogenesis by Interacting with UNC5B. *Developmental Cell*, *20*(1), 33–46. doi:10.1016/j.devcel.2010.12.001
Komatsuzaki, K., Dalvin, S., & Kinane, B. (2002). Modulation of Gia2 signaling by the axonal guidance molecule UNC5H2. *Biochemical and Biophysical Research Communications*, *297*, 898–905.
Korman, N. J., Eyre, R. W., Klaus-Kovtun, V., & Stanley, J. R. (1989). Demonstration of an adhering-junction molecule (plakoglobin) in the autoantigens of pemphigus foliaceus and pemphigus vulgaris. *New England Journal of Medicine*, *321*(10), 631–635.
Krasnow, A. M., Ford, M. C., Valdivia, L. E., Wilson, S. W., & Attwell, D. (2018). Regulation of developing myelin sheath elongation by oligodendrocyte calcium transients in vivo. *Nature Neuroscience*, *21*(1), 24–30. doi:10.1038/s41593-017-0031-y
Kremer, B. E., Adang, L. A., & Macara, I. G. (2007). Septins Regulate Actin Organization and Cell-Cycle Arrest through Nuclear Accumulation of NCK Mediated by SOCS7. *Cell*, *130*(5), 837–850. doi:10.1016/j.cell.2007.06.053
Krull, S., Thyberg, J., Björkroth, B., Rackwitz, H.-R., & Cordes, V. C. (2004). Nucleoporins as Components of the Nuclear Pore Complex Core Structure and Tpr as the Architectural Element of the Nuclear Basket. *Molecular Biology of the Cell*, *15*(September), 4261–4277. doi:10.1091/mbc.E04-03-0165
Kugelmann, D., Waschke, J., & Radeva, M. Y. (2015). Adducin is involved in endothelial barrier stabilization. *PLoS ONE*, *10*(5), 1–16. doi:10.1371/journal.pone.0126213
Kuhlman, P. A., Hughes, C. A., Bennett, V., & Fowler, V. M. (1996). A New Function for Adducin: Calcium/calmodulin-regulated capping of the barbed ends of actin filaments. *Journal of Biological Chemistry*, *271*(14), 7986–7991. doi:10.1074/jbc.271.14.7986
Kuhlmann, T., Lingfeld, G., Bitsch, A., Schuchardt, J., & Bru, W. (2002). Acute axonal damage in multiple sclerosis is most extensive in early disease stages and decreases over time. *Brain*, *125*, 2202–2212.
Kutty, R. K., Kutty, G., Samuel, W., Duncan, T., Bridges, C. C., El-Sherbeeny, A., Nagineni, C. N., Smith, S. B., & Wiggert, B. (2001). Molecular Characterization and Developmental Expression of NORPEG, a Novel Gene Induced by Retinoic Acid. *Journal of Biological Chemistry*, *276*(4), 2831–2840. doi:10.1074/jbc.M007421200
Kye, W. P., Grouse, D., Lee, M., Karnik, S. K., Sorensen, L. K., Murphy, K. J., Kuo, C. J., & Li, D. Y. (2004). The axonal attractant Netrin-1 is an angiogenic factor. *Proceedings of the National Academy of Sciences of the United States of America*, *101*(46), 16210–16215. doi:10.1073/pnas.0405984101
Lamhonwah, A.-M., Leclerc, D., Loyer, M., Clarizio, R., & Gravel, R. A. (1994). Correction of the Metabolic Defect in Propionic Acidemia Fibroblasts by Microinjection of a Full-Length cDNA or RNA Transcript Encoding the Propionyl-CoA Carboxylase beta Subunit. *Genomics*, *19*, 500–505.
Lane, P. W., Bronson, R. T., & Spencer, C. A. (1992). Rostral Cerebellar Malformation, (rcm): A New Recessive Mutation on Chromosome 3 of the Mouse. *The Journal of Heredity*, *83*(4), 315–318.
Laprise, P., Viel, A., & Rivard, N. (2004). Human Homolog of Disc-large Is Required for Adherens Junction Assembly and Differentiation of Human Intestinal Epithelial Cells. *Journal of Biological Chemistry*, *279*(11), 10157–10166. doi:10.1074/jbc.M309843200
Laramé, M., Chabot, C., Cloutier, M., Stenne, R., Holgado-Madruga, M., Wong, A. J., & Royal, I. (2007). The scaffolding adapter Gab1 mediates vascular endothelial growth factor signaling and is required for endothelial cell migration and capillary formation. *Journal of Biological Chemistry*, *282*(11), 7758–7769. doi:10.1074/jbc.M611327200
Larrieu-Lahargue, F., Thomas, K. R., & Li, D. Y. (2012). Netrin Ligands and Receptors: Lessons From Neurons to the Endothelium. *Trends in Cardiovascular Medicine*, *22*(2), 44–47. doi:10.1016/j.tcm.2012.06.010
Larrivée, B., Freitas, C., Trombe, M., Lv, X., DeLafarge, B., Yuan, L., … Eichmann, A. (2007). Activation of the UNC5B receptor by Netrin-1 inhibits sprouting angiogenesis. *Genes and Development*, *21*(19), 2433–2447. doi:10.1101/gad.437807
Lasiene, J., Matsui, A., Sawa, Y., Wong, F., & Horner, P. J. (2009). Age-related myelin dynamics revealed by increased oligodendrogenesis and short internodes. *Aging Cell*, *8*(2), 201–213. doi:10.1111/j.1474-9726.2009.00462.x
Lee, J., Gravel, M., Zhang, R., Thibault, P., & Braun, P. E. (2005). Process outgrowth in oligodendrocytes is

mediated by CNP, a novel microtubule assembly myelin protein. *Journal of Cell Biology*, *170*(4), 661–673. doi:10.1083/jcb.200411047

Lee, S. M., Chin, L. S., & Li, L. (2012). Charcot-marie-tooth disease-linked protein SIMPLE functions with the ESCRT machinery in endosomal trafficking. *Journal of Cell Biology*, *199*(5), 799–816. doi:10.1083/jcb.201204137

Lejmi, E., Leconte, L., Pédron-Mazoyer, S., Ropert, S., Raoul, W., Lavalette, S., … Plouët, J. (2008). Netrin-4 inhibits angiogenesis via binding to neogenin and recruitment of Unc5B. *Proceedings of the National Academy of Sciences of the United States of America*, *105*(34), 12491–12496. doi:10.1073/pnas.0804008105

Lemke, G. (1988). Unwrapping the genes of myelin. *Neuron*, *1*(7), 535–543. doi:10.1016/0896-6273(88)90103-1

Lemke, G., & Reber, M. (2005). RETINOTECTAL MAPPING: New Insights from Molecular Genetics. *Annual Review of Cell and Developmental Biology*, *21*(1), 551–580. doi:10.1146/annurev.cellbio.20.022403.093702

Leonardo, E. D., Hinck, L., Masu, M., Keino-Masu, K., Ackerman, S. L., & Tessier-Lavigne, M. (1997). Vertebrate homologues of C. elegans UNC-5 are candidate netrin receptors. *Nature*, *386*(6627), 833–838. doi:10.1038/386833a0

Leterrier, C., Potier, J., Caillol, G., Debarnot, C., Rueda Boroni, F., & Dargent, B. (2015). Nanoscale Architecture of the Axon Initial Segment Reveals an Organized and Robust Scaffold. *Cell Reports*, *13*(12), 2781–2793. doi:10.1016/j.celrep.2015.11.051

Leung-Hagesteijn, C., Spence, A. M., Stern, B. D., Zhou, Y., Su, M. W., Hedgecock, E. M., & Culotti, J. G. (1992). UNC-5, a transmembrane protein with immunoglobulin and thrombospondin type 1 domains, guides cell and pioneer axon migrations in C. elegans. *Cell*, *71*(2), 289–299. doi:10.1016/0092-8674(92)90357-I

Lewis, J. E., Wahl, J. K., Sass, K. M., Jensen, P. J., Johnson, K. R., & Wheelock, M. J. (1997). Cross-talk between adherens junctions and desmosomes depends on plakoglobin. *Journal of Cell Biology*, *136*(4), 919–934. doi:10.1083/jcb.136.4.919

Li, Y. C., Cheng, C. X., Li, Y. N., Shimada, O., & Atsumi, S. (2005). Beyond the initial axon segment of the spinal motor axon: Fasciculated microtubules and polyribosomal clusters. *Journal of Anatomy*, *206*(6), 535–542. doi:10.1111/j.1469-7580.2005.00418.x

Lockwood, C., Zaidel-Bar, R., & Hardin, J. (2009). The C. elegans Zonula Occludens Ortholog ZOO-1 Cooperates with the Cadherin-Catenin Complex to Recruit Actin during Epidermal Morphogenesis. *Current Biology*, *18*(17), 1333–1337. doi:10.1016/j.cub.2008.07.086.The

Lu, M., Forsberg, L., Höög, A., Juhlin, C. C., Vukojević, V., Larsson, C., Conigrave, A. D., Delbridge, L. W., Gill, A., Bark, C., Farnebo, L. O., & Bränström, R. (2008). Heterogeneous expression of SNARE proteins SNAP-23, SNAP-25, Syntaxin1 and VAMP in human parathyroid tissue. *Molecular and Cellular Endocrinology*, *287*(1–2), 72–80. doi:10.1016/j.mce.2008.01.028

Lu, X., le Noble, F., Yuan, L., Jiang, Q., de Lafarge, B., Sugiyama, D., Bréant, C., Claes, F., F., D. S., Thomas, J. L., Autiero, M., Carmeliet, P., Tessier-Lavigne, M., & Eichmann, A. (2004). The netrin receptor UNC5B mediates guidance events controlling morphogenesis of the vascular system. *Nature*, *432*, 179–186.

Lu, Y. C., Nazarko, O. V., Sando, R., Salzman, G. S., Li, N.-S., Südhof, T. C., & Araç, D. (2015). Structural Basis of Latrophilin-FLRT-UNC5 Interaction in Cell Adhesion. *Structure*, *23*(9), 1678–1691. doi:10.1016/j.str.2015.06.024

Lue, R. A., Brandin, E., Chan, E. P., & Branton, D. (1996). Two independent domains of hDlg are sufficient for subcellular targeting: The PDZ1-2 conformational unit and an alternatively spliced domain. *Journal of Cell Biology*, *135*(4), 1125–1137. doi:10.1083/jcb.135.4.1125

Lue, R. A., Marfatia, S. M., Branton, D., & Chishti, A. H. (1994). Cloning and characterization of hdlg: The human homologue of the Drosophila discs large tumor suppressor binds to protein 4.1. *Biochemistry*, *91*, 9818–9822. doi:10.1073/pnas.91.21.9818

Lyden, D., Young, A. Z., Zagzag, D., Yan, W., Gerald, W., O'Reilly, R., Bader, B. L., Hynes, R. O., Zhuang, Y., Manova, K., & Benezra, R. (1999). Id1 and Id3 are required for neurogenesis, angiogenesis and vascularization of tumour xenografts. *Nature*, *401*, 670–677. doi:10.1038/44334

Macneil, L. T., Hardy, W. R., Pawson, T., Wrana, J. L., & Culotti, J. G. (2009). UNC-129 regulates the balance between UNC-40 dependent and independent UNC-5 signaling pathways. *Nature Neuroscience*, *12*(2), 150–155. doi:10.1038/nn.2256.UNC-129

Manitt, C., Colicos, M. A., Thompson, K. M., Rousselle, E., Peterson, A. C., & Kennedy, T. E. (2001). Widespread Expression of Netrin-1 by Neurons and Oligodendrocytes in the Adult Mammalian Spinal Cord. *Journal of Neuroscience*, *21*(11), 3911–3922.

Manitt, C., Thompson, K. M., & Kennedy, T. E. (2004). Developmental Shift in Expression of Netrin Receptors

in the Rat Spinal Cord : Predominance of UNC-5 Homologues in Adulthood. *Journal of Neuroscience Research*, *77*, 690–700. doi:10.1002/jnr.20199
Medema, R. H., Herrera, R. E., Lam, F., & Weinberg, R. A. (1995). Growth suppression by p16ink4 requires functional retinoblastoma protein. *Proceedings of the National Academy of Sciences of the United States of America*, *92*(14), 6289–6293. doi:10.1073/pnas.92.14.6289
Merz, D. C., Zheng, H., Killeen, M. T., Krizus, A., & Culotti, J. G. (2001). Multiple Signaling Mechanisms of the UNC-6 / netrin Receptors Unc-5 and Unc-40/DCC in Vivo. *Genetics*, *158*, 1071–1080. Retrieved from http://www.ncbi.nlm.nih.gov/pubmed/?term=multiple+signaling+mechanisms+of+the+unc-6%2Fnetrin+receptors+unc-5+and+unc-40%2Fdcc
Mierzwa, A. J., Arevalo, J. C., Schiff, R., Chao, M. V., & Rosenbluth, J. (2010). Role of transverse bands in maintaining paranodal structure and axolemmal domain organization in myelinated nerve fibers: Effect on longevity in dysmyelinated mutant mice. *Journal of Comparative Neurology*, *518*(14), 2841–2853. doi:10.1002/cne.22367
Milkereit, R., Persaud, A., Vanoaica, L., Guetg, A., Verrey, F., & Rotin, D. (2015). LAPTM4b recruits the LAT1-4F2hc Leu transporter to lysosomes and promotes mTORC1 activation. *Nature Communications*, *6*(May), 1–9. doi:10.1038/ncomms8250
Mische, S. M., Mooseker, M. S., & Morrow, J. S. (1987). Erythrocyte adducin: A calmodulin-regulated actin-bundling protein that stimulates spectrin-actin binding. *Journal of Cell Biology*, *105*(6 I), 2837–2845. doi:10.1083/jcb.105.6.2837
Mitchell, K. J., Doyle L., J. L., Serafini, T., Kennedy, T. E., Tessier-Lavigne, M., Goodman, C. S., & Dickson, B. J. (1996). Genetic analysis of Netrin genes in Drosophila: Netrins guide CNS commissural axons and peripheral motor axons. *Neuron*, *17*(2), 203–215. doi:10.1016/S0896-6273(00)80153-1
Miyamoto, Y., Futamura, M., Kitamura, N., Nakamura, Y., Baba, H., & Arakawa, H. (2010). Identification of UNC5A as a novel transcriptional target of tumor suppressor p53 and a regulator of apoptosis. *International Journal of Oncology*, (36), 1253–1260. doi:10.3892/ijo
Mostowy, S., & Cossart, P. (2012). Septins: The fourth component of the cytoskeleton. *Nature Reviews Molecular Cell Biology*, *13*(3), 183–194. doi:10.1038/nrm3284
Muramatsu, F., Kidoya, H., Naito, H., Hayashi, Y., Iba, T., & Takakura, N. (2017). Plakoglobin maintains the integrity of vascular endothelial cell junctions and regulates VEGF-induced phosphorylation of VE-cadherin. *Journal of Biochemistry*, *162*(1), 55–62. doi:10.1093/jb/mvx001
Murcia-Belmonte, V., Coca, Y., Vegar, C., Negueruela, S., de Juan Romero, C., Valiño, A. J., Sala, S., DaSilva, R., Kania, A., Borrell, V., Martinez, L. M., Erskine, L., & Herrera, E. (2019). A Retino-retinal Projection Guided by Unc5c Emerged in Species with Retinal Waves. *Current Biology*, *29*(7), 1149-1160.e4. doi:10.1016/j.cub.2019.02.052
Nakajima, K. I., Hirose, H., Taniguchi, M., Kurashina, H., Arasaki, K., Nagahama, M., Tani, K., Yamamoto, A., & Tagaya, M. (2004). Involvement of BNIP1 in apoptosis and endoplasmic reticulum membrane fusion. *EMBO Journal*, *23*(16), 3216–3226. doi:10.1038/sj.emboj.7600333
Navankasattusas, S., Whitehead, K. J., Suli, A., Sorensen, L. K., Lim, A. H., Zhao, J., Park, K. W., Wythe, J. D., Thomas, K. R., Chien, C. Bin, & Li, D. Y. (2008). The netrin receptor UNC5B promotes angiogenesis in specific vascular beds. *Development*, *135*(4), 659–667. doi:10.1242/dev.013623
Naydenov, N. G., & Ivanov, A. I. (2010). Adducins Regulate Remodeling of Apical Junctions in Human Epithelial Cells. *Molecular Biology of the Cell*, *21*, 3506–3517. doi:10.1091/mbc.E10
Norris, A. D., & Lundquist, E. A. (2011). UNC-6 / netrin and its receptors UNC-5 and UNC-40 / DCC modulate growth cone protrusion in vivo in C . elegans. *Development*, *138*, 4433–4442. doi:10.1242/dev.068841
Noseda, R., Guerrero-Valero, M., Alberizzi, V., Previtali, S. C., Sherman, D. L., Palmisano, M., Huganir, R. L., Nave, K. A., Cuenda, A., Feltri, M. L., Brophy, P. J., & Bolino, A. (2016). Kif13b Regulates PNS and CNS Myelination through the Dlg1 Scaffold. *PLoS Biology*, *14*(4), 1–26. doi:10.1371/journal.pbio.1002440
Odintsova, T. I., Müller, E. C., Ivanov, A. V., Egorov, T. A., Bienert, R., Vladimirov, S. N., Kostka, S., Otto, A., Wittmann-Liebold, B., & Karpova, G. G. (2003). Characterization and analysis of posttranslational modifications of the human large cytoplasmic ribosomal subunit proteins by mass spectrometry and Edman sequencing. *Journal of Protein Chemistry*, *22*(3), 249–258. doi:10.1023/A:1025068419698
Ohno, N., Terada, N., Yamakawa, H., Komada, M., Ohara, O., Trapp, B. D., & Ohno, S. (2006). Expression of Protein 4.1G in Schwann Cells of the Peripheral Nervous System. *Journal of Neuroscience Research*, *84*, 568–577. doi:10.1002/jnr
Ozawa, M., Terada, H., & Pedraza, C. (1995). The fourth armadillo repeat of plakoglobin (γ-catenin) is required for its high affinity binding to the cytoplasmic domains of E-cadherin and desmosomal cadherin Dsg2, and the tumor suppressor APC protein. *Journal of Biochemistry*, *118*(5), 1077–1082. doi:10.1093/jb/118.5.1077
Parada, C. A., & Roeder, R. G. (1999). A novel RNA polymerase II-containing complex potentiates Tat-

enhanced HIV-1 transcription. *EMBO Journal*, *18*(13), 3688–3701. doi:10.1093/emboj/18.13.3688
Patzig, J., Erwig, M. S., Tenzer, S., Kusch, K., Dijab, P., Möbius, W., Goebbels, S., Schaeren-Wiemers, N., Nave, K.-A., & Werner, H. B. (2016). Septin/anillin filaments scaffold central nervous system myelin to accelerate nerve conduction. *ELife*, 1–21. doi:10.1016/j.jmb.2010.10.002
Paul, S., Dansithong, W., Kim, D., Rossi, J., Webster, N. J. G., Comai, L., & Reddy, S. (2006). Interaction of musleblind, CUG-BP1 and hnRNP H proteins in DM1-associated aberrant IR splicing. *EMBO Journal*, *25*(18), 4271–4283. doi:10.1038/sj.emboj.7601296
Peng, Y. F., Mandai, K., Sakisaka, T., Okabe, N., Yamamoto, Y., Yokoyama, S., Mizoguchi, A., Shiozaki, H., Monden, M., & Takai, Y. (2000). Ankycorbin: A novel actin cytoskeleton-associated protein. *Genes to Cells*, *5*(12), 1001–1008. doi:10.1046/j.1365-2443.2000.00381.x
Peters, A. (2002). The effects of normal aging on myelin and nerve fibers: A review. *Journal of Neurocytology*, *31*(8–9), 581–593. doi:10.1023/A:1025731309829
Pilichou, K., Nava, A., Basso, C., Beffagna, G., Bauce, B., Lorenzon, A., Frigo, G., Vettori, A., Valente, M., Towbin, J., Thiene, G., Danieli, G. A., & Rampazzo, A. (2006). Mutations in desmoglein-2 gene are associated with arrhythmogenic right ventricular cardiomyopathy. *Circulation*, *113*(9), 1171–1179. doi:10.1161/CIRCULATIONAHA.105.583674
Pind, S., Slominski, E., Mauthe, J., Pearlman, K., Swoboda, K. J., Wilkins, J. A., Sauder, P., & Natowicz, M. R. (2002). V490M, a common mutation in 3-phosphoglycerate dehydrogenase deficiency, causes enzyme deficiency by decreasing the yield of mature enzyme. *Journal of Biological Chemistry*, *277*(9), 7136–7143. doi:10.1074/jbc.M111419200
Pons, V., Luyet, P. P., Morel, E., Abrami, L., Van Der Goot, F. G., Parton, R. G., & Gruenberg, J. (2008). Hrs and SNX3 functions in sorting and membrane invagination within multivesicular bodies. *PLoS Biology*, *6*(9), 1942–1956. doi:10.1371/journal.pbio.0060214
Przyborski, S. A., Knowles, B. B., & Ackerman, S. L. (1998). Embryonic phenotype of Unc5h3 mutant mice suggests chemorepulsion during the formation of the rostral cerebellar boundary. *Development (Cambridge, England)*, *125*(1), 41–50. Retrieved from http://www.ncbi.nlm.nih.gov/pubmed/9389662
Purohit, A. A., Li, W., Qu, C., Dwyer, T., Shao, Q., Guan, K. L., & Liu, G. (2012). Down syndrome cell adhesion molecule (DSCAM) associates with uncoordinated-5C (UNC5C) in netrin-1-mediated growth cone collapse. *Journal of Biological Chemistry*, *287*(32), 27126–27138. doi:10.1074/jbc.M112.340174
Qian, X., Mruk, D. D., Cheng, Y., & Cheng, C. Y. (2013). RAI14 (retinoic acid induced protein 14) is an F-actin regulator. *Spermatogenesis*, *3*(2), e24824. doi:10.4161/spmg.24824
Qin, Q., Inatome, R., Hotta, A., Kojima, M., Yamamura, H., Hirai, H., Yoshizawa, T., Tanaka, H., Fukami, K., & Yanagi, S. (2006). A novel GTPase, CRAG, mediates promyelocytic leukemia protein-associated nuclear body formation and degradation of expanded polyglutamine protein. *Journal of Cell Biology*, *172*(4), 497–504. doi:10.1083/jcb.200505079
Radeva, M. Y., & Waschke, J. (2018). Mind the gap: mechanisms regulating the endothelial barrier. *Acta Physiologica*, *222*(1), 1–20. doi:10.1111/apha.12860
Rajasekharan, S., Baker, K. A., Horn, K. E., Jarjour, A. A., Antel, J. P., & Kennedy, T. E. (2009). Netrin 1 and Dcc regulate oligodendrocyte process branching and membrane extension via Fyn and RhoA. *Development*, *136*(3), 415–426. doi:10.1242/dev.018234
Rasband, M. N., Tayler, J., Kaga, Y., Yang, Y., Lappe-Siefke, C., Nave, K. A., & Bansal, R. (2005). CNP is required for maintenance of axon-glia interactions at nodes of ranvier in the CNS. *Glia*, *50*(1), 86–90. doi:10.1002/glia.20165
Reuver, S. M., & Garner, C. C. (1998). E-cadherin mediated cell adhesion recruits SAP97 into the cortical cytoskeleton. *Journal of Cell Science*, *111*(8), 1071–1080.
Rios, J. C., Rubin, M., St. Martin, M., Downey, R. T., Einheber, S., Rosenbluth, J., Levinson, S. R., Bhat, M., & Salzer, J. L. (2003). Paranodal interactions regulate expression of sodium channel subtypes and provide a diffusion barrier for the node of ranvier. *Journal of Neuroscience*, *23*(18), 7001–7011. doi:10.1523/jneurosci.23-18-07001.2003
Roberts, J. D., Herkert, J. C., Rutberg, J., Nikkel, S. M., Wiesfeld, A. C. P., Dooijes, D., Gow, R. M., van Tintelen, J. P., & Gollob, M. H. (2013). Detection of genomic deletions of PKP2 in arrhythmogenic right ventricular cardiomyopathy. *Clinical Genetics*, *83*(5), 452–456. doi:10.1111/j.1399-0004.2012.01950.x
Rosenbluth, J. (2009). Multiple functions of the paranodal junction of myelinated nerve fibers. *Journal of Neuroscience Research*, *87*(15), 3250–3258. doi:10.1002/jnr.22013
Rossant, J., & Cross, J. C. (2001). Placental development: Lessons from mouse mutants. *Nature Reviews Genetics*, *2*(7), 538–548. doi:10.1038/35080570
Round, J., & Stein, E. (2007). Netrin signaling leading to directed growth cone steering. *Current Opinion in Neurobiology*, *17*(1), 15–21. doi:10.1016/j.conb.2007.01.003
Sasaki, S., Tabata, H., Tachikawa, K., & Nakajima, K. (2008). The cortical subventricular zone-specific molecule Svet1 is part of the nuclear RNA coded by the putative Netrin receptor gene Unc5d and is

expressed in multipolar migrating cells. *Molecular and Cellular Neuroscience*, *38*(4), 474–483. doi:10.1016/j.mcn.2008.04.002
Schaeren-Wiemers, N., Bonnet, A., Erb, M., Erne, B., Bartsch, U., Kern, F., Mantei, N., Sherman, D., & Suter, U. (2004). The raft-associated protein MAL is required for maintenance of proper axon-glia interactions in the central nervous system. *Journal of Cell Biology*, *166*(5), 731–742. doi:10.1083/jcb.200406092
Scherer, S. S. (1996). Molecular Specializations at Nodes and Paranodes in Peripheral Nerve. *Microscopy Research and Technique*, *34*, 452–461.
Schindelin, J., Arganda-Carreras, I., Frise, E., Kaynig, V., Longair, M., Pietzsch, T., Preibisch, S., Rueden, C., Saalfeld, S., Schmid, B., Tinevez, J. Y., White, D. J., Hartenstein, V., Eliceiri, K., Tomancak, P., & Cardona, A. (2012). Fiji: An open-source platform for biological-image analysis. *Nature Methods*, *9*(7), 676–682. doi:10.1038/nmeth.2019
Schultz, J., Milpetz, F., Bork, P., & Ponting, C. P. (1998). SMART, a simple modular architecture research tool: Identification of signaling domains. *Proceedings of the National Academy of Sciences of the United States of America*, *95*(11), 5857–5864. doi:10.1073/pnas.95.11.5857
Seo, S., Baye, L. M., Schulz, N. P., Beck, J. S., Zhang, Q., Slusarski, D. C., & Sheffield, V. C. (2010). BBS6, BBS10, and BBS12 form a complex with CCT/TRiC family chaperonins and mediate BBSome assembly. *Proceedings of the National Academy of Sciences of the United States of America*, *107*(4), 1488–1493. doi:10.1073/pnas.0910268107
Serafini, T., Kennedy, T. E., Gaiko, M. J., Mirzayan, C., Jessell, T. M., & Tessier-Lavigne, M. (1994). The netrins define a family of axon outgrowth-promoting proteins homologous to C. elegans UNC-6. *Cell*, *78*(3), 409–424. doi:10.1016/0092-8674(94)90420-0
Shao, Q., Yang, T., Huang, H., Alarmanazi, F., & Liu, G. (2017). Uncoupling of UNC5C with polymerized TUBB3 in microtubules mediates netrin-1 repulsion. *Journal of Neuroscience*, *37*(23), 5620–5633. doi:10.1523/JNEUROSCI.2617-16.2017
Shaw, G., Morse, S., Ararat, M., & Graham, F. L. (2002). Preferential transformation of human neuronal cells by human adenoviruses and the origin of HEK 293 cells. *The FASEB Journal : Official Publication of the Federation of American Societies for Experimental Biology*, *16*(8), 869–871. doi:10.1096/fj.01-0995fje
Shepherd, M. N., Pomicter, A. D., Velazco, C. S., Henderson, S. C., & Dupree, J. L. (2012). Paranodal reorganization results in the depletion of transverse bands in the aged central nervous system. *Neurobiology of Aging*, *33*(1), 203.e13-203.e24. doi:10.1016/j.neurobiolaging.2010.08.001
Shibuya, M. (2006). Differential roles of vascular endothelial growth factor receptor-1 and receptor-2 in angiogenesis. *Journal of Biochemistry and Molecular Biology*, *39*(5), 469–478. doi:10.5483/bmbrep.2006.39.5.469
Simons, M., & Nave, K. A. (2016). Oligodendrocytes: Myelination and axonal support. *Cold Spring Harbor Perspectives in Biology*, *8*(1), 1–16. doi:10.1101/cshperspect.a020479
Snaidero, N., Möbius, W., Czopka, T., Hekking, L. H. P., Mathisen, C., Verkleij, D., Goebbels, S., Edgar, J., Merkler, D., Lyons, D. A., Nave, K.-A., & Simons, M. (2014). Myelin membrane wrapping of CNS axons by PI(3,4,5)P3-dependent polarized growth at the inner tongue. *Cell*, *156*(1–2), 277–290. doi:10.1016/j.cell.2013.11.044
Snaidero, N., & Simons, M. (2014). Myelination at a glance. *Cell Science at a Glance*, *127*, 2999–3004. doi:10.1242/jcs.151043
Snider, W. D., & Palavali, V. (1990). Early axon and dendritic outgrowth of spinal accessory motor neurons studied with dii in fixed tissues. *Journal of Comparative Neurology*, *297*(2), 227–238. doi:10.1002/cne.902970206
Sobottka, B., Ziegler, U., Kaech, A., Becher, B., & Goebels, N. (2011). CNS live imaging reveals a new mechanism of myelination: The liquid croissant model. *Glia*, *59*(12), 1841–1849. doi:10.1002/glia.21228
Sohda, M., Misumi, Y., Yamamoto, A., Yano, A., Nakamura, N., & Ikehara, Y. (2001). Identification and Characterization of a Novel Golgi Protein, GCP60, that Interacts with the Integral Membrane Protein Giantin. *Journal of Biological Chemistry*, *276*(48), 45298–45306. doi:10.1074/jbc.M108961200
Son, Y. O., Jang, Y. S., Heo, J. S., Chung, W. T., Choi, K. C., & Lee, J. C. (2009). Apoptosis-inducing factor plays a critical role in caspase-independent, pyknotic cell death in hydrogen peroxide-exposed cells. *Apoptosis*, *14*(6), 796–808. doi:10.1007/s10495-009-0353-7
Spassky, N., Castro, F. De, Bras, B. Le, Heydon, K., Quéraud-LeSaux, F., Bloch-gallego, E., Chédotal, A., Zalc, B., & Thomas, J.-L. (2002). Directional Guidance of Oligodendroglial Migration by Class 3 Semaphorins and Netrin-1. *Journal of Neuroscience*, *22*(14), 5992–6004.
Spiliotis, E. T. (2010). Regulation of microtubule organization and functions by septin GTPases. *Cytoskeleton*, *67*(6), 339–345. doi:10.1002/cm.20448
Spiliotis, E. T., Hunt, S. J., Hu, Q., Kinoshita, M., & Nelson, W. J. (2008). Epithelial polarity requires septin coupling of vesicle transport to polyglutamylated microtubules. *Journal of Cell Biology*, *180*(2), 295–303. doi:10.1083/jcb.200710039

Spiliotis, E. T., Kinoshita, M., & Nelson, W. J. (2005). A mitotic septin scaffold required for mammalian chromosome congression and segregation. *Science*, *307*(5716), 1781–1785. doi:10.1126/science.1106823
Srivatsa, S., Parthasarathy, S., Britanova, O., Bormuth, I., Donahoo, A. L., Ackerman, S. L., Richards, L. J., & Tarabykin, V. (2014). Unc5C and DCC act downstream of Ctip2 and Satb2 and contribute to corpus callosum formation. *Nature Communications*, 1–15. doi:10.1038/ncomms4708
Stadler, S. C., Polanetz, R., Meier, S., Mayerhofer, P. U., Herrmann, J. M., Anslinger, K., Roscher, A. A., Röschinger, W., & Holzinger, A. (2005). Mitochondrial targeting signals and mature peptides of 3-methylcrotonyl-CoA carboxylase. *Biochemical and Biophysical Research Communications*, *334*(3), 939–946. doi:10.1016/j.bbrc.2005.06.190
Strand, D., Unger, S., Corvi, R., Hartenstein, K., Schenkel, H., Kalmes, A., Merdes, G., Neumann, B., Krieg-Schneider, F., Coy, J. F., Poustka, A., Schwab, M., & Mechler, B. M. (1995). A human homologue of the Drosophila tumour suppressor gene l(2)gl maps to 17p11.2-12 and codes for a cytoskeletal protein that associates with nonmuscle myosin II heavy chain. *Oncogene*, *11*(2), 291–301.
Stucke, V. M., Timmerman, E., Vandekerckhove, J., Gevaert, K., & Hall, A. (2007). The MAGUK Protein MPP7 Binds to the Polarity Protein hDLG1 and Facilitates Epithelial Tight Junction Formation. *Molecular Biology of the Cell*, *18*, 1744–1755. doi:10.1091/mbc.E06
Su, M.-W., Merz, D. C., Killeen, M. T., Zhou, Y., Zheng, H., Kramer, J. M., Hedgecock, E. M., & Culotti, J. G. (2000). Regulation of the UNC-5 netrin receptor initiates the first reorientation of migrating distal tip cells in Caenorhabditis elegans. *Development*, *127*(3), 585–594. Retrieved from http://www.ncbi.nlm.nih.gov/pubmed/10631179
Su, W.-H., Mruk, D. D., Wong, E. W. P., Lui, W.-Y., & Cheng, C. Y. (2012). Polarity Protein Complex Scribble/Lgl/Dlg and Epithelial Cell Barriers. *Advances in Experimental Medicine and Biology*, *763*, 149–170. doi:10.1016/j.cortex.2009.08.003.Predictive
Sugimoto, Y., Taniguchi, M., Yagi, T., Akagi, Y., Nojyo, Y., & Tamamaki, N. (2001). Guidance of glial precursor cell migration by secreted cues in the developing optic nerve. *Development*, *128*, 3321–3330.
Susuki, K., Otani, Y., & Rasband, M. N. (2016). Submembranous cytoskeletons stabilize nodes of Ranvier. *Experimental Neurology*, *283*, 446–451. doi:10.1016/j.expneurol.2015.11.012
Susuki, X. K., Zollinger, X. D. R., Chang, K., Zhang, C., Huang, C. Y., Tsai, X. C., Galiano, X. M. R., Liu, Y., Benusa, S. D., Yermakov, L. M., Griggs, X. R. B., Dupree, J. L., & Rasband, X. M. N. (2018). Glial BII Spectrin Contributes to Paranode Formation and Maintenance. *Journal of Neuroscience*, *38*(27), 6063–6075. doi:10.1523/JNEUROSCI.3647-17.2018
Tai-Nagara, I., Yoshikawa, Y., Numata, N., Ando, T., Okabe, K., Sugiura, Y., … Kubota, Y. (2017). Placental labyrinth formation in mice requires endothelial FLRT2/UNC5B signaling. *Development (Cambridge)*, *144*(13), 2392–2401. doi:10.1242/dev.149757
Tao-Cheng, J. H., & Rosenbluth, J. (1983). Axolemmal differentiation in myelinated fibers of rat peripheral nerves. *Developmental Brain Research*, *9*(3), 251–263. doi:10.1016/0165-3806(83)90023-8
Tarabykin, V., Stoykova, A., Usman, N., & Gruss, P. (2001). Cortical upper layer neurons derive from the subventricular zone as indicated by Svet1 gene expression. *Development*, *128*(11), 1983–1993.
Tavender, T. J., Sheppard, A. M., & Bulleid, N. J. (2008). Peroxiredoxin IV is an endoplasmic reticulum-localized enzyme forming oligomeric complexes in human cells. *Biochemical Journal*, *411*(1), 191–199. doi:10.1042/BJ20071428
Torrents, D., Estévez, R., Pineda, M., Fernández, E., Lloberas, J., Shi, Y. B., Zorzano, A., & Palacín, M. (1998). Identification and characterization of a membrane protein (y + L amino acid transporter-1) that associates with 4F2hc to encode the amino acid transport activity y + L. A candidate gene for lysinuric protein intolerance. *Journal of Biological Chemistry*, *273*(49), 32437–32445. doi:10.1074/jbc.273.49.32437
Tsai, H., Tessier-lavigne, M., & Miller, R. H. (2003). Netrin 1 mediates spinal cord oligodendrocyte precursor dispersal. *Development*, *130*, 2095–2105. doi:10.1242/dev.00424
Tu, T., Zhang, C., Yan, H., Luo, Y., Kong, R., Wen, P., Ye, Z., Chen, J., Feng, J., Liu, F., Wu, J. Y., & Yan, X. (2015). CD146 acts as a novel receptor for netrin-1 in promoting angiogenesis and vascular development. *Cell Research*, *25*(3), 275–287. doi:10.1038/cr.2015.15
Uchida, T., Myers, M. G., & White, M. F. (2000). IRS-4 Mediates Protein Kinase B Signaling during Insulin Stimulation without Promoting Antiapoptosis. *Molecular and Cellular Biology*, *20*(1), 126–138. doi:10.1128/mcb.20.1.126-138.2000
Uhlén, M., Fagerberg, L., Hallström, B. M., Lindskog, C., Oksvold, P., Mardinoglu, A., … Pontén, F. (2015). Tissue-based map of the human proteome. *Science*, *347*(6220). doi:10.1126/science.1260419
Unsain, N., Bordenave, M. D., Martinez, G. F., Jalil, S., Von Bilderling, C., Barabas, F. M., Masullo, L. A., Johnstone, A. D., Barker, P. A., Bisbal, M., Stefani, F. D., & Cáceres, A. O. (2018). Remodeling of the Actin/Spectrin Membrane-associated Periodic Skeleton, Growth Cone Collapse and F-Actin Decrease during Axonal Degeneration. *Scientific Reports*, *8*(1), 1–16. doi:10.1038/s41598-018-21232-0
Unsain, N., Stefani, F. D., & Cáceres, A. (2018). The actin/spectrin membrane-associated periodic skeleton in

neurons. *Frontiers in Synaptic Neuroscience*, *10*(MAY), 1–8. doi:10.3389/fnsyn.2018.00010
Visser, J. J., Cheng, Y., Perry, S. C., Chastain, A. B., Parsa, B., Masri, S. S., Ray, T. A., Kay, J. N., & Wojtowicz, W. M. (2015). An extracellular biochemical screen reveals that FLRTs and Unc5s mediate neuronal subtype recognition in the retina. *ELife*, *4*, 1–27. doi:10.7554/eLife.08149
Wang, R., Wei, Z., Jin, H., Wu, H., Yu, C., Wen, W., Chan, L., & Wen, Z. (2009). Autoinhibition of UNC5b Revealed by the Cytoplasmic Domain Structure of the Receptor. *Molecular Cell*, *33*(6), 692–703. doi:10.1016/j.molcel.2009.02.016
Wang, V. Y., & Zoghbi, H. Y. (2001). Genetic regulation of cerebellar development. *Nature Reviews Neuroscience*, *2*(7), 484–491. doi:10.1038/35081558
Watanabe, K., Tamamaki, N., Furuta, T., Ackerman, S. L., Ikenaka, K., & Ono, K. (2006). Dorsally derived netrin 1 provides an inhibitory cue and elaborates the "waiting period" for primary sensory axons in the developing spinal cord. *Development*, *133*(7), 1379–1387. doi:10.1242/dev.02312
Waxman, S. G. (1980). Determinants of Conduction Velocity in Myelinated Nerve Fibers. *Muscle & Nerve*, *3*(2), 141–150.
Wetzel-Smith, M., Hunkapiller, J., Bhangale, T., Srinivasan, K., Maloney, J., Atwal, J., … Graham, R. (2014). A rare mutation in UNC5C predisposes to Alzheimer`s disease and increases neuronal cell death. *Nature Medecin*, *20*(12), 1452–1457. doi:10.1038/jid.2014.371
Williams, M. E., Wu, S. C. Y., McKenna, W. L., & Hinck, L. (2003). Surface Expression of the Netrin Receptor UNC5H1 is Regulated through a Protein Kinase C-Interacting Protein/Protein Kinase-Dependent Mechanism. *Journal of Neuroscience*, *23*(36), 11279–11288. doi:10.1523/jneurosci.23-36-11279.2003
Wilson, B. D., Ii, M., Park, K. W., Suli, A., Sorensen, L. K., Larrieu-Lahargue, F., Urness, L. D., Suh, W., Asai, J., Kock, G. A. H., Thorne, T., Silver, M., Thomas, K. R., Chien, C.-B., Losordo, D. W., & Li, D. Y. (2006). Netrins Promote Developmental and Therapeutic Angiogenesis. *Science*, *313*(5787), 640 LP – 644. doi:10.1126/science.1124704
Wingate, R. J. T., & Hatten, M. E. (1999). The role of the rhombic lip in avian cerebellum development. *Development*, *126*(20), 4395–4404.
Winnay, J. N., Boucher, J., Mori, M., Ueki, K., & Kahn, C. R. (2010). A Novel Interaction Between the Regulatory Subunit of PI 3-Kinase and X-box Binding Protein-1 Modulates the Unfolded Protein Response. *Nature Medecin*, *16*(4), 438–445. doi:10.1021/acssynbio.5b00266.Quantitative
Wolf, D., Hofbrucker-MacKenzie, S. A., Izadi, M., Seemann, E., Steiniger, F., Schwintzer, L., Koch, D., Kessels, M. M., & Qualmann, B. (2019). Ankyrin repeat-containing N-Ank proteins shape cellular membranes. *Nature Cell Biology*, *21*(10), 1191–1205. doi:10.1038/s41556-019-0381-7
Wolswijk, G., & Balesar, R. (2003). Changes in the expression and localization of the paranodal protein Caspr on axons in chronic multiple sclerosis. *Brain*, *126*(7), 1638–1649. doi:10.1093/brain/awg151
Woods, D. F., & Bryant, P. J. (1991). The discs-large tumor suppressor gene of Drosophila encodes a guanylate kinase homolog localized at septate junctions. *Cell*, *66*(3), 451–464. doi:10.1016/0092-8674(81)90009-X
Woods, D. F., Hough, C., Peel, D., Callaini, G., & Bryant, P. J. (1996). Dlg protein is required for junction structure, cell polarity, and proliferation control in Drosophila epithelia. *Journal of Cell Biology*, *134*(6), 1469–1482. doi:10.1083/jcb.134.6.1469
Wu, L. M. N., Williams, A., Delaney, A., Sherman, D. L., & Brophy, P. J. (2012). Report Increasing Internodal Distance in Myelinated Nerves Accelerates Nerve Conduction to a Flat Maximum. *Current Biology*, *22*(20), 1957–1961. doi:10.1016/j.cub.2012.08.025
Xia, W., & Liang, F. (2011). 4.1G promotes arborization and tight junction formation of oligodendrocyte cell line OLN-93. *Journal of Cellular Physiology*, *227*(6), 2730–2739. doi:10.1002/jcp.23017
Xu, K., Zhong, G., & Zhuang, X. (2013). Actin, spectrin, and associated proteins form a periodic cytoskeletal structure in axons. *Science*, *339*(6118), 452–456. doi:10.1126/science.1232251
Xu, S., Ha, C. H., Wang, W., Xu, X., Yin, M., Jin, F. Q., Mastrangelo, M., Koroleva, M., Fujiwara, K., & Jin, Z. G. (2016). PECAM1 regulates flow-mediated Gab1 tyrosine phosphorylation and signaling. *Cellular Signalling*, *28*(3), 117–124. doi:10.1016/j.cellsig.2015.12.007
Yamagishi, S., Hampel, F., Hata, K., Del Toro, D., Schwark, M., Kvachnina, E., Bastmeyer, M., Yamashita, T., Tarabykin, V., Klein, R., & Egea, J. (2011). FLRT2 and FLRT3 act as repulsive guidance cues for Unc5-positive neurons. *EMBO Journal*, *30*(14), 2920–2933. doi:10.1038/emboj.2011.189
Yamanaka, T., Horikoshi, Y., Sugiyama, Y., Ishiyama, C., Suzuki, A., Hirose, T., Iwamatsu, A., Shinohara, A., & Ohno, S. (2003). Mammalian Lgl Forms a Protein Complex with PAR-6 and aPKC Independently of PAR-3 to Regulate Epithelial Cell Polarity. *Current Biology*, *13*, 734–743. doi:10.1016/S0960-9822(03)00244-6
Yasugi, T., Vidal, M., Sakai, H., Howley, P. M., & Benson, J. D. (1997). Two classes of human papillomavirus type 16 E1 mutants suggest pleiotropic conformational constraints affecting E1 multimerization, E2 interaction, and interaction with cellular proteins. *Journal of Virology*, *71*(8), 5942–5951. doi:10.1128/jvi.71.8.5942-5951.1997

Yasunaga, M., Ipsaro, J. J., & Mondragón, A. (2012). Structurally similar but functionally diverse ZU5 domains in human erythrocyte ankyrin. *Journal of Molecular Biology*, *417*(4), 336–350. doi:10.1016/j.jmb.2012.01.041

Young, K. M., Psachoulia, K., Tripathi, R. B., Dunn, S. J., Cossell, L., Attwell, D., Tohyama, K., & Richardson, W. D. (2013). Oligodendrocyte dynamics in the healthy adult CNS: Evidence for myelin remodeling. *Neuron*, *77*(5), 873–885. doi:10.1016/j.neuron.2013.01.006

Zeitler, J., Hsu, C. P., Dionne, H., & Bilder, D. (2004). Domains controlling cell polarity and proliferation in the Drosophila tumor suppressor scribble. *Journal of Cell Biology*, *167*(6), 1137–1146. doi:10.1083/jcb.200407158

Zhu, M., Wang, F., Yan, F., Yao, P. Y., Du, J., Gao, X., Wang, X., Wu, Q., Ward, T., Li, J., Kioko, S., Hu, R., Xie, W., Ding, X., & Yao, X. (2008). Septin 7 interacts with centromere-associated protein E and is required for its kinetochore localization. *Journal of Biological Chemistry*, *283*(27), 18916–18925. doi:10.1074/jbc.M710591200

Zhu, Y., Chen, G., Lv, F., Wang, X., Ji, X., Xu, Y., Sun, J., Wu, L., Zheng, Y. T., & Gao, G. (2011). Zinc-finger antiviral protein inhibits HIV-1 infection by selectively targeting multiply spliced viral mRNAs for degradation. *Proceedings of the National Academy of Sciences of the United States of America*, *108*(38), 15834–15839. doi:10.1073/pnas.1101676108